Theme IIb: Interaction of different structural elements and assemblies

II b

Interaction entre différents éléments

Wechselwirkung zwischen verschiedenen Konstruktionsgliedern

Interaction of different Structural Elements and Assemblies

Leere Seite
Blank page
Page vide

IIb

Frame-Bracing Interaction in Multi-Storey Buildings

Interaction de charpente et ancrages dans des bâtiments à plusieurs étages

Zusammenwirken von Rahmen und Verbänden in mehrgeschossigen Bauten

JOSEPH A. YURA
Associate Professor of Civil Engineering
The University of Texas at Austin
Austin, Texas, USA

LE-WU LU
Professor of Civil Engineering
Lehigh University
Bethlehem, Pennsylvania, USA

1. Introduction

The bracing system in a multi-story building frame is designed to serve three specific fractions: 1) to prevent overall frame buckling under gravity load, 2) to resist story shear when the frame is subjected to combined gravity and lateral loads, and 3) to control lateral deflection (or drift) of the frame (1). Approximate methods for selecting bracing sizes are available in the literature (1,2,3) and are used in design practice. In these methods, it is generally assumed that the frame itself resist only the gravity load and that the bracing system is required to carry all the shear existing in a given story. No interaction between the frame and the bracing system is considered.

At low levels of applied loads, the frame would usually remain elastic and the interaction problem can be examined by using any conventional method of structural analysis. In a tall building frame, however, the presence of the secondary moment (or P-Δ moment) may cause the structure to respond non-linearly and a second-order analysis is required in order to determine the exact manner of interaction. The complexity of the interaction problem increases at high load levels when the frame becomes partially yielded. Any yielding in the frame tends to reduce its overall stiffness. A change in the distribution of the story shear between the frame and the bracing system will take place.

An analytical and experimental study has been carried out to investigate the interaction problem in low multi-story steel buildings. The study considers the behavior of diagonally braced frames in the elastic and elastic-plastic range and up to the maximum load. This discussion is a brief summary of the experimental program and the results obtained from two frame tests. Some analytical results related to the test frames are also included.

2. Test Frames and Loading Program

The frames tested in the experimental study are full size three-story, two-bay welded frames fabricated from rolled wide-flange shapes. A total of four frames were tested, two of which were loaded by gravity loads only (Frame 1 and 2). The remaining two (Frames 3 and 4) were subjected to combined gravity and lateral loads. The description presented herein pertains only to the frames. The frames were designed by the plastic method (1), with the girders proportioned for 1.7 times the working dead and live loads. Figure 1 shows the member sizes, exterior and interior connections, and the fixed base details of the test frames. Theoretically speaking, all structural components (girders and columns) in the frames designed by this method would reach their maximum capacity at the same load. However, because of variation of cross sectional and material properties, it was not possible to exactly achieve this condition in all the tests. Nevertheless, based on handbook section properties and a uniform yield stress of 36 ksi (minimum specified yield stress of A36 steel) for all members, the design shown in Fig. 1 was closely balanced.

The diagonal bracing was designed as a tension system and the cross sectional area was determined to meet certain drift limitation. Because of clearances the bracing could not be placed in the plane of the frame. The total

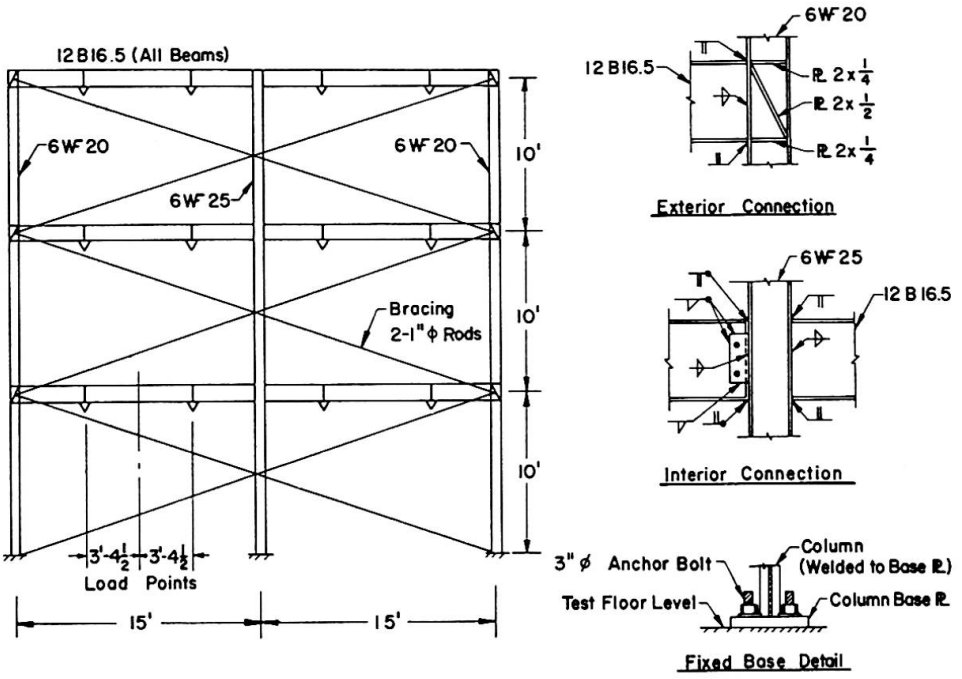

FIG. 1 TEST SPECIMENS

bracing area (1.57 sq. in.) was supplied by two, 1-in. diameter rods (slenderness ratio of 1520). One rod was placed on each side of the frame so that the resultant force would act in the plane of the frame. The bracing was prestressed before the testing operation to remove the sag and to offset slackening due to column shortening during testing. A detailed description of the fixtures used to attach the bracing to the frame and of the general test setup can be found elsewhere (4,5).

Although a pair of diagonal braces was provided in each story, only one was effective in resisting the story shear. This is because the slender braces used could sustain only a small compressive force. However, the "compression" brace in the test frame was made partially effective by the prestressing operation. A residual tensile force was present in all the braces after prestressing. When lateral loads were applied to the frame, both the tension brace and the compression brace would resist the loads provided that the net force in the compression brace was tensile. The compression brace eventually became ineffective when the net force changed to compression.

A checkerboard pattern of live loads was used in testing Frame 3. The loading pattern tends to produce a more critical bending moment condition (single curvature) in the interior columns. Frame 4 was tested with full gravity loads on all the girders. The loading conditions at the ultimate load of the two frames are shown in Fig. 2.

FIG. 2 LOADING CONDITION AT ULTIMATE LOAD

The loading program that was followed in testing Frame 3 consisted of four phases (Fig. 3):

Phase I Dead load on all the girders. The applied loads on the first and second floor girders increased from zero to 13.6 kips.

Phase II Checkerboard live load. The loads on the girders of alternate bays increased from 13.6 kips to 27.8 kips.

Phase III Wind load up to 4.5 kips applied at each floor level. All gravity loads were maintained at 13.6 kips or 27.8 kips.

Phase IV Proportional increase of gravity and wind loads. At the end of Phase III, the loads had the approximate proportions shown in Fig. 2. These proportions were maintained until a maximum of gravity load of 35.4 kips was reached in the heavily loaded girders. At this load, the girders failed due to the formation of plastic mechanism.

The loads of 13.6 kips, 27.8 kips and 4.5 kips represent, respectively, the factored (load factor = 1.30) dead load, dead plus live load, and wind load.

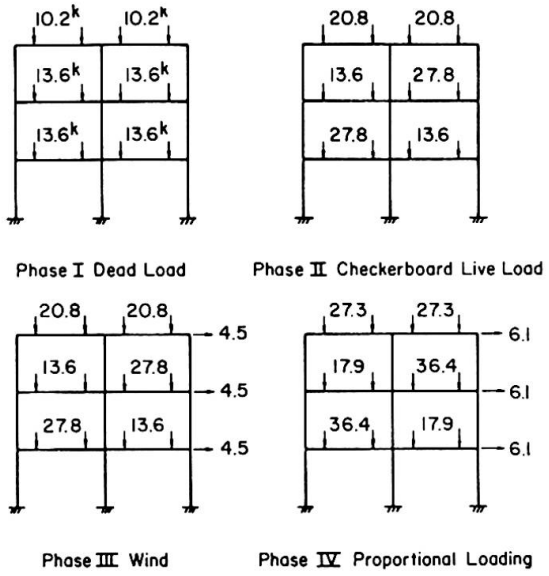

FIG. 3 LOADING PROGRAM FOR FRAME 3

For Frame 4, the load proportions shown in Fig. 2 were maintained throughout the test. The maximum girder load attained was 36.2 kips.

3. Theoretical Interaction in the Elastic Range

As elastic analysis of the test frames was performed to determine the theoretical interaction between the frame and the bracing system at low levels of the applied load. In general the amount of lateral load the frame resists depends on its stiffness relative to the bracing stiffness. The interaction of the test frame and various bracing sizes is illustrated in Fig. 4. The solid line on the right side shows the manner in which the total story shear is distributed between the frame and the bracing. For the bottom story, the sum of the frame shear and bracing shear must always equal 3.0 kips (neglecting any shear existing in the story induced by the secondary moment). Since the frame stiffness is assumed to remain constant, the theoretical interaction for various bracing areas will be a straight line. If the bracing is infinitely stiff, it will resist all the shear and the drift index Δ/h will be zero (point a). On the other hand, if the stiffness of the bracing is zero, then the frame will carry all the shear. In this case the frame is completely unbraced, and its Δ/h is equal to 0.0012 (point b). A straight line connecting these two points

defines the frame bracing interaction. The solid curve in the left portion of Fig. 4 shows the relationship between the bracing area furnished and the resulting deflection of the frame. This curve is constructed by using the information (bracing shear and story deflection) given in the right portion of the figure. The dashed curve is based on the assumption that only the bracing resists the story shear.

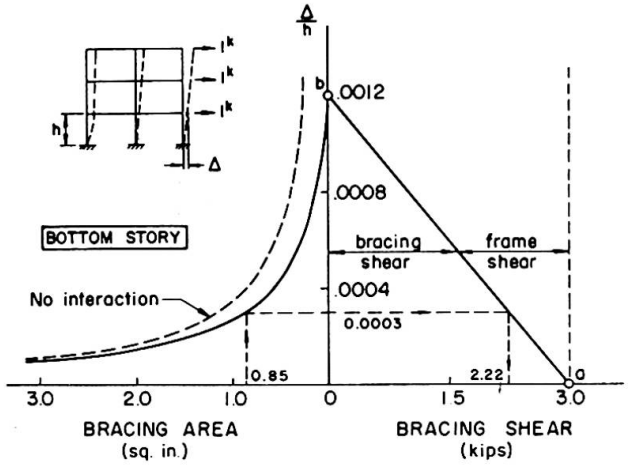

FIG. 4 THEORETICAL ELASTIC INTERACTION

The interaction between the frame and the bracing will change as soon as yielding takes place in the frame. The analysis presented above must be modified because of the reduction of frame stiffness caused by yielding. It is, therefore, necessary to know the locations of the plastic hinges before performing the analysis.

4. Experimental Results

Frame 3 - Lateral Loading Program (Phase III): As explained in Section 2, the lateral loads in Frame 3 were applied after a checkerboard pattern of factored gravity loads had been placed on the girders. The gravity load factor used was 1.30. Since the frame was designed for a load factor of 1.70, no plastic mechanism was expected to form in any of the girders at the beginning of the lateral loading program. There was, however, yielding in several parts of the heavily loaded girders near the interior columns. One plastic hinge formed in the first floor girder at a short distance away from the interior connection.

Figure 5 shows the shears developed in the columns and the bracing in the bottom story along with the total applied wind shear and the secondary shear caused by P-Δ moment. The bracing did not resist all the applied shear because

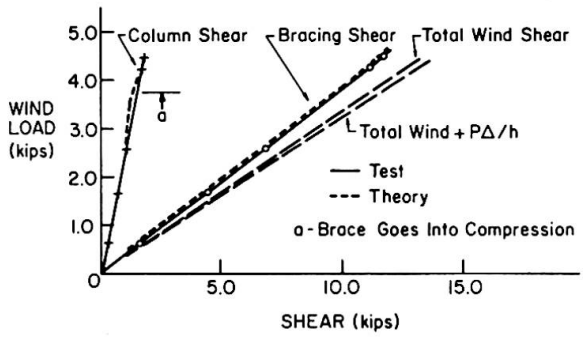

FIG. 5 RESULTS OF FRAME 3 TEST (LATERAL LOADING)

of the frame resistance. The theoretical shears carried by the frame and the bracing are shown by the dotted curves, and the theory shows excellent with the test results. The theory considers the effect of yielded zones developed during the application of the gravity loads. The calculations show that the frame stiffness is reduced about 25% by yielding. This reduced the contribution of the frame in resisting story shear from 14% (elastic frame) to 12% when all braces are in tension. Point a in Fig.5 denotes the points at which the "compression" brace goes into compression, and the frame resistance increases to 22%.

Frame 3 - Proportional Loading Program (Phase IV): The final loading phase was the application of loads in the proportions shown in Fig. 2. The applied wind shear with the corresponding shears in the columns and the bracing for the bottom story are shown in Fig. 6. The P-Δ shear at maximum load amounts to about 9% of the total wind shear. The shear in the bracing is greater than the combined wind and P-Δ shears even though the frame should carry 22% of the total shear as observed previously. This is caused by the large shears produced by the gravity loads due to the formation of plastic hinges in the frame.

As plastic hinges form in an unsymmetrical manner, the frame becomes unsymmetrical and even symmetrical gravity loads will cause shear in each story. Figure 7 shows how the shear in the bottom story is increased as plastic hinges form due to the checkerboard gravity loads. The results are derived for a frame with an infinitely stiff brace (no sidesway). The test frame corresponds to case (c) at the start of the proportional loading. The theoretical shear produced is 6.96 times greater than the shear in the elastic frame. The shear due to the gravity loads corresponding to case (c) is shown in Fig. 6 added to the effects of wind and P-Δ. The gravity load shear amounts to 37% of the wind shear applied during the proportional loading phase.

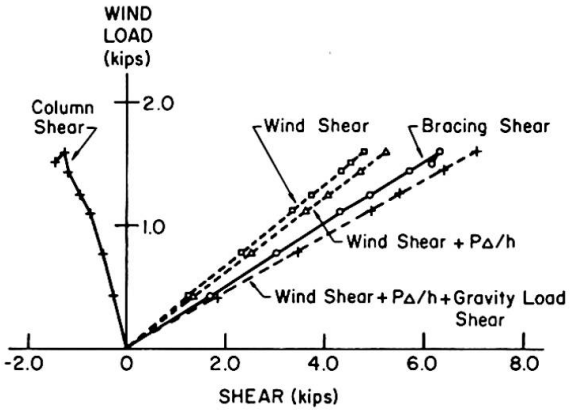

FIG. 6 RESULTS OF FRAME 3 TEST (PROPORTIONAL LOADING)

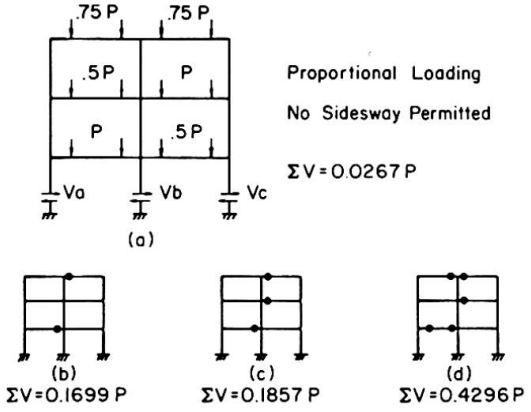

FIG. 7 GRAVITY LOAD SHEARS

Frame 4 - Proportional Loading: The frame was tested under proportionally increasing gravity loads and wind shear (Fig. 2). Because gravity loads were

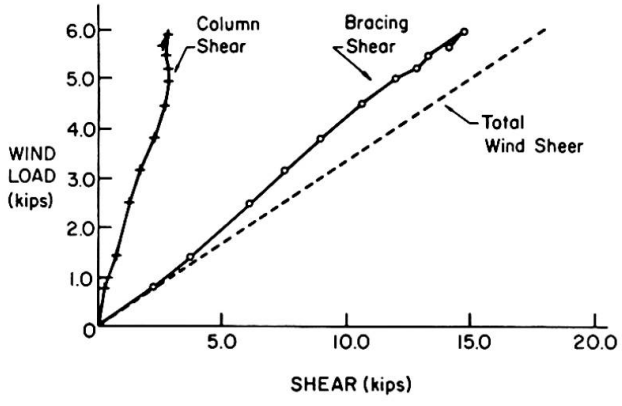

FIG. 8 RESULTS OF FRAME 4 TEST

applied symmetrically to all the girders the plastic hinge pattern developed in the frame was also symmetrical. The shear caused by the gravity loads was negligibly small. The results of this test, as shown in Fig. 8, are similar to those obtained from Phase III of the previous test.

5. Conclusions

Based on the results of this study, the following conclusions may be drawn with regard to frame-bracing interaction in low multi-story buildings:

1. The use of diagonal bracing is a very effective way to control drift and the reduce instability effect (P-Δ moment).

2. The amount of total story shear carried by the frame is significant (amounting to 20 to 30% of the total shear for the test frames).

3. In the elastic range, the distribution of story shear between the frame and the bracing system is nearly constant and can be predicted by conventional structural theory (instability effect need not be considered).

4. In the inelastic range, there is a tendency for the bracing shear to increase. This is due to the reduction of frame stiffness caused by yielding.

5. Under unsymmetrical gravity loads, the force to be resisted by the bracing system may exceed the applied story shear. Because of the gravity loads an additional shear of significant magnitude may develop in the columns after the frame is partially yielded in an unsymmetrical manner.

References

1. "Plastic Design of Multi-Story Frames" by G. C. Driscoll, Jr. et al, 1965 Summer Conference Lecture Notes, Lehigh Univ. 1965.
2. "Wind Bracing" by H. V. Spurr, McGraw-Hill, 1930.
3. "Lateral Support for Tier Buildings" by T. V. Galambos, Engineering Journal, AISC, Vol. 1, No. 1, Jan. 1964.
4. "The Strength of Braced Multi-Story Steel Frames" by J.A. Yura, Ph.D. Dissertation, Lehigh Univ., 1965.
5. "Ultimate Load Tests on Braced Multi-Story Frames" by J.A. Yura and L.W. Lu, Journal of the Structural Division, ASCE, Vol. 95, No. ST10, October 1969.

Summary

The results of an analytical and experimental study on the interaction between a rigid frame and its internal bracing system are presented. The study pertains to low multi-story steel frames subjected to combined gravity load and wind. It is shown that the amount of story shear carried by the bracing depends on the relative stiffness of the bracing to that of the frame. The ratio between bracing shear and frame shear changes significantly when the frame is stressed into the inelastic range.

Shear-Wall Bracing Criteria for Tall Buildings

Critères d'interaction entre cadre et noyau dans des maisons tours

Interaktionskriterien für Scheiben-Rahmen-Kombinationen in Hochhäusern

S. TALWAR
Department of Civil Engineering
M.Z. COHN
Solid Mechanics Division
University of Waterloo, Waterloo, Ontario, Canada

INTRODUCTION

In current design practice rigid jointed building frames are classified as braced and unbraced [1], [2]. The recommended design results in widely different member proportions for the two classes of frames. However, no clear guidance on the basis for this classification is offered in the literature.

Some studies of the bracing problem are concerned with the shear truss type of bracing [3], [4]. The results of these studies are not applicable to shear wall bracing because of the basic difference in behaviour of the shear wall and the shear truss types of bracings.

The object of this paper is twofold, (1) to identify the roles that lateral bracing plays in limiting sway movements in building frames, and, (2) to present related criteria in order that sway effects can be eliminated from the design of frames with shear wall bracing.

ROLE OF LATERAL BRACING

The current practice of designing braced frames suggests that:

1. Lateral displacements of frames under their horizontal loads should be small and no larger than a specified allowable limit. The criterion controlling the sway movements is referred to as the *lateral displacement criterion*.
2. Lateral stiffness of a braced system should be such that sway instability effects, before the ultimate stage, are small. The criterion developed for this purpose is referred to as the *stability criterion*.
3. Relative stiffnesses of the frame and its bracing should be such that a major portion of the lateral loads is assigned to the bracing elements, resulting in a design for which the frame proportions are controlled by gravity loads alone. The criterion that ensures such a behaviour is referred to as the *primary loading criterion*.
4. Moments and joint rotations of the frame members due to unsymmetrical gravity loading and/or geometry should be similar to the behaviour under infinitely stiff lateral restraints. The shear wall criterion intended to produce such a response is referred to as the *symmetric loading criterion*.

The object of this paper is to study the satisfaction of the above criteria for shear wall braced frames.

THE ANALYTICAL MODEL

The main features of the analytical model adopted for developing criteria 1 to 3 are (Fig. 1):

1. The columns of a multibay frame are lumped in a single continuous column which is restrained at every floor level by beams with pinned far ends.
2. The shear walls are represented by a single cantilever wall.
3. The interconnection between the equivalent frame and wall components is made by axially rigid pinned linkages.
4. The effect of axial loading on member stiffness is neglected, but the P-Δ effects are taken into account.

Similar models have been extensively used in past [5], [6], [7] and the approximations resulting from the adopted approach do not significantly affect the results of this study.

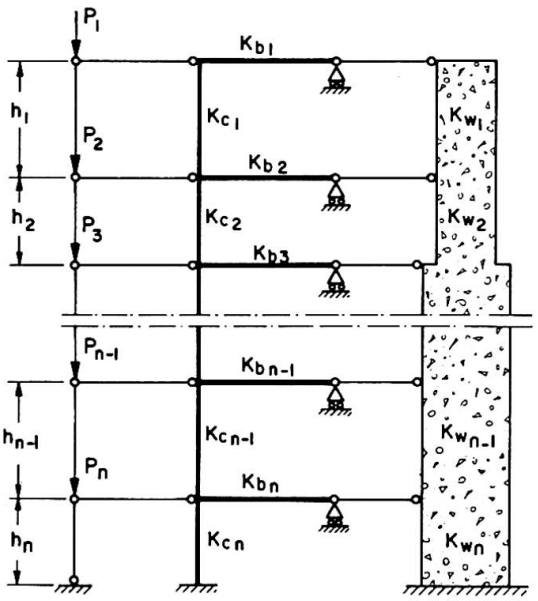

Fig. 1 Analytical Model

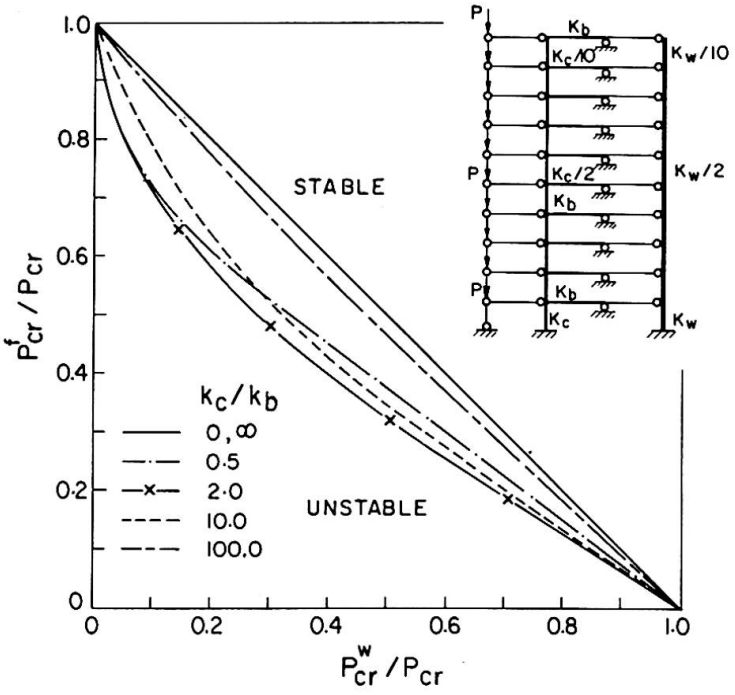

Fig. 2 Interaction of Critical Loads

DEVELOPMENT OF CRITERIA

The study shows that three parameters P_{cr}, P^w_{cr} and P^f_{cr} i.e., the critical loads associated with the lateral buckling of the structure, the free-standing wall and the unbraced frame respectively, control the development of the criteria. P^w_{cr} and P^f_{cr} are independent parameters, whereas P_{cr} depends upon the buckling loads and shapes of the frame and wall components. The interaction of these parameters for a ten story structure is shown in Fig. 2.

1. *Lateral Displacement Criterion*: In a single story model, a lateral force H causes a story rotation $\rho = H/P_{cr}$. The axial load P increases this primary rotation by a multiplier $\beta = 1/(1 - P/P_{cr})$. Thus, the relationship $\rho = \beta H/P_{cr}$ accounts for both the primary and secondary displacements of a single story model.

The validity of a similar relationship for multi-story structures is studied. An investigation on a number of frames suggests that the maximum story rotation ρ_m in a multi-story structure, in which the ratio of lateral to gravity loads, H/P, at all floors is constant, is approximately given by:

$$\rho_m = c\beta\, H/P_{cr} \tag{1}$$

where the constant c depends primarily on the relative stiffness of the beams in the structure and β, as defined above, is a multiplier accounting for the P–Δ effect. The value of c(which is 1.0 for infinitely stiff beams) may be taken as 1.2 for all practical unbraced frames and 1.5 for cantilever walls. For frames braced according to the criteria in this paper, a value of c = 1.4 seems appropriate. The correlation of eq. (1) with the exact values of ρ_m is good.

In real structures, H and P generally are not in a constant ratio. Assuming the total gravity load distributed in the same manner as the lateral loads, eq. (1) yields only slightly conservative values of ρ_m.

Then eq. (1) expresses the lateral displacements in terms of the critical loads. If the serviceability conditions limit ρ_m to an allowable value ρ_a, eq. (1) with c = 1.4 yields:

$$P_{cr}/P \geq (1.4/\rho_a)(H/P) + 1 \tag{2}$$

Current building codes [1],[2] leave the matter of the allowable lateral displacements open. Various technical committees [8],[9] limit the maximum horizontal sway under wind forces to 1/500 of the overall height of the structure. Reference [9] allows an alternative interpretation of this limitation as "the ratio of the relative lateral story displacement to the story height, assuming a more or less uniform story height". Accordingly, accepting $\rho_a = 1/500$, the lateral displacement criterion for design wind load becomes:

$$P_{cr}/P \geq 700\, H/P + 1 \tag{3}$$

2. *Stability Criterion*: The sway instability phenomenon affects the behaviour of structures mainly through the amplification of their primary lateral displacements, which may result due to horizontal loads or lack of symmetry in geometry or loading. In braced buildings the effects of such an amplification are completely neglected [1],[2]. In order for this practice to be justified, the value of the maximum sway multiplier must be negligible. Any value which may be considered negligible for this purpose is subjective. In this paper, an amplification of 5% at working loads and of 10–15% at the ultimate stage is considered acceptable.

Lateral displacement studies have shown that the multiplier of ρ_m is $1/(1-P/P_{cr})$. This also happens to be the maximum amplification for any story rotation. If the assumption introduced with the displacement criterion is accepted, a limitation on the maximum amplification of 5% at working loads yields:

$$P_{cr}/P \geqslant 20 \tag{4}$$

If a structure is designed to remain elastic until the ultimate stage, with a load factor of 1.25 (for combined lateral and gravity loading) this amplification becomes about 7% and with a load factor of 1.7 (for gravity loads alone) its magnitude becomes about 9%.

If the beams of a structure develop plastic hinges at their right ends before the ultimate stage and the frame is braced according to the criteria in this paper, the maximum amplification of primary story rotations increases to about 12% for the combined loading and to about 16% for gravity loading alone.

3. *Primary Loading Criterion*: The extent to which a frame contributes in resisting the applied lateral forces depends upon the relative stiffnesses of the frame and the shear wall. If critical loads are taken as a measure of stiffness, the lateral loads carried by the shear wall should bear some relationship to P^w_{cr}/P^f_{cr}. In fact, in a single story model, the distribution of lateral shears between the wall and the frame follows strictly this ratio.

In multi-story structures, such proportionality in individual stories does not exist, but the shear distribution is determined by the relative stiffnesses of the wall and the frame [7].

Studies on multi-story structures indicate that the average percentage of shear carried by the shear wall in different stories is approximately proportional to the parameter P^w_{cr}/P_{cr} with the critical loads evaluated with a distribution of P similar to H. One such study is presented in Fig. 3. In this figure, i refers to the number of stories from the top and the dotted curve also represents the average wall shear. The deviation from the average of wall shear percentages in individual stories varies with the type of frame and wall and the loading, but is mainly controlled by the ratio P^w_{cr}/P_{cr}: the larger is this ratio, the smaller is the deviation. From Fig. 3, it is clear that values of P^w_{cr}/P_{cr} above about 0.5 help the frame to a lesser degree in the lower part of the structure. A smaller value of this parameter causes a disproportionately large increase of the shears carried in the lower part of the frame. Thus, it is recommended that for braced frames:

$$P^w_{cr} \geqslant 0.5\, P_{cr} \tag{5}$$

This is a necessary but not sufficient provision for ensuring that the frame can be designed for gravity loads only.

4. *Symmetric Loading Criterion*: The case of a single column frame is considered. The column is loaded by joint moments of different ratios. Comparisons are made between column end moments and rotations for two cases: (a) column laterally restrained by a finite shear restraint, and (b) column with infinite shear restraint. Such studies indicate that a column bent in double curvature without sway exhibits the largest departure from the no sway behaviour. This case is more critical for joint rotations than for end moments. Denoting the average rotations for the sway cases by $\bar{\theta}$ and for the no sway case by θ, the behaviour of this model is described by:

$$\bar{\theta}/\theta = 1+[12k_c/h-P^f_{cr}]/P_{cr} \tag{6}$$

With P_{cr} corresponding to a shear restraint $\alpha_\ell = 12k_c/h$, this ratio ranges from 2 for no rotational to 1 for infinite rotational restraint. This value of the shear restraint α_ℓ has been found adequate for reinforced concrete columns [10] and is used as a basis for developing this criterion.

The behaviour of double curvature frame columns, loaded primarily by moments at their joints, is approximated from eq. (6) as:

$$\bar{\theta}/\theta = 1 + [(1/i)\,(12k_c/h)-(k_c/\Sigma k_c)P^f_{cr}]\,(\bar{H}^f/\bar{H}^c)/P_{cr} \tag{7}$$

where $\bar{H}^f/\bar{H}^c$ is the ratio of the no sway frame shear to the column shear under the loading being investigated, Σk_c denotes the summation of column stiffnesses EI_c/h over the story i (counting from top) containing the column under consideration, and P_{cr} corresponds to equal distribution of gravity loads between floors. The correlation of behaviour predicted by eq. (7) with the exact analyses is satisfactory. From the comparison of eqs. (6) and (7), it follows that restraint equivalent to $\alpha_\ell = 12k_c/h$ for the single column model is provided if:

$$P_{cr} = \text{Max.}[(1/i)(12k_c/h)+(k_c/\Sigma k_c)P^f_{cr}]\,\bar{H}^f/\bar{H}^c \tag{8}$$

This criterion need only be applied to a column with the maximum H^c in a story under a loading causing a maximum unbalanced shear $\bar{H}^f$. The critical story will usually be one of the few top or bottom stories of the structure.

Whereas the previous criteria apply to the service conditions, eq. (8) refers to the ultimate stage. This criterion may not be critical for elastic frames since $\bar{H}^f$ is usually small, but it may prove to be the most critical if applied to a pseudoelastic frame similar to the one described earlier for the stability criterion. In limit design, with materials having limited ductility, the use of this pseudoelastic frame for applying eq. (8) is recommended. For such frames, the contribution of P^f_{cr} may be dropped from either side of eq. (8) which thus simplifes to:

$$P^w_{cr} = \text{Max.}[(1/i)(12k_c/h)(\bar{H}^f/\bar{H}^c)] \tag{9}$$

DESIGN EXAMPLE

A twelve story four bay reinforced concrete frame, Fig. 4, with the preliminary member sizes and moments of inertia in Table 1, is to be designed for collapse at the specified ultimate loads. The frames are 20 ft. apart and carry a service live load of 100 lb/sq.ft., a wind load of 20 lb/sq.ft. and a dead load of 50 lb/sq.ft. The load is transferred to the frame through cross beams 7 ft. apart. The materials have $f'_c = 4$ ksi and $f_y = 60$ ksi. The preliminary design is based on American practice [1]. Gross moments of inertia are used for columns while some adjustments for cracking are made in computing the moments of inertia for the beams, which include a 3.5 in. slab on the top.

With these data, the gravity load per story is P = 305 kips or 1.05 EI_c/h^2 with $E = 60{,}000\sqrt{f'_c}$. The wind load per story is H = 5 kips, giving a ratio H/P = 1/61. From eq. (3), a value of $P_{cr}/P = 12.45$ is required for the displacement criterion. This factor is less than the minimum $P_{cr}/P = 20$ required for the stability criterion, which yields a minimum value $P_{cr} = 21\ EI_c/h^2$.

A stability analysis of the continuous column modelling the frame by Grinter's approach [5], yields $P^f_{cr} = 17.14\ EI_c/h^2$. Assuming that the shear wall stiffness varies along its height as the sum of column stiffnesses $P^w_{cr} = 0.107\ EI_w/h^2$. Studies of the interaction between P_{cr}, P^f_{cr} and P^w_{cr} show that with the type of frame and shear wall in this example, $P^w_{cr}/P_{cr} = 0.5$ requires $P^f_{cr}/P_{cr} = 0.33$, so that $P^w_{cr}/P^f_{cr} = 1.5$. Thus, in order to satisfy the primary loading criterion, a $P^w_{cr} \geq 1.5\ P^f_{cr}$ is required. This results in a minimum $I_w/I_c = 1.5 \times 17.14/0.107 = 240$ yielding a shear wall critical load $P^w_{cr} = 25.71\ EI_c/h^2$ which is greater than $P_{cr} = 21\ EI_c/h^2$ required for the stability and the displacement criteria.

The frame is analysed (no sway) for full loading on all beams with their right ends assumed hinged. Columns on line D (Fig. 4) exhibit higher values of $k_c\bar{H}^f/i\bar{H}^c$ in all stories, indicating that a larger amount of bracing is required for this column line. This results from a smaller end span carrying a lighter loading. Determining the amount of bracing for this column line, however, is considered unreasonable because of the smaller shears associated with this column line. Columns on lines B and C carry maximum shears in all stories and are made the basis for satisfactions of the symmetric loading criterion. For either of these column lines the maximum $k_c\bar{H}^f/i\bar{H}^c = 2.88\ EI_c/h$ occurs in the top story and, from eq. (9), a minimum $P^w_{cr} = 34.56\ EI_c/h^2$, and corresponding ratio $I_w/I_c = 34.56/0.107 = 322$ are found.

Thus, the symmetric loading criterion controls the stiffness of the shear wall required to brace the frame in this example. However, if the frame is to be designed for an elastic ultimate stage, the primary loading criterion will control, since under a loading maximizing $\bar{H}^f$ the value of $\bar{H}^f/\bar{H}^c$ in eq. (8) is relatively small.

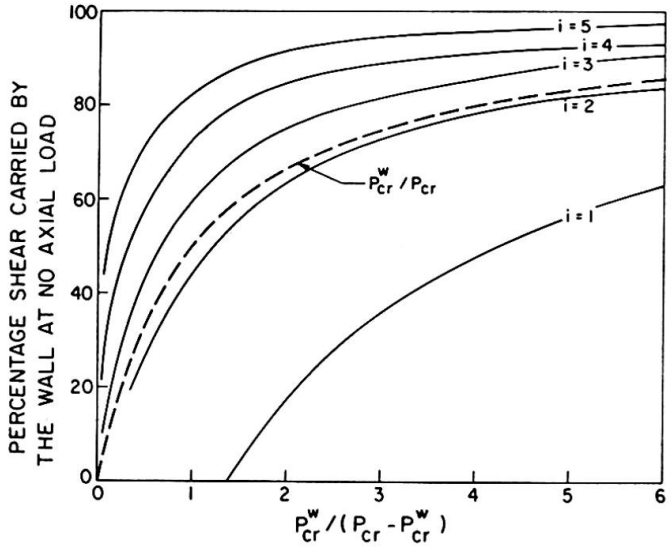

Fig. 3 Typical Lateral Load Distribution

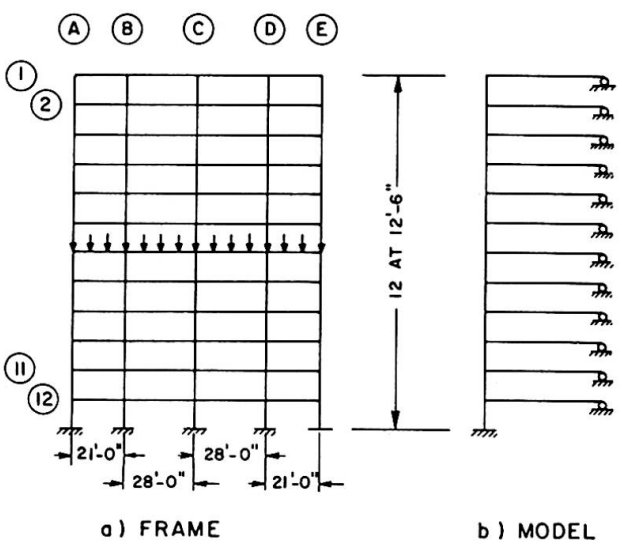

Fig. 4 Example Frame

TABLE 1

PROPERTIES OF EXAMPLE FRAME

STORIES	FRAME						MODEL	
	EXT. COLUMNS		INT. COLUMNS		BEAMS		COLUMNS	BEAMS
	Section (in. x in.)	I	Section (in. x in.)	I	Section (in. x in.)	I	k	k
1	12 x 12	I_c	12 x 12	I_c	12 x 24	$12I_c$	$5k_c$	$100\ k_c$
2	12 x 12	I_c	12 x 12	I_c			$5k_c$	
3	12 x 12	I_c	12 x 14	$1.6\ I_c$			$6.8\ k_c$	
4	12 x 12	I_c	12 x 14	$1.6\ I_c$			$6.8\ k_c$	
5	12 x 12	I_c	14 x 18	$3.95I_c$			$13.85k_c$	
6	12 x 12	I_c	14 x 18	$3.95I_c$			$13.85k_c$	
7	12 x 14	$1.6\ I_c$	16 x 21	$7.15I_c$			$24.65k_c$	
8	12 x 14	$1.6\ I_c$	16 x 21	$7.15I_c$			$24.65k_c$	
9	14 x 14	$1.85I_c$	18 x 21	$8.05I_c$			$27.85k_c$	
10	14 x 14	$1.85I_c$	18 x 21	$8.05I_c$			$27.85k_c$	
11	16 x 16	$3.16I_c$	21 x 21	$9.40I_c$			$34.52k_c$	
12	16 x 16	$3.16I_c$	21 x 21	$9.40I_c$			$34.52k_c$	

CONCLUSIONS

The purpose of the study is to develop criteria for braced frames when shear walls are used as lateral supports in tall buildings. Four basic criteria are used to develop the equations. Only the shear walls extending over the full height of the frame are considered. No allowance is made for the stiffening effects of partitions and cladding or any torsional effects arising out of an unsymmetry in the plan of the building. The study demonstrates that all the proposed criteria can be satisfied by placing suitable limits on the critical loads of the structural system and its frame and shear wall components.

The parameters used in the study may be too time consuming for exact calculations in design offices. However, if the analytical model suggested in this paper is accepted, such calculations may futher be simplified by developing standard design aids.

ACKNOWLEDGEMENT

The study is based on a Ph.D. dissertation prepared by the first author and is a part of a comprehensive research on the application of limit design to reinforced concrete structures, being conducted in the Department of Civil Engineering at the University of Waterloo under the direction of the second author. The financial support of the National Research Council of Canada, under grant A 4789, is gratefully acknowledged.

REFERENCES

1. "Building Code Requirements for Reinforced Concrete", ACI 318-71, American Concrete Institute, Detroit, 1971.
2. "Specification for the Design, Fabrication and Erection of Structural Steel for Buildings", AISC, New York, 1969.
3. GOLDBERG, J.E., "On the Lateral Buckling of Multistory Building Frames with Shear Bracing", *Final Report Sixth IABSE Congress*, Stockholm, 1960, pp. 231-240.
4. GALAMBOS, T.V., "Lateral Support for Tier Buildings", *Engineering Journal, AISC*, Vol. 1, No. 1, January 1964, pp. 16–19.
5. GRINTER, L.E., "Theory of Modern Steel Structures", Vol. 2, The MacMillan Company, New York, 1957.
6. DESCHAPELLES, BERNARDO J., "Analytical Model for Lateral Load Effect on Buildings", *Journal of the Structural Division, ASCE*, Vol. 96, No. ST 6, Proc. Paper 7328, June 1970, pp. 1025–1048.
7. KHAN, FAZLUR R., and SBAROUNIS, JOHN A., "Interaction of Shear Walls and Frames" , *Journal of the Structural Division,ASCE*, Vol. 90, No. ST 3, Proc. Paper 3957, June 1964, pp. 285–335.
8. ACI Committee 435, "Allowable Deflections", *ACI Journal*, Proceedings, Vol. 65, No. 6, June 1968, pp. 433-444.
9. ACI Committee 442, "Response of Buildings to Lateral Forces", *ACI Journal*, Proceedings Vol. 68, No. 2, Feb. 1971, pp. 81–106.
10. PFRANG, E.O., "Behaviour of Reinforced Concrete Columns with Sidesway", *Journal of the Structural Division, ASCE*, Vol. 92, No. St. 3, Proc. Paper 4853, June, 1966, pp. 225–250.

NOTATION

E	= Modulus of elasticity.
f_c'	= Concrete cylinder strength.
f_y	= Steel yield strength.
h	= Story height.
H	= Lateral forces at floor level.
$\bar{H}^c, \bar{H}^f, \bar{H}^w$	= Lateral shears on a column, frame and wall, respectively.
I	= Moment of inertia.
I_c, I_w	= Moments of inertia of a column and a wall, respectively.
k	= EI/L for a member.
k_b, k_c	= EI/L for a beam and a column, respectively.
n	= Number of stories in a structure.
P_{cr}	= Critical load of a structure against lateral buckling.
P_{cr}^f, P_{cr}^w	= Same as P_{cr} but for the unbraced frame and the free standing shear wall respectively.
$\alpha_\varrho = \bar{H}/\rho$	= Lateral restraint magnitude.
β	$= 1/(1 - P/P_{cr})$.
$\theta, \bar{\theta}$	= Average end rotations of a column, sway prevented and allowed, respectively.
Δ	= Relative lateral movement between consecutive floors.
ρ	$= \Delta/h$.
ρ_a	= Allowable value of ρ for serviceability.
ρ_m	= Maximum value of ρ in a structure.

SUMMARY

The object of the paper is to derive rational criteria for shear wall bracing of tall building concrete frames with particular reference to limit design. Four basic conditions referred to as 1) *lateral displacement*, 2) *stability* 3) *primary loading* and 4) *symmetrical loading criteria* are developed. Approximate relations for practical design based on these criteria are suggested and their application to a typical building is illustrated on a numerical example.

Das Zusammenwirken von Trägern verschiedener Biege- und Schubsteifigkeit

Interaction between Girders of Different Flexural and Shear Stiffness

Interaction entre poutres à différentes rigiditées de flexion et de cisaillement

FRANTIŠEK FALTUS
Professor an der Technischen Hochschule
in Prag, CSSR

Dieser Beitrag zu Thema IIb des Einführungsberichtes soll daran erinnern, dass bei der Berechnung des Zusammenwirkens verschiedener Arten aussteifender Verbände eine gewisse Vorsicht geboten ist. Gewöhnlich werden die angreifenden Kräfte einfach im Verhältnis der Steifigkeit auf die einzelnen Verbände verteilt, wobei die Steifigkeit als die Belastung zur Erzeugung der Durchbiegung "Eins" aufgefasst wird. Ist z.B. ein Stahlskelettbau/Fig. 1/mit zwei Fachwerkwänden A1, A2 und einem Betonkern B gegen Windbelastung gestützt und setzt man die Geschossdecken als

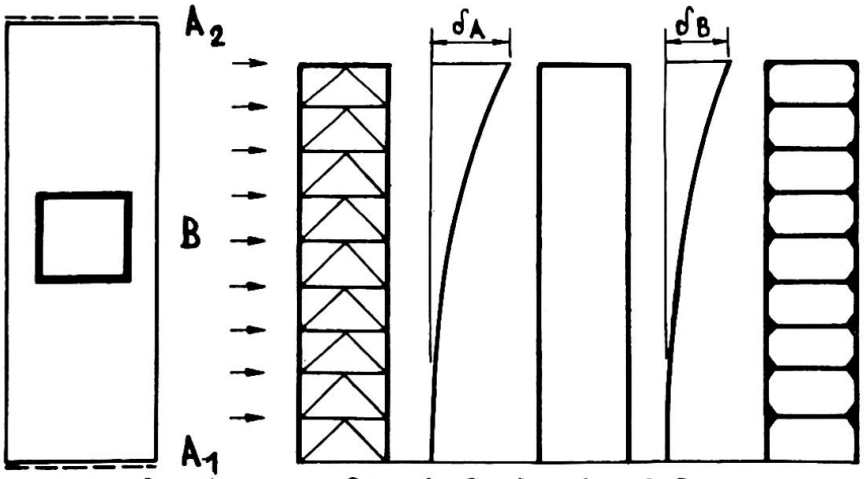

FIG. 1

starr voraus, so rechnet man oft einfach wie folgt: Es sei δ_A die Durchbiegung des Verbandes A, bzw, δ_B des Verbandes B unter Belastung w=1, dann weist man von der Gesamtbelastung W den Verbänden A jeden Anteil $W_A = W\delta_B/(\delta_A + 2\delta_B)$ und dem Verband B den Anteil $W_B = W\delta_A/(\delta_A + 2\delta_B)$ zu. Dieser Vorgang ist nur richtig, wenn die Biegelinien beider Verbände affin sind, denn nur dann werden die Belastungen W_A und W_B nicht nur an den Trägerenden, sondern auch in jedem Stockwerk gleiche Durchbiegungen erzeugen. Sind die Biegelinien nicht affin,

müssen in den einzelnen Geschosshöhen weitere Reaktionskräfte wirken, welche den Ausgleich der Form erzwingen, wie z.B. ausführlich in [1] gezeigt wurde. Bei vielgeschossigen Bauten können wir statt mit einer diskreten, mit einer kontinuierlichen Verteilung der Reaktionskräfte, also mit den Differentialgleichungen der Biegelinien rechnen.

Untersuchen wir als einfaches Beispiel den Fall zweier Kragträger mit über die ganze Länge ℓ konstanten Querschnitten nach Fig.2. Die Steifigkeitsverhältnisse sollen durch folgende Werte gegeben sein.

Die Biegesteifigkeit: $\varepsilon_1 = \frac{E_0 J_0}{E_1 J_1}$, $\varepsilon_2 = \frac{E_0 J_0}{E_2 J_2}$

Die Schubsteifigkeit: $\beta_1 = \frac{E_0 J_0}{G_1 \omega_1 F_1 \ell^2}$, $\beta_2 = \frac{E_0 J_0}{G_2 \omega_2 F_2 \ell^2}$

Der Wert $E_0 I_0$ bezieht sich auf einen beliebigen Vergleichsträger, die Indizes 1 und 2 bezeichnen Träger 1 und 2. Für einen Rechteckquerschnitt ist $\omega = 5/6$, für einen Vollwandträger $\omega = 1$, wenn F die Stehblechfläche bedeutet. Für Fachwerkträger ist F die Fläche des Stehbleches eines gedachten Vollwandträgers gleicher Schubverformung wie die vorhandene Ausfachung. Das Verhalten der Träger charakterisieren die Werte

$$\alpha^2 = \frac{\varepsilon_1 + \varepsilon_2}{\beta_1 + \beta_2} \quad \text{und} \quad \delta_1 = \frac{\varepsilon_2 \beta_1 - \varepsilon_1 \beta_2}{(\varepsilon_1 + \varepsilon_2)(\beta_1 + \beta_2)}$$

Die für die Berechnung massgebenden Grössen bewegen sich in praktischen Fällen etwa in folgenden Grenzen, wenn h die Trägerhöhe und ℓ die Kraglänge bedeuten:

für Rechteckquerschnitte $\beta = 0{,}26/\varepsilon h^2/\ell^2/$,
für Blechträger bis etwa $\beta = 1{,}2\ \varepsilon h^2/\ell^2$
für Fachwerkträger ist β bis etwa $10\,\varepsilon\, h^2/\ell^2$

Grosse Werte β erhalten wir bei Fachwerkträgern mit grossen Gurtflächen /schwerbelastete Säulen/und leichter Ausfachung, welche nur auf die Windbelastung dimensioniert ist. Hiemit ergibt sich

$\varepsilon_1 : \varepsilon_2$ etwa 0,5 bis 5
α etwa (1 bis 3) h/ℓ und $|\delta|$ etwa 0 bis 1.

Der Wert $\delta = 0$ entspricht zwei ähnlichen Vollwand oder Fachwerkträgern, δ wird gross beim Zusammenwirken von Vollwand- mit Fachwerkträgern. Die grössten Werte nimmt $|\delta|$ an, wenn einer der Träger ein Rahmenträger ist.

Aus der Differentialgleichung der Biegelinie mit Berücksichtigung der Querkräfte

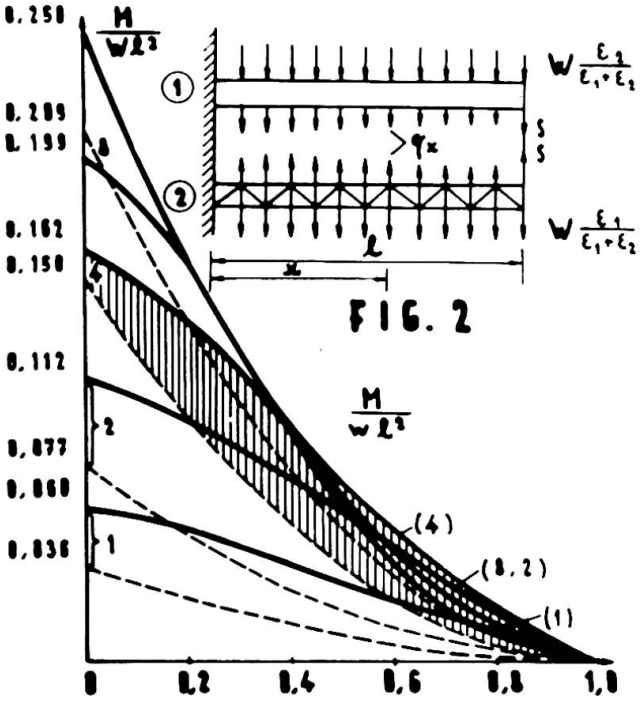

FIG. 3

FIG. 2

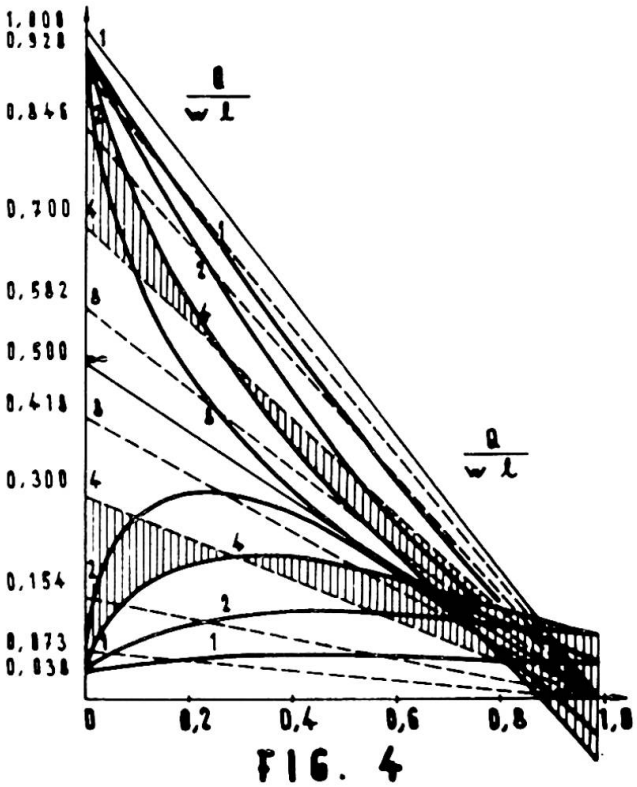

FIG. 4

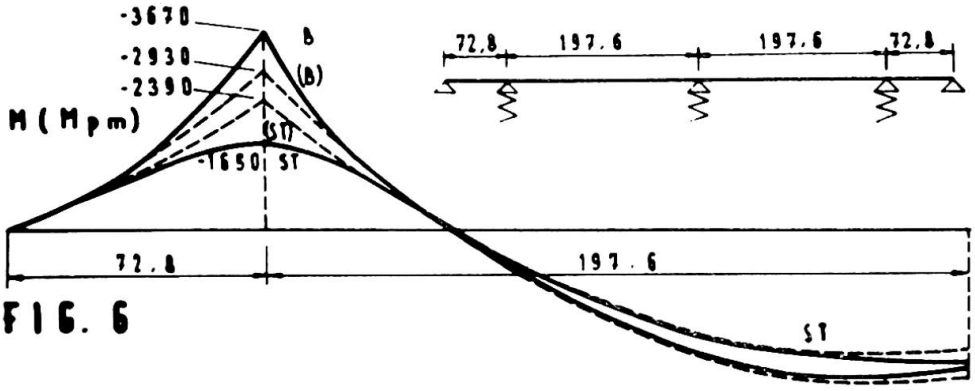

FIG. 6

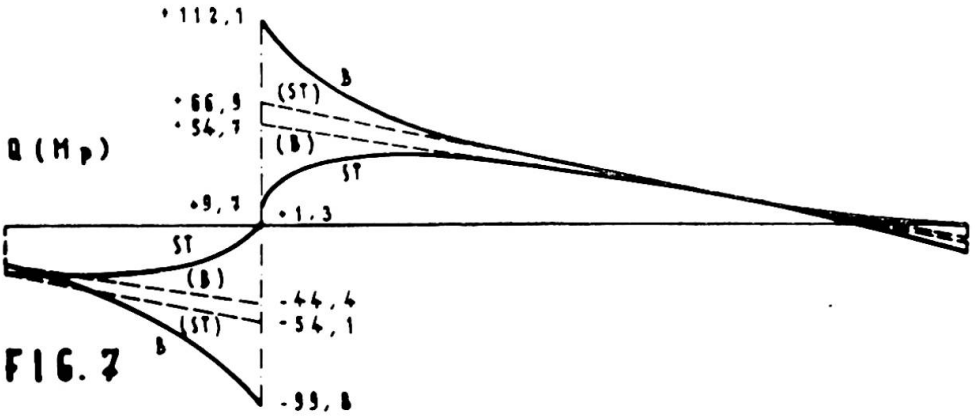

FIG. 7

$$\frac{d^2 y}{d x^2} = \frac{M}{E J} + \frac{d Q}{G \omega F d x} = \varepsilon \left(M + \beta \frac{d Q}{d x} \right)$$

erhalten wir die Gleichung unseres Problemes mit

$$\frac{d^2 y_1}{d x^2} = \frac{d^2 y_2}{d x^2}$$

da die Biegelinien in ihrem ganzen Verlauf der Voraussetzung nach identish sein sollen und daher auch ihre zweiten Ableitungen.

Wenn wir annehmen, dass sich die äussere Belastung auf die beiden Träger im Verhältniss der Biegesteifigkeiten verteilt,

$$w_1 = \frac{\varepsilon_1}{\varepsilon_1 + \varepsilon_2} \qquad w_2 = \frac{\varepsilon_2}{\varepsilon_1 + \varepsilon_2}$$

ergibt sich die Differentialgleichung für die Reaktionskräfte q_x mit

$$q_x - \frac{l^2}{\alpha^2} q_x'' = 0$$

mit der Lösung für $\xi = \frac{x}{l}$

$$q_x = C_1 \cosh \alpha \xi + C_2 \sinh \alpha \xi .$$

Mit den Auflager- und Randbedingungen der Fig.2 ist

$$C_1 = - \frac{\delta w \alpha}{\cosh \alpha} \left(\sinh \alpha + \frac{1}{\alpha} \right)$$

$$C_2 = \delta x \alpha$$

$$q = \frac{\delta w \alpha}{\cosh \alpha} \left[\sinh \alpha (1 - \xi) + \frac{1}{\alpha} \cosh \alpha \xi \right]$$

$$M_{1x} = \frac{\varepsilon_1}{\varepsilon_1 + \varepsilon_2} \frac{w (1-\xi)^2 l^2}{2} + \frac{l^2}{\alpha^2} \left(\delta w + C_1 \cosh \alpha \xi + C_2 \sinh \alpha \xi \right)$$

$$Q_{1x} = \frac{\varepsilon_1}{\varepsilon_1 + \varepsilon_2} w (1 - \xi) l - \frac{l}{\alpha} \left(C_1 \sinh \alpha \xi + C_2 \cosh \alpha \xi \right)$$

In den Fig. 3 und 4 sind der Verlauf der Momente und Querkräfte für einen der Praxis entnommenen Fall angegeben.

Es sei

$$1/E_0 J_0 = 1/E_1 J_1 = 1/E_2 J_2 = 1,4 \cdot 10^{-8} \quad [t, m]$$

$$\text{ALSO } \varepsilon_1 = \varepsilon_2 = 1$$

und $\beta_1 = 40 \left(\frac{m}{l} \right)^2$, $\beta_2 = 1000 \left(\frac{m}{l} \right)^2$ entsprechend einer Betonwand von 11,3 m Breite und 25 cm Dicke, bzw. einem Fachwerkträger von 12m Breite und starken, für die Deckenbelastungen bemessenen Gurten und schwachen, nur der Winbelastung entsprechenden Diagonalen. Hieraus ergibt sich α zu

$$\alpha = \frac{l}{22,8} \quad [m]$$

Um den Einfluss verschiedener Schlankheiten zu zeigen, sind die Ergebnisse für $\alpha = 1,2,3,8,\infty$, also für Höhen l=22,8,45,4, 91,2 bzw. 182,4 m berechnet. Je grösser die Höhe, umso geringer wird der verhältnissmässige Einfluss der Schubverformung. Der Fall $\alpha = \infty$ entspricht einem Trägerpaar mit ähnlichen Biegeli-

nien. Der Wert δ ist in allen Fallen $\delta = -0{,}462$. Die in Fig.3 bzw. 4 mit vollen linien eingetragenen Werte von M bzw. Q entsprechen der genaueren Berechnung.

Verteilt man die Belastung W in erster Annäherung gemäss den Biegesteifigkeiten, entpräche dies hier einer gleichen Belastung beider Träger. Bei etwas genauerer Berechnung wird die Belastung in umgekehrtem Verhältnis der Durchbiegungen mit Einrechnung der Verformungen durch Querkräfte verteilt. Wir erhalten dann die gestrichelt eingezeichneten Werte. Auch hier sind die Unterschiede zu den Werten der genauen Berechnung noch verhältnismässig gross wie anschaulich die schraffierten Flächen für $\alpha = 4$, also für einen Bau von 91 m Höhe zeigen. Der schubsteife Betonkern übernimmt an der Einspannstelle fast die gesamte Querkraft. Die Unterschiede in der Verteilung der Momente ist zwar geringer, aber doch beachtenswert und zeigt, dass eine genauere Rechnung notwendig ist.

Es sei hier noch an den in /1/ und /2/ genauer beschriebenen Fall der Berechnung der Fahrbahnkonstruktion der grossen Bogenbrücke über die Moldau bei Ždákov erinnert. Zur Erhöhung der seitlichen Stabilität des 330 m weit gespannten Stahlbogens /Fig. 5/ wurden die Fahrbahntafel als Durchlaufträger auf 5 Stützen ausgeführt und übernimmt so einen Grossteil der Windbelastung quer zur Brückenachse. Ursprünglich war geplant, den Fahrbahnrost aus zwei Fahrbahnhauptträgern mit horizontalem Fachwerkwindverband

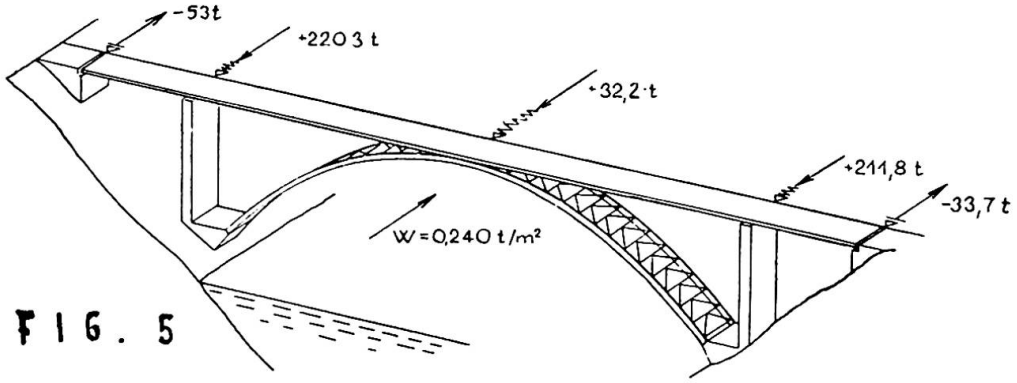

FIG. 5

und einer Betonplatte nur in Verbund mit den Querträgern auszuführen. In der Vorberechnung wurde die Belastung im umgekehrten Verhältnis der Durchbiegungen in Brückenmitte verteilt. Diese sind für eine Belastung 1Mp/m und einen frei aufliegenden Träger von 190 m Spannweite aus Normal- und Querkräften

für die Betontafel $y = 0{,}244 + 0{,}002 = 0{,}246$ m
für die Stahlkonstruktion $y = 0{,}254 + 0{,}045 = 0{,}299$ m

Die sich daraus ergebenden Momente und Querkräfte sind in Fig. 6 und 7 mit /B/ und /ST/ bezeichnet und gestrichelt eingetragen. Die genauere Berechnung, deren Ergebnis in Fig.6 und 7 mit B und ST bezeichnet und mit vollen Linien eingetragen ist, ergab, dass in der Nähe der Auflagerraktionen die schubsteife Betonplatte fast die gesamten Querkräfte und einen Grossteil der Momente übernehmen müsste. Es wurde daher die Betonplatte auch in Verbund mit den Fahrbahnhauptträgern ausgeführt und der Fachwerk-

windverband weggelassen. Es entstand also ein Verbundträger von 541 m Länge mit einer durchlaufenden Betonplatte mit den stählernen Fahrbahnhauptträgern als Gurten, welcher eine eindeutige Übertragung der Momente und Querkräfte sicherstellt.

Literatur: /1/ Faltus,Schindler:Der Einfluss der Schubverformung biegesteifer Träger. Acta Technica ČSAV 1963, Seite 27-62.

/2/ Faltus,Zeman: Die Bogenbrücke über die Moldau bei Ždákov. Der Stahlbau 1968. Seite 332-339.

Zusammenfassung:

Es wird die genauere Berechnung des Zusammenwirkens zweier Träger mit über die Länge konstanten Querschnitten angegeben und an zwei Beispielen der Fehler gezeigt, zu welchem die Vernachlässigung der Schubverformungen führen kann.

Bracing System Composed of High-Strength Steel Bars as Adopted in Aseismic Design of a High-Rise Building

Système de raidissement composé de barres de haute résistance adoptées pour un immeuble de plusieurs étages soumis aux séismes

Aussteifungssystem aus Stahlstäben hoher Festigkeit, wie es beim Entwurf erdbebengeschützter hoher Gebäude angewendet wird

KAZUO WAKABAYASHI
Struc. Engr.

MASAYOSHI KAWAMURA
Eng. D., Struc. Engr.

Nikken Sekkei Ltd
Japan

SHIZUO BAN
Eng. D., Prof. Emeritus
Kyoto University

MINORU YAMADA
Eng. D., Prof.
Kobe University

Japan

1. Introduction

The bracing system as a structural element can increase the rigidity of a building and enables it to resist effectively against overturning moment more economically than if the genuine rigid frame is used. The conventional bracing system usually insures satisfactory results as far as wind resistance is concerned. It, however, often turns out to be unsuitable for the aseismic design of a building because the rigidity usually becomes too high and inadequately distributed if such a bracing system is used. Consequently, it ends up in a structure subject to large shear forces and liable to unsatisfactory earthquake responses. This means that the merits of the bracing system needs to be evaluated quite differently depending on whether the design must be wind-resistant only or aseismic as well as wind-resistant.

This report deals with a case wherein the bracing system composed of high strength steel bars was assessed through the tests and the computations on braced frame units in an attempt to find a structural system which could provide a sufficient strength without adversely increasing rigidity. The bracing system as described above was adopted actually for the 26-storeyed KTC Building (the Kobe Commerce, Industry and Trade Center Building in Kobe, Japan).

2. Bracing System with High-Strength Steel Bars

For the section design of the members of high-rise building subject to lateral forces (wind load and seismic excitation), it is a general practice to determine the sections on the basis of elastic theory for the loads that occur frequently, and on the basis of elasto-plastic theory for the loads that occur less frequently.

Because the bracing system increases the rigidity of a building particularly in lower storeys and the braces themselves have large share in shear rigidity, the lateral force is concentrated in the brace system, thereby causing large stress in bracing. Thus, if mild steel with ordinary strength is used for such braces, the existing stress in the braces is likely to reach the yield point readily by the external force which may occur rather frequetnly, Consequently, the structure might retain a residual deflection even after external force is removed. This phenomenon is not desirable because it virtually lowers

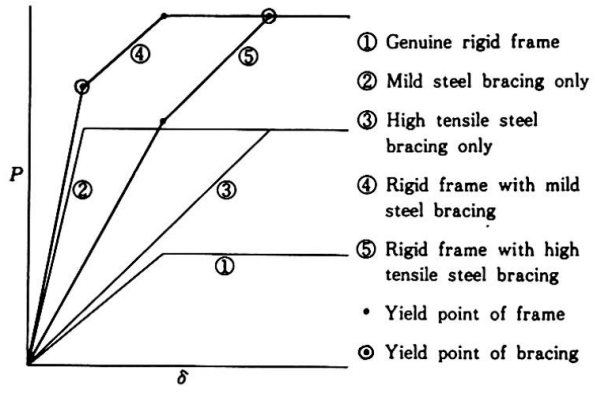

Fig. 1 Idealized expression of bracing system

the initial rigidity of building. Moreover, large axial forces will be concentrated on the braced end columns under lateral load. The foregoing disadvantage can be greatly eliminated if high strength steel bars are used for those braces because the use of such bars gives the structure a wider elastic range without pronounced increase of the rigidity. Fig.1 represents idealized expression of the structural phenomena described above. Thus, such a bracing system insures a structural system with adequate rigidity distribution which results in more satisfactory earthquake responses.

The KTC Building is featured by a structural system as shown in Figs. 2 and 3. Its main framework is composed of a core made up of frames braced with high strength steel bars and of perimeter frames which are in the form of a genuine rigid frame. The sharing and distribution of shear forces among these and other frames during an earthquake are indicated in Fig. 4. A structure well balanced under both wind load and seismic excitation was made possible by a brace system consisting of high strength steel bars (27 - 32 mm in diam., upset and threaded at both ends).

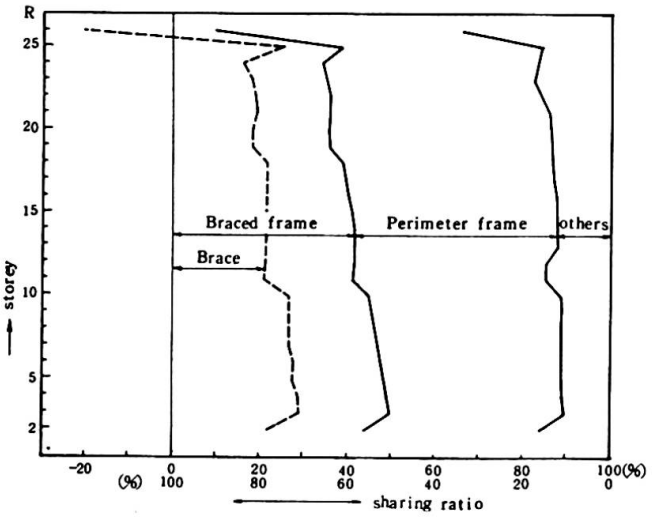

Fig. 4 Seismic load sharing

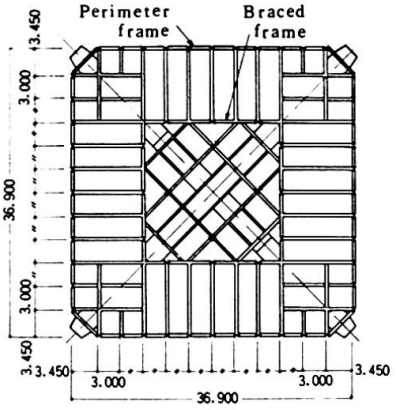

Fig. 2 Beam plan

3. Experiments

3.1 Test Specimens

Two types of specimens were prepared. F-2 was a 2-storeyed single-bay braced frame and F-1 was a non-braced rigid frame for comparison, both reduced to 1/2 of the actual structure in scale. The columns and beams of the specimens were designed to have the section modulus (Z) approximately equal to 1/8 of that of the actual members except for the intermediate beam which, in consideration of the influence of adjoining members, was designed to have a Z-value approximately equal to 1/4 of the actual

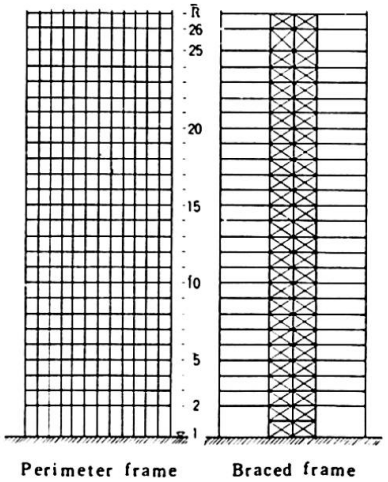

Fig. 3 Structural system

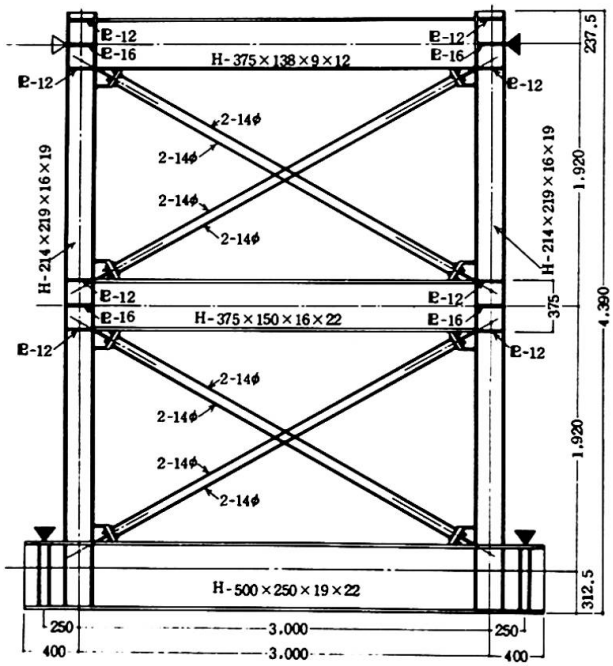

Fig. 5 Test specimen F-2

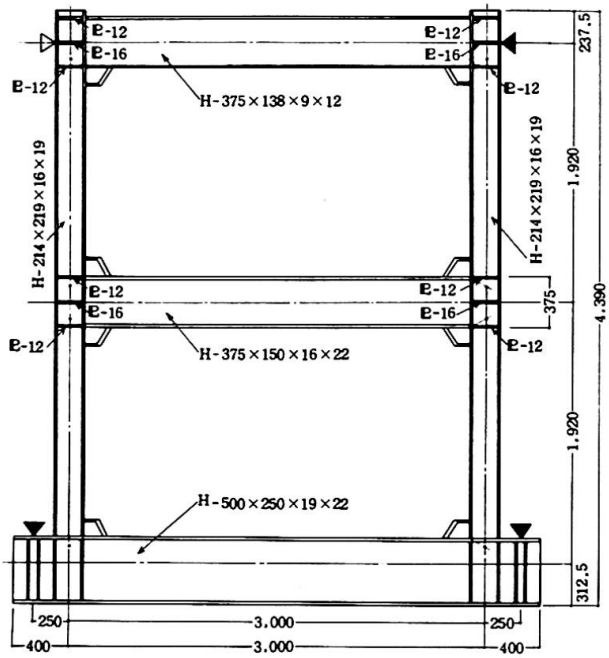

Fig. 6 Test specimen F-1

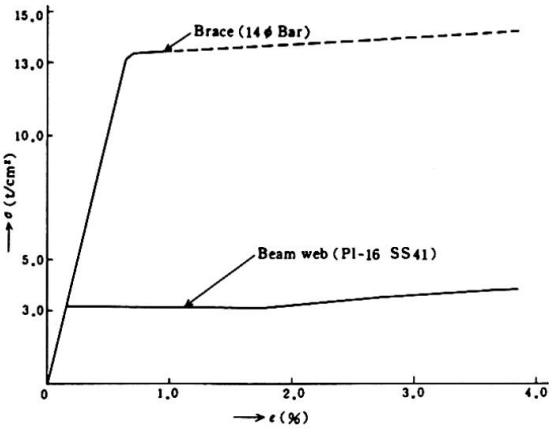

Fig. 7 $\sigma - \varepsilon$ relationship

Table 1 Materials

PL-thickness	Member	Quality	Yield point (t/cm²)	Tensile strength (t/cm²)	Elongation (%)
PL- 9	Beam web	SS41	3.56	4.70	31.3
PL-12	Beam flange	SS41	2.78	4.28	31.3
PL-16	Beam web	SS41	3.17	4.32	31.0
PL-22	Beam flange	SS41	2.84	4.65	31.0
PL-16	Column web	SM50A	3.74	5.39	29.3
PL-19	Column flange	SM50A	3.88	5.37	31.0
14φ	Brace	Gr.4	12.8	13.6	7.5

member. The sectional area of bracing bars was about 1/4 of the actual area. The qualities and mechanical properties of steels used are shown in Fig.7 and Table 1.

3.2 Results of the Experiments

The results of the experiments are shown in Figs. 8 through 11 by the solid lines. Figs. 8 and 9 show the load-deflection relationships at the top of columns in upper and lower storeys of F-2 and F-1 specimens respectively. Figs. 10 and 11 show the load-curvature relationships calculated from the strains measured with wire strain gauges at the top and bottom of the cross section (marked by o) of column and beams of specimens F-2 and F-1 respectively. The photos show the specimen F-2 in final state after the test.

3.3 Analyses

The stress and deformation analyses of frames were made by the "plastic hinge method". The relationship between bending moment (M) and curvature (ϕ) in each member was assumed to be purely elasto-plastic as shown in Fig. 12. Then, the elastic analyses were made of the deformation which took place between the

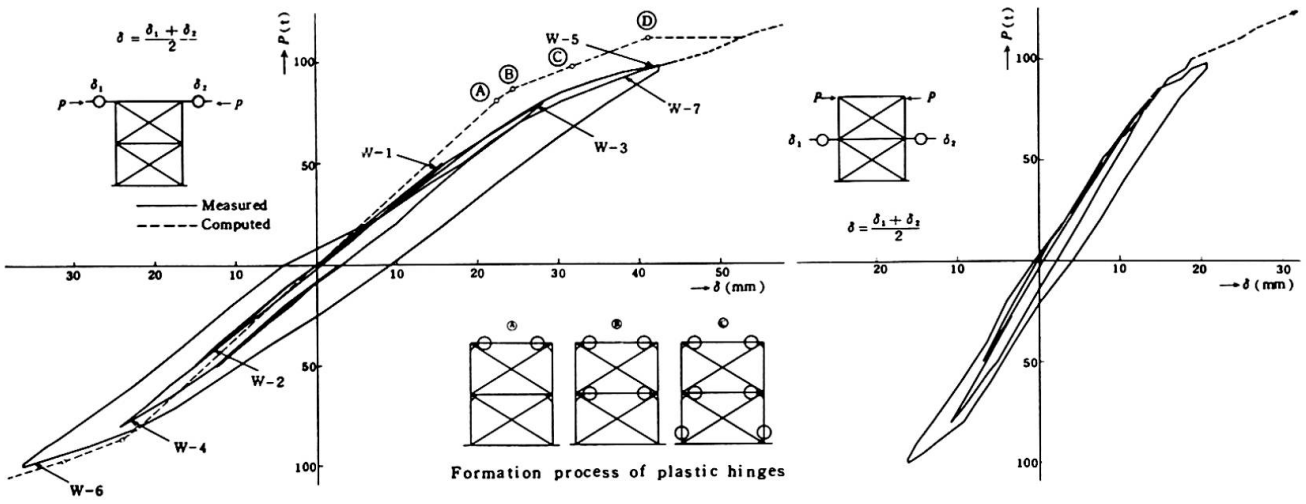

Fig. 8 Load - deflection relationships F - 2

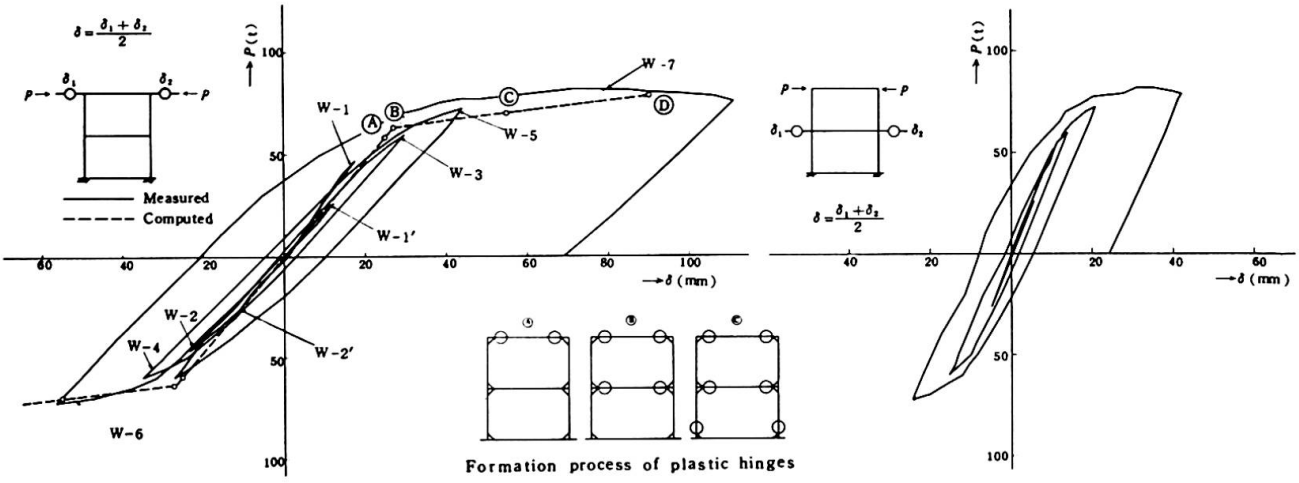

Fig. 9 Load - deflection relationships F - 1

stage where a certain plastic hinge was formed and the next stage where another plastic hinge was formed. The results of analyses are shown by a dotted line in Figs. 8 and 9.

The assumptions used in analyses were as follows:

(1) The sections of end portions of columns and beams were calculated inclusive of the gusset portions.
(2) Bending, shearing and axial deformation was considered for the calculation of columns and beams.
(3) Shearing deformation in the joint panels was considered.
(4) Braces were assumed as pinned at both ends, taking the eccentricity from the panel center into account.
(5) The eccentricity was dealt with by extending rigid arms from the column-beam intersections in line diagram.

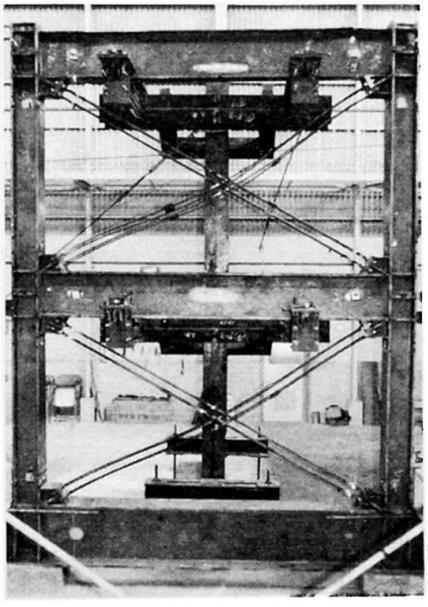

Final state of specimen F - 2 after the test

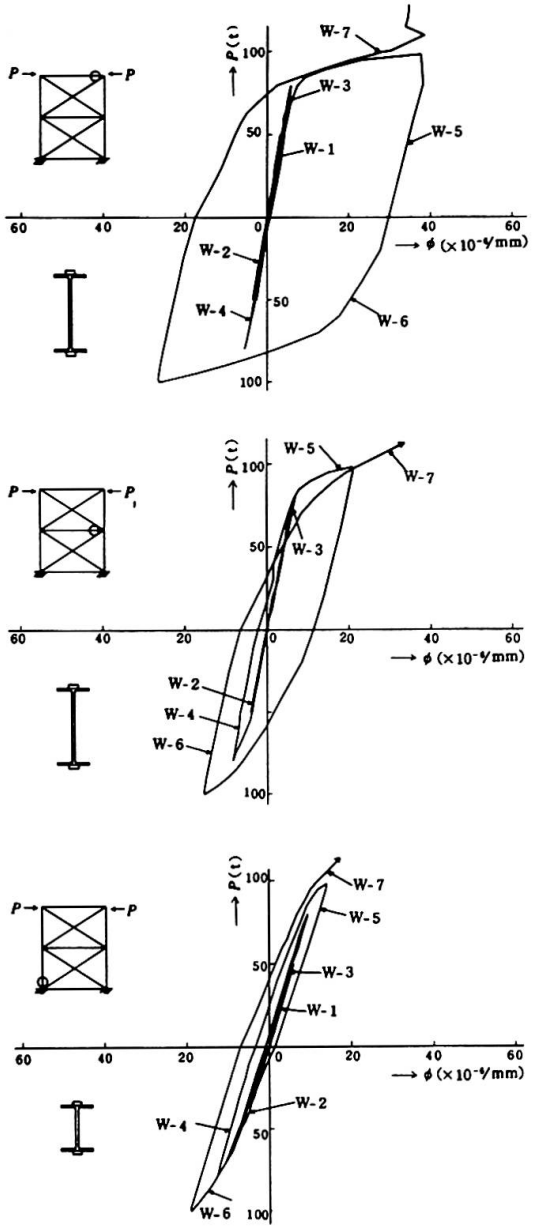

Fig 10 Load - curvature relationships F - 2

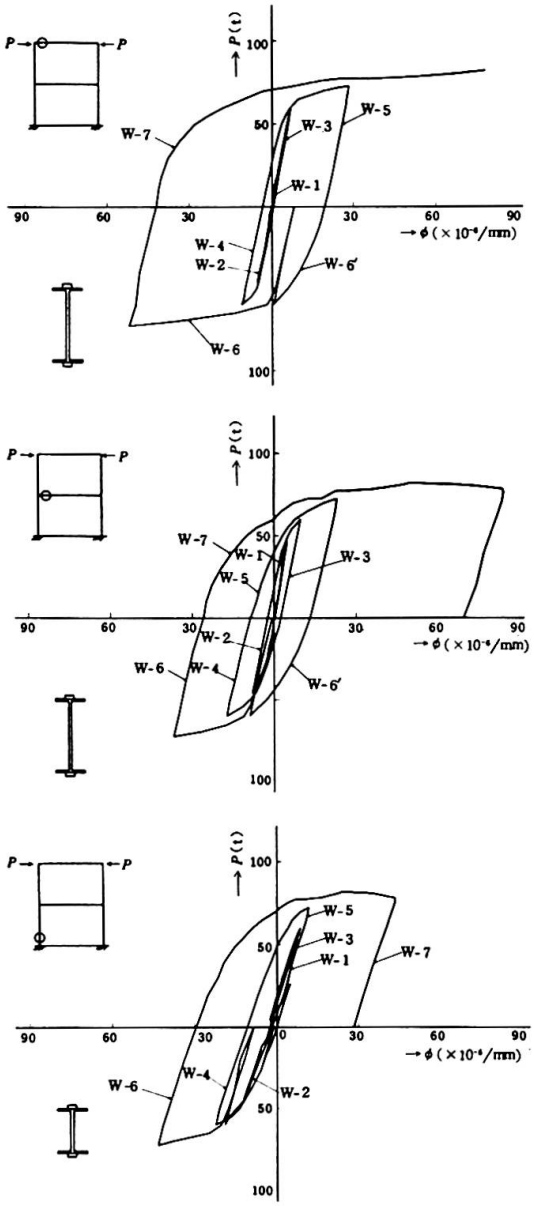

Fig. 11 Load - curvature relationships F - 1

(6) Axial deformation of the braces was considered.

3.4 Discussions

The results of analyses and experiments are in reasonably good agreement with regard to the rigidity, strength and plastic-hinge formation process both in the elastic and the elasto-plastic ranges. As for the load-deformation relationship of the frames, in spite of the occurrence of the local and lateral bucklings at the final stage (see Fgis. 13 and 14), the frames exhibited stabilized behaviors showing increased strength as the deformation progressed until extremely large deformation took place. The reduction of the initial rigidity due to cyclic loading was not noticeable. The high strength steel bar braces were still in elastic range even after a large deformation had occurred in the rigid frame, and the braces as tension bars coped well with the deformation of rigid frame.

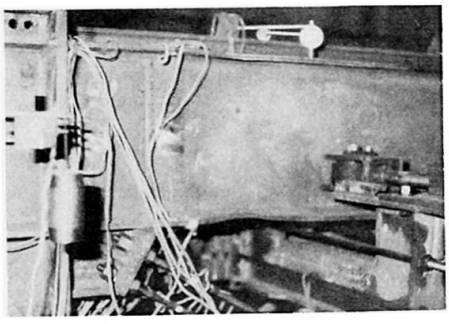

Final state of specimen F−2 after the test

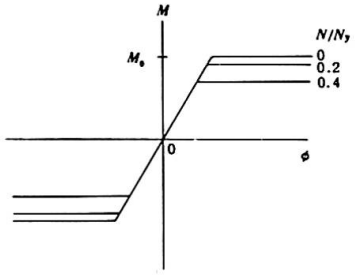

Fig. 12 Assumed M – ϕ relationship

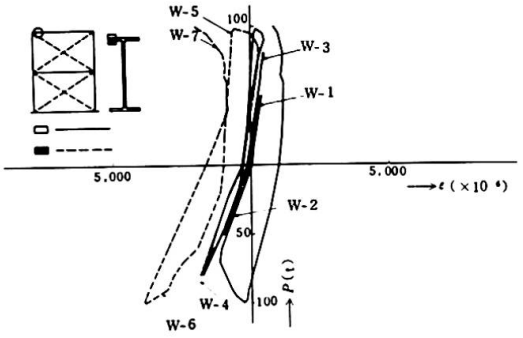

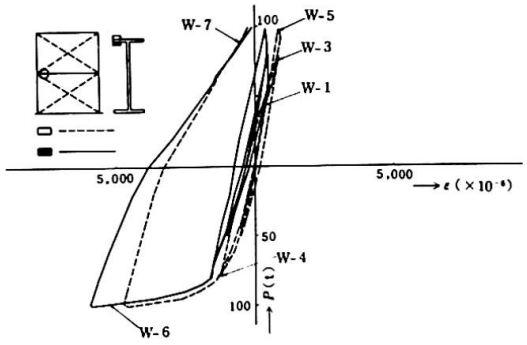

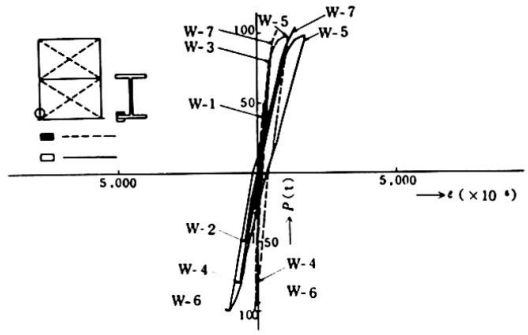

Fig. 13 Load – strain relationships F – 2 (Local buckling)

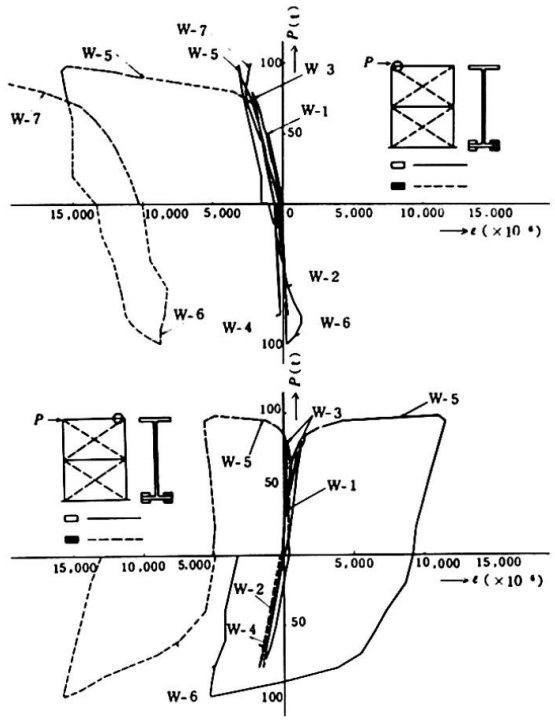

Fig. 14 Load – strain relationships F – 2 (Lateral buckling)

Bibliography

(1) Finzi, L. : Interaction of Different Structural Elements : Introductory Report, 9th Congr. IABSE, Amsterdam 1972, pp. 86-88.

(2) Kawamura, M., Wakabayashi, K., Ban, S., Kobori, T. : Dynamic Design of High-Rise Building subjected to Wind and Seismic Loads : Preliminary Publication, 9th Congr. IABSE, Amsterdam 1972.

(3) Ban, S., Kobori, T., Yamada, M., Kawamura, M., Wakabayashi, K. : Researches on the Structural Design of the KTC Bldg. : Annual Convention of the Architectural Institute of Japan, August 1969, pp. 1105-1118.

Summary

In aseismic design of high-rise buildings, high-strength steel bar bracing contributes to the desired selection of the values of rigidity and their distribution in a building and thus insures satisfactory earthquake responses.

The structural behaviours of such bracing system were studied by the cyclic lateral load tests on 1/2 scale models. From the test results, it was proved that high strength steel bar provides a satisfactory and adequate material for the bracing system of high-rise buildings which must be earthquake-resistant.

Influence of Diaphragms on Behaviour of Box Girders with Deformable Cross Section

Influence d'entretoises sur le comportement de poutres en caisson à section déformable

Einfluss der Querträger auf das Verhalten von Kastenträgern mit deformierbarem Querschnitt

FUJIKAZU SAKAI
Research Engineer
Steel Structure Division
Kawasaki Heavy Industries, Ltd.
Hyogo, Japan

TOSHIE OKUMURA
Professor
Dept. of Civil Engineering
Faculty of Engineering
University of Tokyo
Tokyo, Japan

1. INTRODUCTION

Thin-walled structures, which have recently been applied very often in the field of civil engineering, have got big-sized and complicated remarkably. In designing such structures three-dimensional analyses have been getting essential to harmonize safety with economy. At present, however, we cannot say that the interaction between their structural elements is fully considered in their design.

One of interaction problems is the distortional deformation of box-girders and the influence of diaphragms on it. The conventional theory of thin-walled beams, based on the assumption of non-distortional deformation, cannot be applied to the above problem. Therefore diaphragms are designed from experience rather than on a theoretical basis, and there seems to be no clear specification on their design in any country. 1),2)

The subject of this paper is to analyze theoretically and experimentally the distortional behaviour of box-girders and the interaction between box-girders and diapharagms.

There are two methods in analyzing thin-walled structures. One is the finite element method (F.E.M.), and the other is the folded plate theory.*) In this paper, we modefied Vlasov's folded plate theory and applied it to the analyses of straight box-girders with rectangular and ribbed trapezoidal cross section and curved box-girders. Theoretical results obtained agreed well with experimental ones. We also developed the finite strip method, which is a kind of F.E.M., 10) and compared results from both theories. The comparison shows that there is not so marked difference between both theories with respect to primary stresses and deformations. 11)

2. FUNDAMENTAL EQUATIONS OF A STRAIGHT SINGLE BOX GIRDER 12)

2.1 Assumed displacement functions

We consider a ribbed trapezoidal cross section, as shown in Fig. 1, and assume the followings:

1. The cross section is uniaxially symmetrical.
2. The ribs exist concentratedly on the contour line of the cross section.

---

*) For example, the references 3),4),5),6),7),8) and 9)

3. The shear stresses in the ribs are negligible.
4. Each plate element resists only in-plane forces.*)

Let us the displacements in the axial direction and in the direction tangent to the cross-section contour line as follows (Fig. 2):

$$u(z,s)=\sum_{i=1}^{4}\varphi^{(i)}(s)\,U_i(z) \tag{1-a}$$

$$v(z,s)=\sum_{j=1}^{4}\psi^{(j)}(s)\,V_j(z) \tag{1-b}$$

where $\varphi^{(i)}$ and $\psi^{(j)}$ are generalized coordinates, and U_i and V_j are generalized displacements. If the generalized coordinates are given as shown in Fig. 3 and 4, the generalized displacements represent the following physical meanings:

U_1: Axial displacement — V_1: Twist angle
U_2: Rotation about x axis — V_2: Deflection in x direction
U_3: Rotation about y axis — V_3: Deflection in y direction
U_4: Warping rate — V_4: Distortion rate

In Fig. 3.(d) α_1 and α_2 are determined from the following orthogonal condition:

$$\oint\varphi^{(3)}\varphi^{(4)}dF=0 \tag{2}$$

In Fig. 4.(a) y_S are determined from the following orthogonal condition:

$$\oint\psi^{(1)}\psi^{(3)}tds=0 \tag{3}$$

Similarly β_1 and β_2 in Fig. 4.(d) are obtained from the following assumption that a unit shear flow of pure torsion does not work for the displacement $\psi^{(4)}$:

$$\oint\psi^{(3)}\psi^{(4)}tds=0\quad,\quad\oint\psi^{(4)}1tds=0 \tag{4}$$

where d_W is the length of a perpendicular from the shear center to a web.

2.2 Fundemental equations

Applying the principle of virtual work for the assumed displacements u and v, we obtain the following fundamental equations:

$$EFU_1''+p_1=0 \tag{5}$$
$$EJ_\omega U_2''-GF_w(U_2+V_2')+p_2=0 \tag{6}$$
$$EJ_y U_3''-GF_f(U_3+V_3')+p_3=0 \tag{7}$$
$$EJ_w U_4''-G\{B_{44}U_4-B_{34}(U_3+V_3')-C_{41}V_3'-C_{44}V_4'\}+p_4=0 \tag{8}$$
$$G(C_{41}U_4'+D_{11}V_1''+D_{14}V_4'')+q_1=0 \tag{9}$$
$$GF_w(U_2'+V_2'')+q_2=0 \tag{10}$$
$$G\{F_f(U_3'+V_3'')+B_{34}U_4'\}+q_3=0 \tag{11}$$
$$G(C_{44}U_4'+D_{14}V_1'+D_{44}V_4'')+q_4=0 \tag{12}$$

where E and G are elastic constants, F, I_x, ... and D_{44} are cross-sectional constants, and p_1, p_2, ... and q_4 are generalized loads.

When it is necessary to take into consideration the influence of transverse plate-bending, we must add the term $\oint M_s\rho_s^{(4)}ds$ to the left side of the equation (12), where $\rho_s^{(4)}$ is the curvature due to the displacement $\psi^{(4)}$.

Now for a distortional load shown in Fig. 5,

*) In the case of very a few diaphragms the influence of transverse plate-bending is significant, as mentioned in 2.2.

$$p_1 = p_2 = p_3 = p_4 = q_2 = q_3 = 0 \tag{13}$$

then we have only to deal with the simaltaneous equations (7), (8), (9), (11) and (12).

2.3 Cross-sectional forces

The relation between stresses and displacements is as follows:

$$\sigma_z = E\sum_{i=1}^{4} \varphi^{(i)} U_i' \tag{14-a}$$

$$\tau_{zs} = G\sum_{j=1}^{4} (\psi^{(i)} V_j' + \varphi^{(j)} U_j) \tag{14-b}$$

We define cross-sectional forces as N,Mx,My,B,H,Qx,Qy and Q. Then stresses are related with cross-sectional forces as follows:

$$\sigma_z = \frac{N}{F} + \frac{M_x}{I_x} y + \frac{M_y}{I_y} x + \frac{B}{I_w} \varphi^{(4)} \tag{15-a}$$

$$\tau_{zs} = \frac{D_{44} H - D_{14} Q}{D_{11} D_{44} - D_{14}^2} \psi^{(1)} + \frac{Q_y}{F_w} \psi^{(2)} + \frac{Q_x}{F_f} \psi^{(3)} + \frac{D_{14} H + D_{11} Q}{D_{11} D_{44} - D_{14}^2} \psi^{(4)} \tag{15-b}$$

2.4 Diaphragms

We assume that diaphragms cannot resist forces out of their own planes. Diaphragm stresses, as shown in Fig. 6, are obtained as follows:

$$\tau_h = \frac{Q_d / t_d}{(b_l \beta_1 + b_u \beta_2 + 2h) d_w} \quad , \quad \tau_u = \tau_h \frac{b_l}{h} \quad , \quad \tau_l = \tau_h \frac{b_u}{h} \tag{16}$$

Where Q_d is a distortional reaction from the girder to the diaphragm.

3. THE CASE OF RECTANGULAR(BIAXIALLY SYMMETRICAL) CROSS SECTION 13)

3.1 Fundamental equations and solutions

In the case of biaxially symmetrical cross section, $b_u=b_l=b$ and $t_u=t_l=t$ results in:

$$y_s = 0, \; d_w = b/2, \; \alpha_1 = \alpha_2 = hb/4, \; \beta_1 = \beta_2 = h/b \tag{17}$$

Therefore $B_{34}=0$ and the system of the equations (7) and (11) is independent of the system of the equations (8),(9) and (12) for distortional loads.

When we must take into consideration the influence of transverse plate-bending, the equation (12) becomes as follows:

$$G(C_{44} U_4' + D_{14} V_1' + D_{44} V_4'') - E\left(\frac{8}{b/t_b^3 + h/t_h^3}\right) V_4 + q_4 = 0 \tag{18}$$

The equation system (8), (9) and (18) coincides with the equations which V. Z. Vlasov derived from his closed beam-shell theory.

Numerical calculations were made by using Fourier series and the transfer matrix method. The transfer matrix method is efficient in the cases of variable cross section, deformable diaphragm and complicated boundary condition such as continuous girders. In Table 1 and 2 are shown the field matrix and the point matrix.14)

3.2 Model test

The above-mentioned theory were checked with a model test. The models are three simple-supported box-girders with 6 mm plate thickness, 50 cm x 30 cm cross section and 5 m span length. One and five intermediate diaphragms are placed at two of them, which are called A501 and A505. No intermediate diaphragm is placed at the other, A500.

Fig. 7 and 8 show illustrations of the comparison between the theoretical and experimental results. Fig. 7 shows the displacements in the perpendicular direction due to a distortional load. The fine lines correspond to the c=0 (the equation (12)) and the thick lines correspond to the case c≠0 (the equation (18)). Fig. 8 shows the warping stress and the transverse membrane stress. It can be seen

from both figures that the membrane equations and Vlasov's equations are confirmed by the experiment.

3.3 Considerations on diaphragm designing

There is close relation between spacing and rigidity in diaphragm designing. Spacing and rigidity should not be determined independently, but in this paper we consider these problems separately.

3.3.1 Spacing

We investigate the influence of diaphragm spacing by the following numerical examples under the condition that infinitely rigid diaphragms are placed at a uniform interval:

Cross sections: (1) 1.0 m x 1.0 m, (2) 1.0 m x 1.5 m,
(3) 1.0 m x 2.0 m, (4) 1.0 m x 2.5 m,
(5) 1.0 m x 3.0 m

Span length: l=10 m - 80 m

Numbers of diaphragm: 0 - 10

Fig. 9 shows the relationship between maximum values of warping moment and numbers of diaphragm when the same quantity of uniform distortional load is distributed along each span. It indicates that we can consider two critical points with respect to diaphragm spacing.

1. The number of diaphragms needed so that stresses or displacements do not exceed limited values
2. The number of diaphragms needed so that the membrane equations are valid

3.3.2 Rigidity

We investigate the influence of diaphragm rigidity by a numerical example of box-girder with variable cross section, as shown in Fig. 10. The relationship between maximum values of warping moment and rigidity (thickness) of diaphragms is shown in Fig. 11, which indicates that diaphragms may be considered as infinitely rigid even if they are comparatively thin.

4. THE CASE OF RIBBED TRAPEZOIDAL CROSS SECTION

4.1 Characteristics of trapezoidal box-girders

We investigate the characteristics of trapezoidal box-girders by comparing numerical results of rib-stiffened simple-supported girders with three types of cross section in Fig. 12. The thickness of their webs and bottom flanges is adjusted so that each cross section has the same area and moment of inertia about the x axis.

The results obtained show that as the number of diaphragms increases, warping stresses approach gradually zero and shear stresses approach gradually Bredt's values in each girder, but as a trapezoid of cross section becomes sharp, stresses increase. Diaphragm stresses are shown in Fig. 13, from which it is seen that as a trapezoid of cross section becomes sharp, the stresses become greater if the diaphragms have the same thickness.

4.2 Considerations on diaphragm designing

We investigate the stresses of girder and diaphragm on the basis of numerical results in the case that infinitely rigid diaphragms are placed at a uniform distance on a girder of the cross section shown in Fig. 12.(b). σ_b and τ_B, which are normal stresses due to bending about the x axis and shear stresses due to pure torsion (Bredt's values) respectively, are used in order to compare absolute values of stresses due to the distortional load.

For a uniform distortional load, as shown in Fig. 14, the influence of distortion decreases rapidly as the number of diaphragms increases. For a concentrated distortional load, as shown in Fig. 15 and 16, it depends on load positions. If the load acts at a diaphragm point, the influence of distortion almost vanishes, but if

the load acts away from diaphragm points, comparatively great stresses are produced due to the influence of distortion, although diaphragm spacing is close.

Diaphragm stresses are illustrated in Fig. 17 and 18, They have the same tendency as girder stresses. When the load acts at a diaphragm point, the shear stress of the diaphragm is almost constant regardless of diaphragm spacing,, and almost equal to the value calculated on the assumption that a distortional moment due to the load is resisted only by the diaphragm. This fact indicates that we may estimate shear stresses of diaphragms acted upon by a concentrated distortional load, if they are rigid, on the above assumption. This estimation is on the safety side for deformable diaphragms in practical application.

5. CURVED BOX- GIRDERS

5.1 Fundamental equations

In curved girders F.E.M. is applicable, too. 15),16),6) In this paper we apply fundametal equations of curved box-girder based on the folded plate theory.

In curved box-giders, it is tedious to choose generalized coordinates satisfying orthogonal conditions, as seen in straight box-girders. This is appreciable, for example, from the fact that the neutral axis does not pass through the center of cross section. The influence of initial curvature enforces us to consider three-dimensional displacement functions, because axial strains are produced by the displacement in the radial direction.

Let us assume the displacements in the directions of the coordinate α , s and r (Fig. 19) as follows: 17), 18)

$$\left.\begin{aligned} u(\alpha,s) &= \sum_{i=1}^{4} \varphi^{(i)}(s)\, U_i(\alpha) \\ v(\alpha,s) &= \sum_{i=1}^{4} \psi_v^{(i)}(s)\, V_i(\alpha) \\ w(\alpha,s) &= \sum_{i=1}^{4} \psi_w(s)\, V_i(\alpha) \end{aligned}\right\} \qquad (19)$$

where $\varphi^{(i)}$, $\psi_v^{(j)}$ and $\psi_w^{(j)}$ are generalized coordinates, and U_i and V_j are generalized displacements.

Applying the principle of virtual work for the assumed displacements, we obtain the fundamental equations as follows:

$$\left.\begin{aligned} \sum_{j=1}^{4} EA_{ij}\frac{U_j''}{R_o^2} - \sum_{j=1}^{4}(EB_{ij}^{*}+GB_{ij})\frac{V_j'}{R_o} + \sum_{j=1}^{4} GC_{ij}\,U_j + p_i &= 0 \\ \sum_{j=1}^{4} GD_{ij}\frac{V_j''}{R_o^2} + \sum_{j=1}^{4}(EE_{ij}^{*}+GE_{ij})\frac{U_j'}{R_o} + \sum_{j=1}^{4} EF_{ij}\,V_j + q_i &= 0 \end{aligned}\right\} \quad (i=1,2,3,4) \quad (20\text{—a,b,c,d,e,f,g,h})$$

where A_{ij}, B_{ij}, ... and F_{ij} are cross-sectional constants and p_i and q_i are generalized loads.

When we must take into consideration the influence of transverse plate-bending, the term $\oint M_s \rho_s^{(4)} ds$ is added to the left side of the equation (20-h).

5.2 Model test

We compare theoretical and experimental results by a model test. Model were supported simply. The theoretical results were obtained after consideration of the influence of transverse plate-bending and stretching. The results showed that the influence of transverse plate-stretching is not important to primary stresses and the influence of transverse plate-bending vanishes as the number of diaphragms increases, in the same manner as straight girders.

Fig. 20 shows the deflections due to an eccentric load at the centers of the inner and outer web. The inner loading produces greater deflection for the case of no intermediate diaphragm, while the outer loading produces greater deflection for the case of intermediate diaphragms. Fig. 21 shows the normal stress distri-

bution due to an eccentric load at the 1/4 point of the span. The normal stress for the case of no intermediate diaphragm is twice as great as the one for the case of intermediate diaphragms, and if there is no intermediate diaphragm, distortion affects curved box-girders to the same extent as longitudinal bending.

6. CONCLUSIONS

We come to the following conclusions from the above theoretical and experimental results:

1) The cross-sectional distortion has a great influence on the behaviour of a box girder, when a distortional load acts upon it.

2) The characteristics of a diaphragm for distortional loads are considered as follows:

a) Decrease of stresses and increase of rigidity in a girder
b) Keeping cross-sectional shapes unchangeable
c) Reduction of distortional loads into torsional loads
d) Distinguishing plate membrane actions from plate bending actions
e) Introduction and distribution of loads

3) There are almost the same tendencies in curved box giders as in straight box girders with respect to distortional behaviours and diaphragm characteristics. The inner loading produces more severe condition than the outer loading for a curved box girder with very a few diaphragms.

4) Diaphragm spacing should be determined so that warping stresses are within a limited value, for example 10%, of the maximum bending stress for a uniformly distributed load, providing that it needs to check by calculations for a concentrated load.

5) Diaphragms may be considered as rigid, even if they are comparatively thin. When a usual diaphragm is acted upon by a concentrated load, it is practical to calculate the shear stress on the assumption that it is infinitely rigid.

7. ACKNOWLEDGEMENT

This study is much owing to Mr. Katsuhito Aono in the service of Japan Highway Corporation, who was a graduate student at University of Tokyo. The authors wish to thank him for his cooperation in experiments and calculations.

8. LIST OF REFERENCES

1) "Trends in the Design of Steel Box Girder Bridges", Subcommittee on Box Girder Bridges, ASCE-AASHO Committee on Flexural Members, Proc. ASCE, ST3, June 1967
2) "Progress Report on Steel Box Girder Bridges", Subcommittee on Box Girder Bridges, ASCE-AASHO Committee on Flexural Members, Proc. ASCE, ST4, April 1971
3) Greene, B. E.: "Calculation of Stresses in a Swept Multicell Cantilever Box Beam by the Direct Stiffness Method and Comparison with Test Results", The Boeing Company, Oct. 1960
4) Sanbongi, S.: "Analysis of Box Beams" (in Japanese). Text on the Structural Analysis by Matrix Methods, JSSC, March 1968
5) Cheung, Y. K.: "Analysis of Box Girder Bridges by Finite Strip Method", Paper for the 2nd Int. Sym. on Concrete Bridge Design, Chicago, March 1969
6) Chapman, J. C., Dowling, P. J., Lim, P. T. K. & Billington, C. J.: "The Structural Behaviour of Steel and Concrete Box Girder Bridges", Structural Engineer, No 3, March 1971
7) Vlasov, V. Z.: "Thin-walled Elastic Beams", Publ. for the

National Science Foundation, 1961
8) Nomachi, S.: "On the Flexural-torsion of Thin-walled Rectangular Box-girders with Rigid Diaphragms at a Uniform Interval" (in Japanese), Proc. JSCE, No 146, Oct. 1967
9) Abdel-Samad, S. R., Wright, R. N. & Robinson, A. R.: "Analysis of Box Girders with Diaphragms", Proc. ASCE, STIO, Oct. 1968
10) Okumura, T. & Sakai, F.: "The Relation between Finite Element Methods and the Folded Plate Theory" (in Japamese), Proc. the National Symposium on the Matrix Methods of Structural Analysis, May 1969
11) Okumura, T. & Sakai, F.: "An Approach to Statical Analysis of Threedimensional Structures Consisting of Thin Flat Plates and Its Applications", Trans, JSCE, Vol. 2, Part 1, 1970
12) Okumura, T. & Sakai, F.: "The Fundamental Equations and the Analysis of Diaphragms of Trapezoidal Ribbed Box Girders" (in Japanese), under contribution to Proc. JSCE
13) Okumura, T. & Sakai. F.: "The Cross-sectional Deformation of Box-girders and the Influence of Intermediate Diaphragms", Trans. JSCE. Vol. 2, Part 1, 1971
14) Okumura, T. & Sakai, F.: "Analysis of Box Girders with Deformable Cross Section by the Transfer Matrix Method" (in Japanese), Proc. the National Symposium on the Matrix Methods of Structural Analysis, June 1971
15) Sisodiya, R. G., Cheung, Y. K. & Ghali, A.: "Finite Element Analysis of Skew, Curved Box-girder Bridges", Publ. IABSE, Dec. 1970
16) Sakai, F.: "Statical Behaviour of Three-dimensional Structures consisting of Thin Plates and Shells" (in Japanese), Dr. Eng. Thesis, University of Tokyo, March 1970
17) Aono, K.: "Analysis of Curved Box Girders Considering Cross-sectional Distortion" (in Japanese), M. Eng. Thesis, University of Tokyo, March 1971
18) Sakai, F.: "The Cross-sectional Deformation of Curved Box Girders and the Influence of Diaphragms" (in Japanese), Preprint of the Annual Meeting of JSCE Kansai Branch, May 1971

SUMMARY

The subject of this paper is to analyze the distortional behaviour of box girders and the girder-diaphragm interaction and to investigate the effects of diaphragms. The fundamental equations of straight rib-stiffened trapezoidal box girders and rectangular curved box girders are presented, based on the folded plate theory. The experimental results agree with the theoretical ones and confirm the assumption of the theory. Some investigations are carried out on diaphragm designing, that is, diaphragm rigidity and spacing.

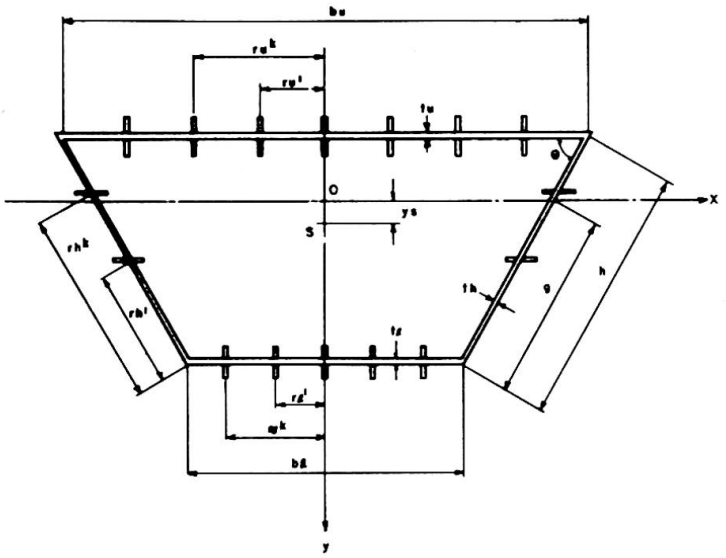

Fig. 1 A Ribbed Trapezoidal Cross Section.

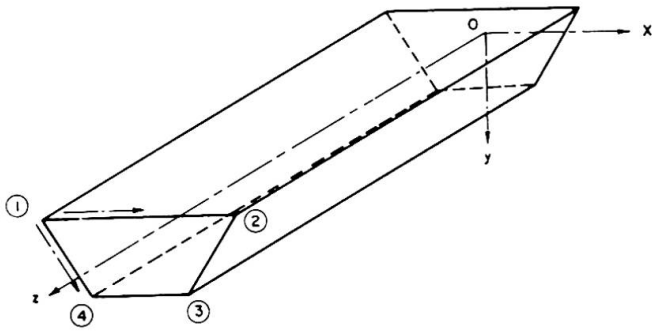

Fig. 2 Coordinates

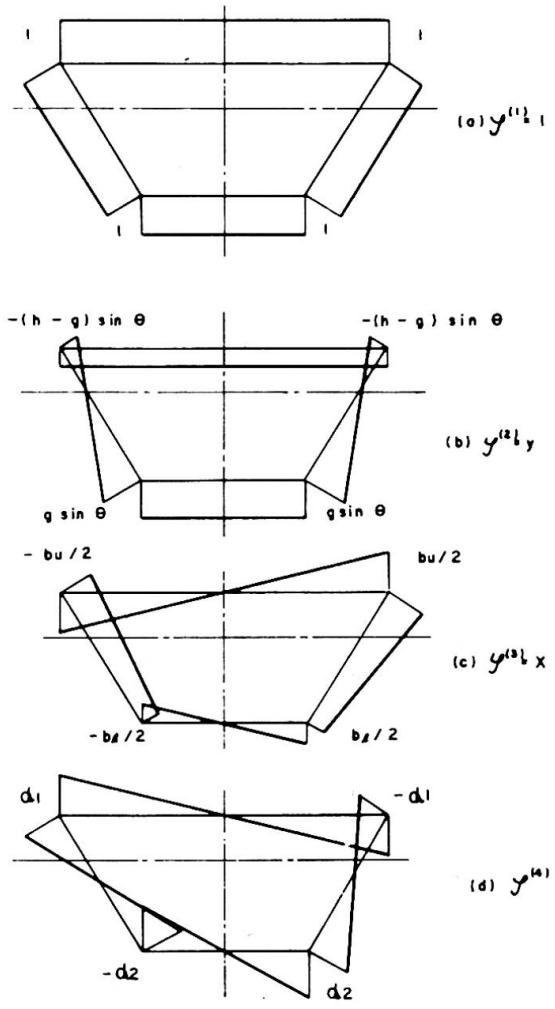

Fig. 3 Generalized Coordinates $\varphi^{(i)}$

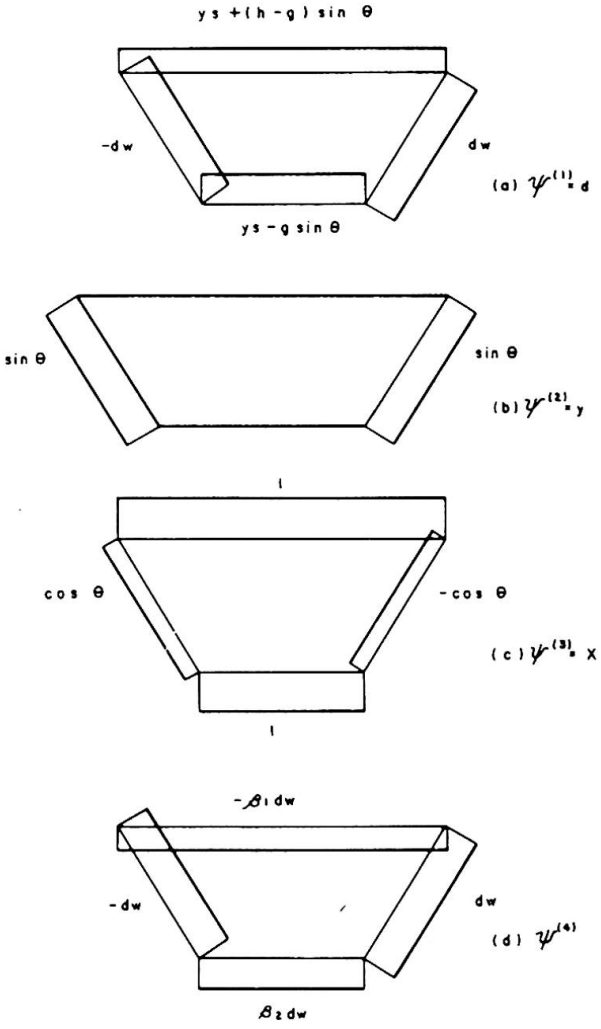

Fig. 4 Generalized Coordinates $\psi^{(i)}$

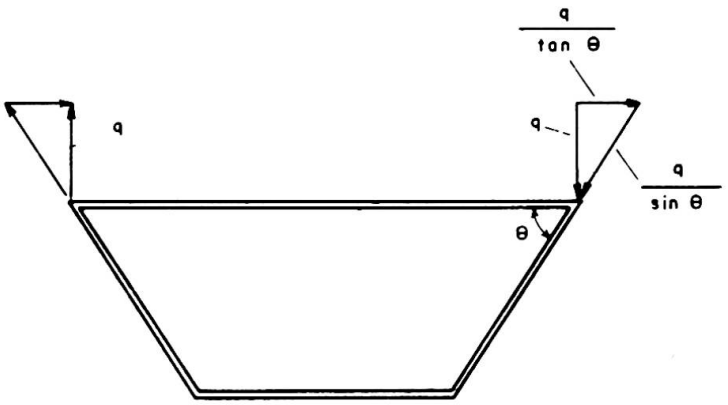

Fig. 5 A Distortional Load

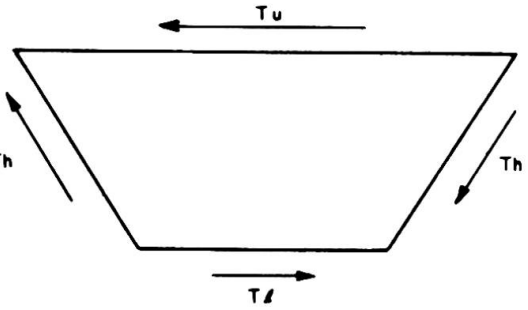

Fig. 6 Diaphragm Shear Stresses

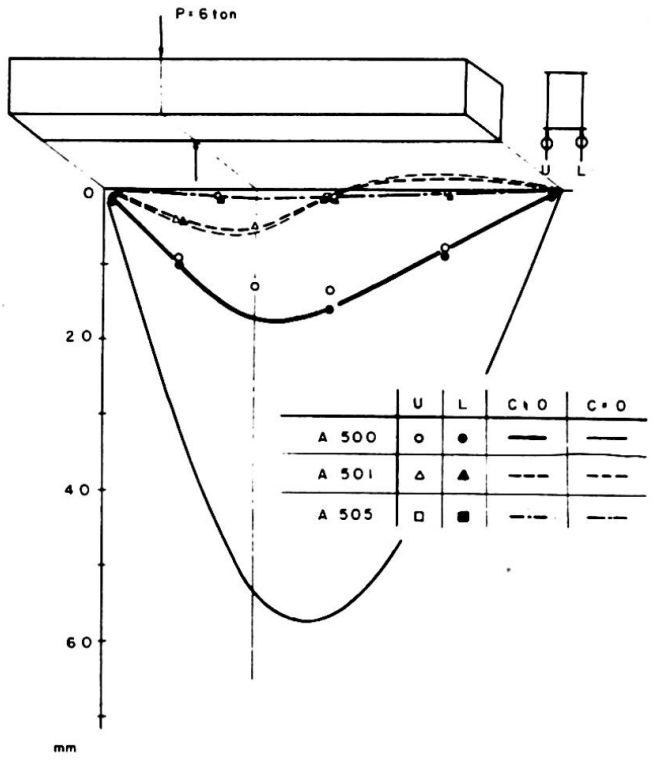

Fig. 7 Comparison of Displacements

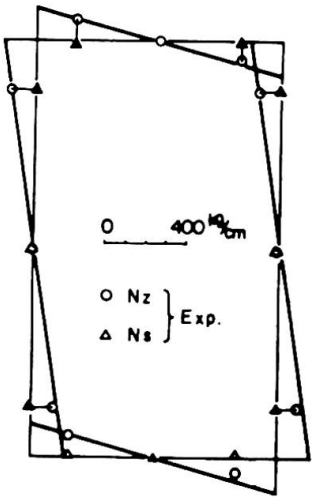

Fig. 8 Warping Stress at the Center

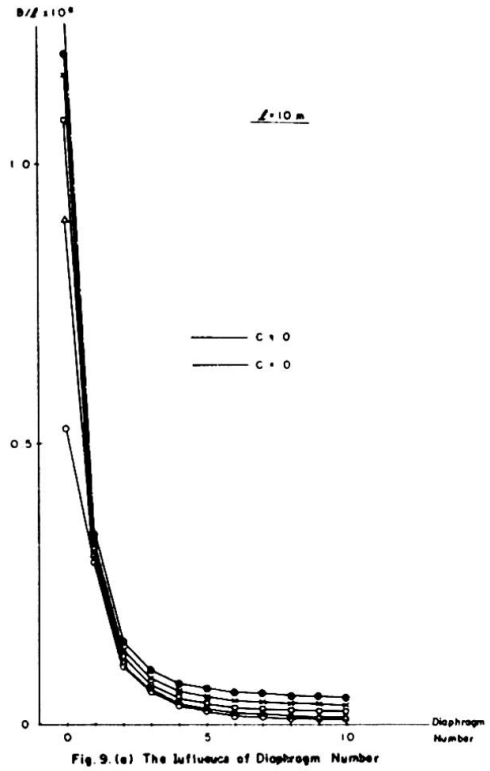

Fig. 9. (a) The Influence of Diaphragm Number

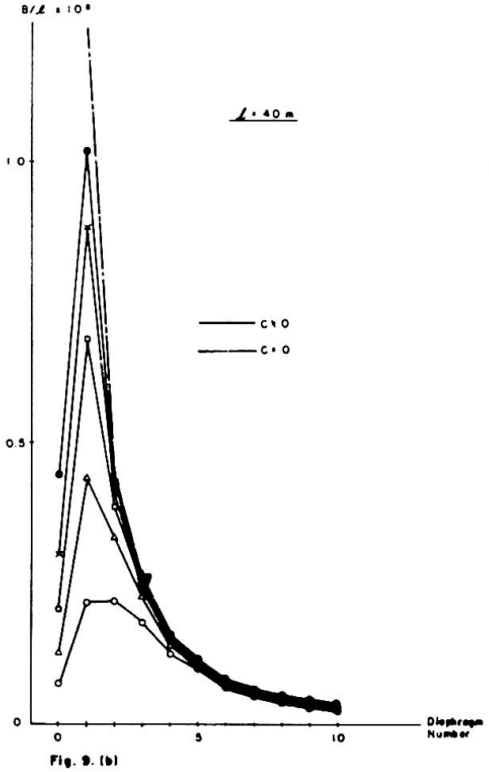

Fig. 9. (b)

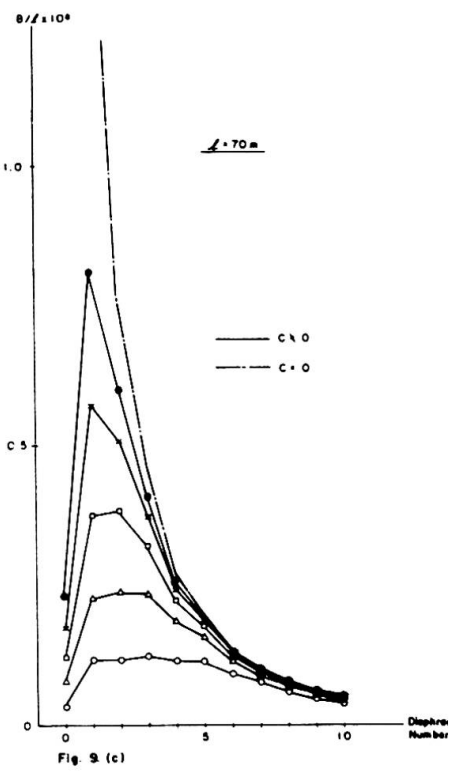

Fig. 9. (c)

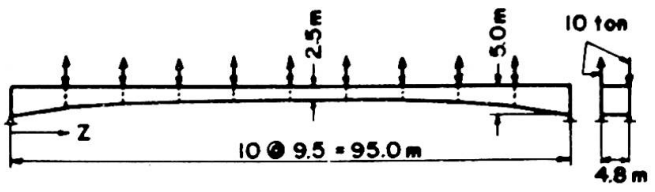

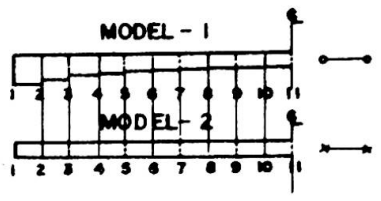

tb = 25 mm
th = 17 mm

Fig. 10 A Numerical Model of Variable Cross Section

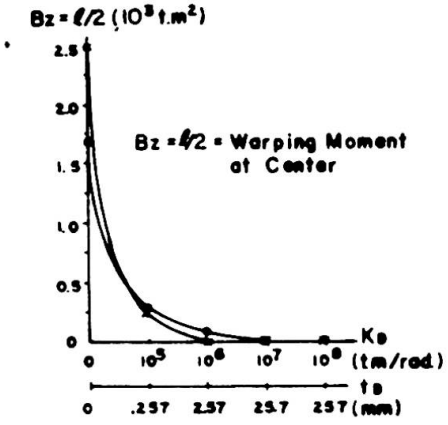

Fig. 11 Influence of Diaphragm Rigidity

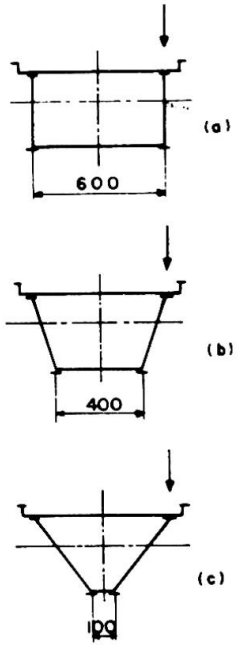

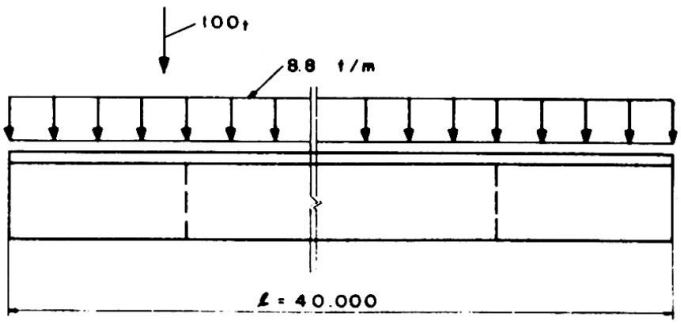

	F (cm^2)	Ix (cm^4)	Iy (cm^4)	Iw (cm^6)
(a)			1.83×10^8	3.72×10^{12}
(b)	$\times 10^4$ 0.360	$\times 10^8$ 0.841	1.39	2.88
(c)			1.01	2.55

Fig. 12 Cross Sections for Comparison

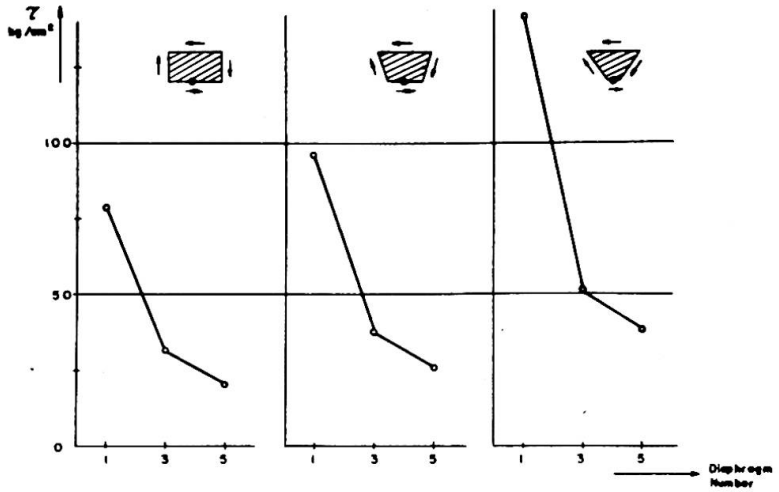

Fig. 13 Maximum Diaphragm Stress (ts = 20 mm)

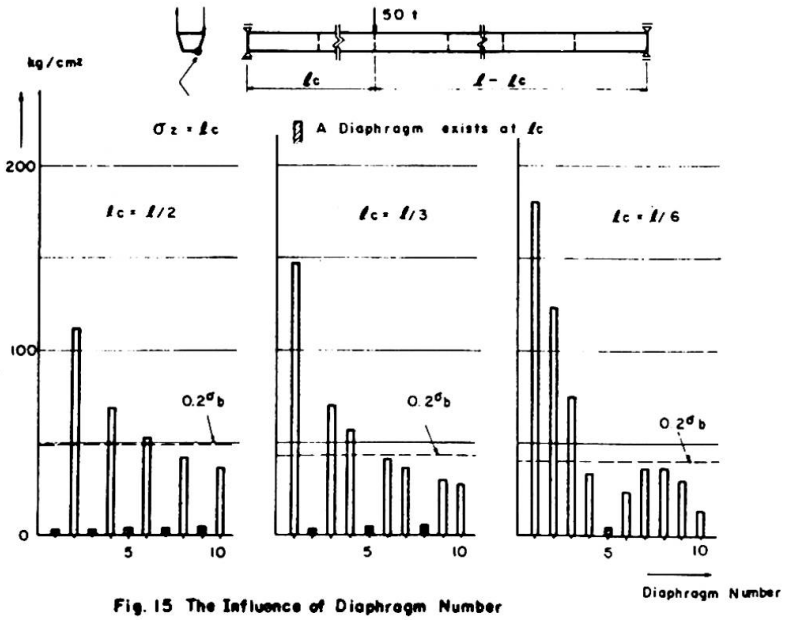

Fig. 15 The Influence of Diaphragm Number

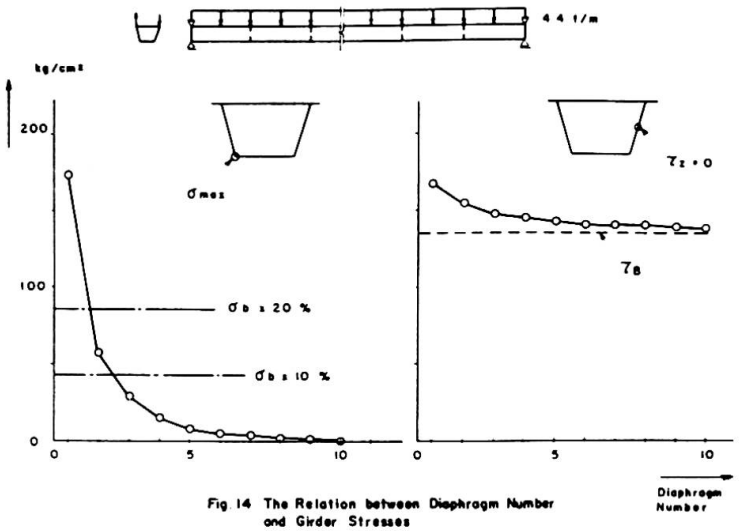

Fig. 14 The Relation between Diaphragm Number and Girder Stresses

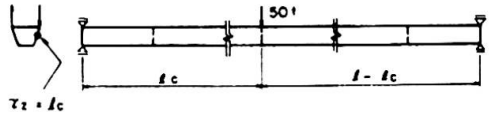

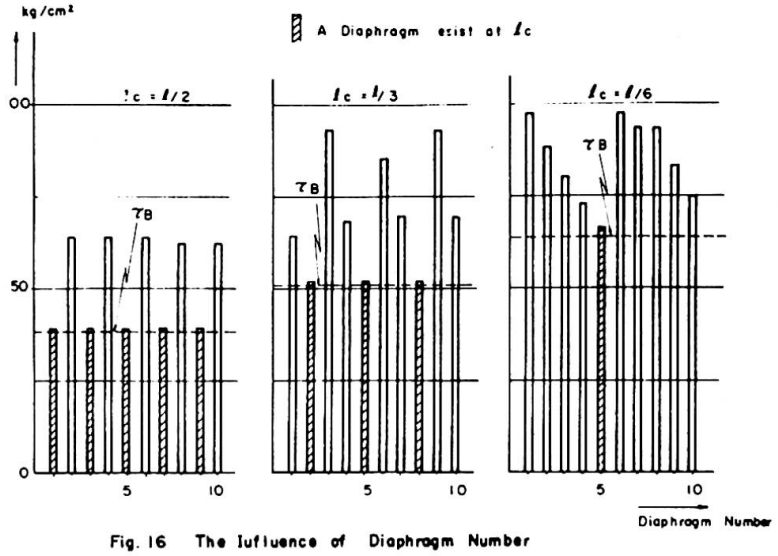

Fig. 16 The Influence of Diaphragm Number

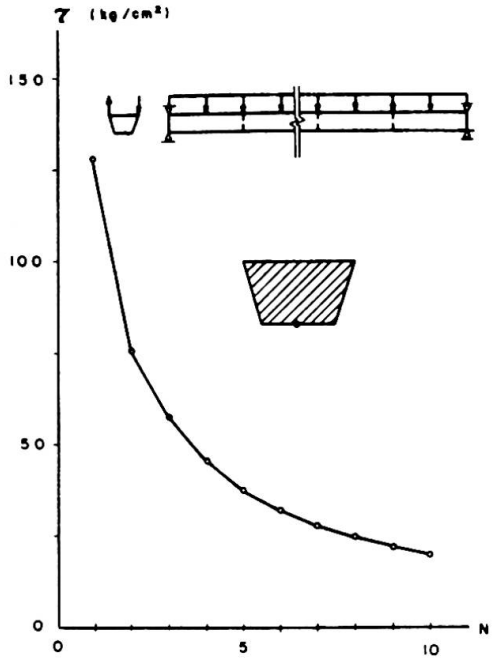

Fig. 17 The Influence of Diaphragm Number on Diaphragm Stress

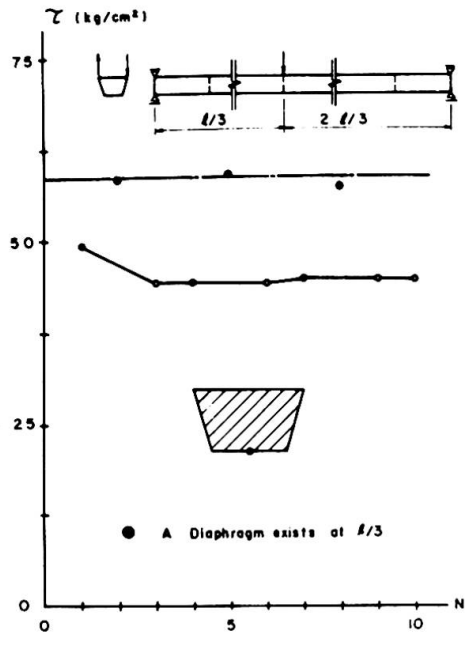

Fig. 18 The Influence of Diaphragm Number on Diaphragm Stress

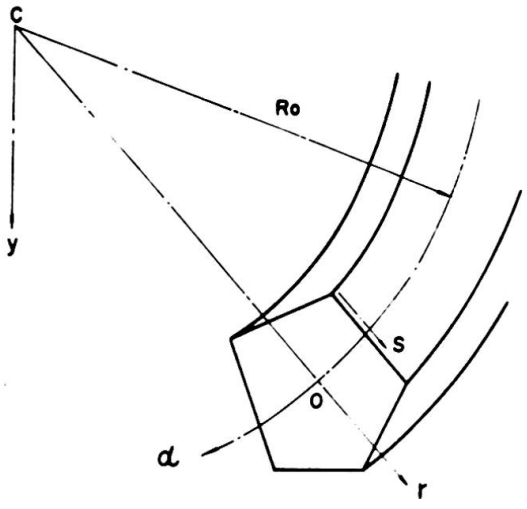

Fig. 19 Coordinates for Curved Box Girders

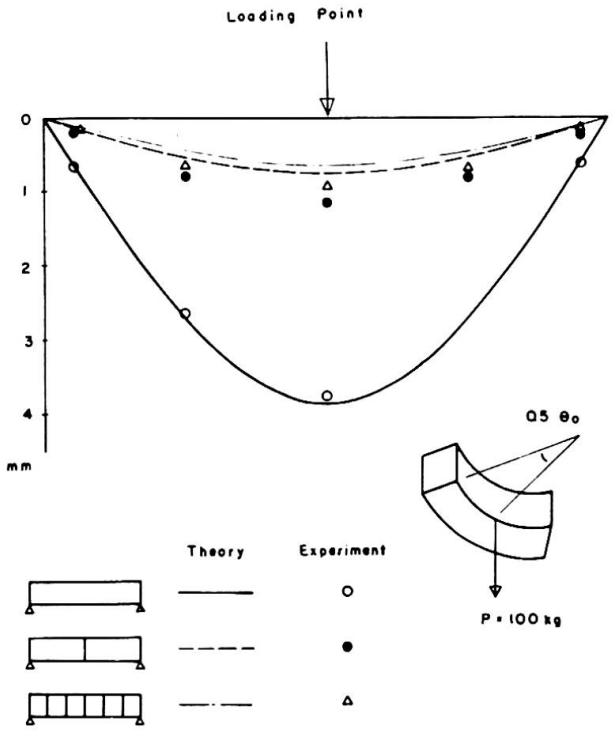

Fig. 20 (a) Deflection by Inner Loading

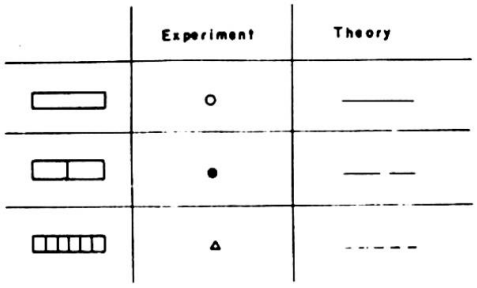

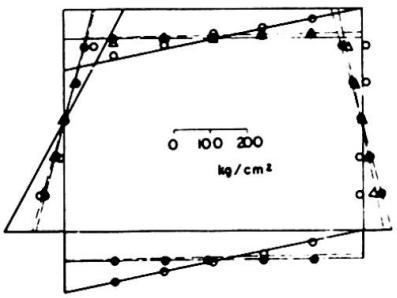

Fig. 21 Warping Stress at 5/12 α_o
(Outer Loading at 1/4 α_o)

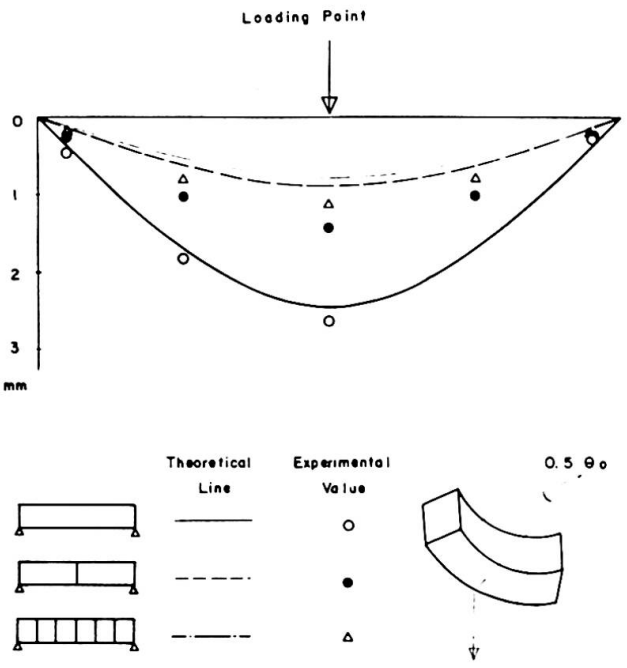

Fig. 20 (b) Deflection by Outer Loading

$$
\begin{bmatrix}
1 & -\ell & 0 & -\gamma_2\ell & \frac{\ell^2}{2a} & \frac{\ell^3}{6a}+\gamma_1\ell & P_X \\
 & 1 & 0 & 0 & -\frac{\ell}{a} & \frac{\ell^2}{2a} & P_U \\
 & & 1 & \gamma_1\ell & 0 & \gamma_2\ell & P_B \\
 & & & 1 & 0 & 0 & P_H \\
 & 0 & & & 1 & -\ell & P_B \\
 & & & & & 1 & P_Q \\
 & & & & & & 1
\end{bmatrix}
$$

$$
1 = \frac{b_1}{b_1^2 - b_2^2} \quad , \quad 2 = \frac{b_2}{b_1^2 - b_2^2}
$$

Table 1. Field Matrix

$$
\begin{bmatrix}
1 & 0 & 0 & 0 & 0 & 0 & 0 \\
0 & 1 & 0 & 0 & 0 & 0 & 0 \\
0 & 0 & 1 & 0 & 0 & 0 & 0 \\
0 & 0 & -K_H & 1 & 0 & 0 & H^{(i)} \\
0 & -K_B & 0 & 0 & 1 & 0 & B^{(i)} \\
-K_Q & 0 & 0 & 0 & 0 & 1 & Q^{(i)} \\
0 & 0 & 0 & 0 & 0 & 0 & 1
\end{bmatrix}
$$

Table 2. Point Matrix

Lateral Buckling Strength of Girders with Bracing Systems

Résistance de voilement latéral de poutres raidies

Seitliche Beulsteifigkeit ausgesteifter Träger

YUHSHI FUKUMOTO
Associate Professor

MASAHIRO KUBO
Research Assistant

Department of Civil Engineering
Nagoya University
Nagoya, Japan

INTRODUCTION

The girder-bracing structural systems which consist of two or more parallel main girders and lateral and/or sway bracings between them are commonly used in steel girder bridges. The characteristics required of the bracing systems are to counteract lateral buckling of the girders and to give adequate bracing in order to provide the required lateral support condition at the bracing points.

The load carrying capacity of braced beams and the bracing requirements for the plastically designed beams are investigated extensively at Lehigh University[1), 2), 3)]. Elastic lateral buckling of beams with lateral restraint at the intermediate supports are treated in Refs. 4)-8) as the bifurcation problem and in Refs. 9),10),11) including the initial imperfections. Diaphragm-braced columns and beams are studied extensively at Cornell University[12), 13), 14)] and their studies are cited by Professor Finzi in his Introductory Report[15)].

In this paper the lateral buckling strength of two parallel girders with bracing system between them is solved in bending and the bracing effects on the buckling strength of main girders are discussed using stiffness parameters in the bracings. The optimum relative stiffnesses of the bracings which provide full bracing to girders are determined in which full bracing is defined to possess effectiveness to immovable supports in lateral and torsional at the bracing points. Lateral buckling strength of main girders is obtained in the inelastic range with assumed distributions of residual stresses while the bracing remains in elastic.

Tests are also conducted in this study. Total of eleven specimens are tested under uniform bending and the results of critical moments, buckled configurations, effective length, are compared with the theoretical ones. Bracing forces are also measured during test.

THEORETICAL ANALYSIS

Theoretical elastic and inelastic lateral buckling solutions are obtained by considering the total energy in the system as shown in Fig. 1. Girders with constant cross section are either simply supported or clamped at the both ends.

The total potential energy T in the system is

$$T = V + U + B \qquad (1)$$

in which V=the internal strain energy stored in the main girders, U=the potential energy of the external loads, and B=the internal strain energy stored in the bracing system. In the lateral bracing as shown in Fig. 2 the strain energy B[16] is

$$B = \frac{F_a}{2}\sum(\bar{u}_{Ai}-\bar{u}_{Bj})^2 + 2F_m\sum(\beta_{Ai}^2+\beta_{Ai}\beta_{Bj} +\beta_{Bj}^2) + 2F_{\bar{m}}\sum(\bar{u}_{Ai}'^2+\bar{u}_{Ai}'\bar{u}_{Bj}'+\bar{u}_{Bj}'^2) \qquad (2)$$

in which $F_a=E_bA_b\cos^2\theta/L_b$, $F_m=E_bI_{b\xi}\cos^2\theta/L_b$, $F_{\bar{m}}=E_bI_{b\eta}/L_b$, A_b=cross sectional area of one member, $I_{b\xi}$, $I_{b\eta}$ =moments of inertia of one member about ξ and η axes, respectively. η-ζ plane is in the vertical plane including the member ends i and j.

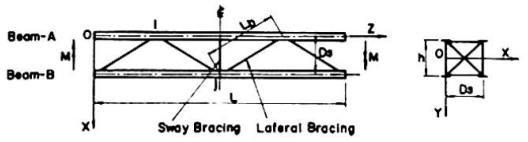

Fig. 1

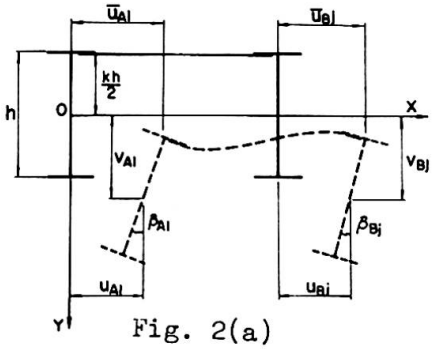
Fig. 2(a)

Horizontal displacement $\bar{u}_{Ai}$ at the bracing point is equated to the displacements u_{Ai} and β_{Ai} about the shear center as,

$$\bar{u}_{Ai} = u_{Ai}-\frac{kh}{2}\beta_{Ai},\quad \bar{u}_{Bj} = u_{Bj}-\frac{kh}{2}\beta_{Bj} \qquad (3)$$

In the sway bracing as shown in Fig. 3 the strain energy B is,

$$B = F_{ad}\sum\beta_i^2 + 12F_{ms}\sum\beta_i^2 + 12F_{\bar{m}s}\sum\bar{u}_i'^2 \qquad (4)$$

in which $F_{ad}=E_bA_bh^2\cos^2\alpha/L_d$, $F_{ms}=E_bI_{b\xi}/L_s$, $F_{\bar{m}s}=E_bI_{b\eta}/L_s$, L_d =length of a strut, and L_s =length of a diagonal member.

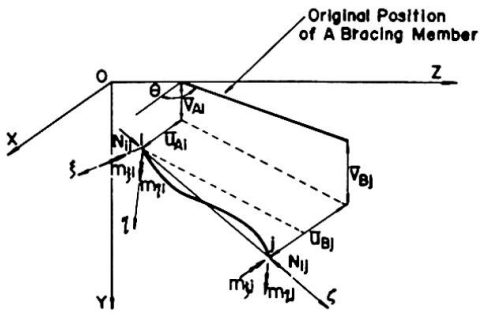

Fig. 2(b)

The critical moment M_{cr} can be obtained by assuming the buckled configurations as trigonometric series which satisfy the boundary conditions at the both ends and solving the characteristic equations of the coefficients which extremize the total potential energy.

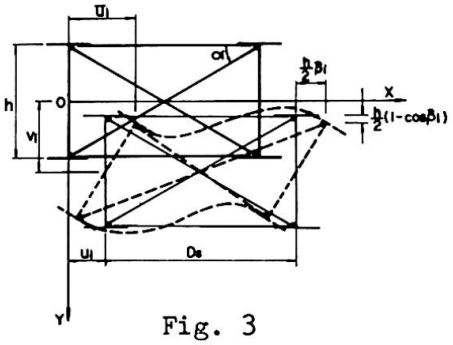
Fig. 3

Fig. 4 shows the elastic and inelastic lateral buckling strength curves for three different residual stress patterns with the maximum compressive stress of $\sigma_{rc}=0.3\sigma_y$[17),18)]. The curves for H-200×100×5.5×8mm beam represent the basic strength curves when unbraced. The following numerical examples are carried out for the same cross section having the residual stress pattern (1).

NUMERICAL EXAMPLES

The authors derived the relationships of the critical moment with the slenderness ratio and the stiffness parameters δ and γ in the bracing system, where δ and γ are defined as follows,

$$\delta = A_b/A_c,\quad \gamma_\xi = I_{b\xi}/I_c,\quad \gamma_\eta = I_{b\eta}/I_c \qquad (5)$$

in which A_b= area of one bracing member

$A_c=A_f+\frac{1}{6}A_w$= area of a compression flange, and web of girder, respectively. I_c =moment of inertia of the compressive area A_c, $I_c \cong I_f=bt^3/12$.

Lateral Bracing : Fig. 5 shows the buckling strength curves with lateral bracing along the compression flange for four different δ and γ values. Bracing deformation is considered in the vertical plane, that is, $\gamma=\gamma_\xi$, and γ_η-effect on the buckling strength is almost negligible compared to γ_ξ-effect. Distance between two parallel girders in this case is D_s=50cm. In this figure fully braced B-curve indicates the buckling strength when beam B is fully supported at the bracing points in order to meet $u_i=\beta_i=0$ and fully braced A-curve is for beam A. The fully braced B-curve is, in this case, practically important for the design purpose. Fig. 6 is another presentation of M_{cr}-L/r_y-δ-γ curves. In this figure horizontal lines M_{cr}/M_y=0.86, 0.76, 0.69 and 0.52 represent the buckling strength for the fully braced B-curve with the specified L/r_y values, respectively. And γ-values which will be read at the intersections of the horizontal and curved lines give the optimum relative stiffness γ_{opt}=0.07,0.13, 0.23 and 0.28, respectively for the specified δ=0.01. Fig. 7 shows the relationship between the buckling strength and the braced point in the web height. k=1, 0, and -1 mean the beam braced at the tension flange,shear center (=centroid in this case) and compression flange, respectively. The bracing effect against the buckling strength is almost the same if the bracing points are in the compression zone of the main girders due to bending.

Sway Bracing : Fig. 8 shows the buckling strength curves with sway bracing at the span center. The curves are bounded by the unbraced and full bracing limits. Since the sway bracing possesses the effectiveness in rotation at the braced section, angle of rotation β_i=0 is only required to meet the full bracing condition.

Effective length : Fig. 9 shows the relations between the unbraced length λ L and the effective length λ_eL which delivers the same critical moment between the simply supported pinned ends. The curves are for full bracing strength in three different

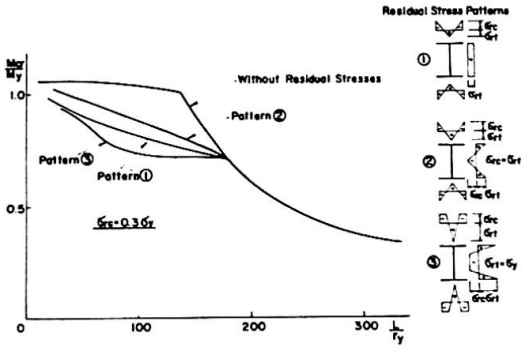

Fig. 4

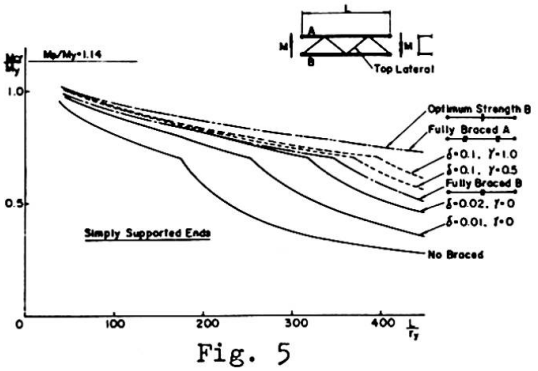

Fig. 5

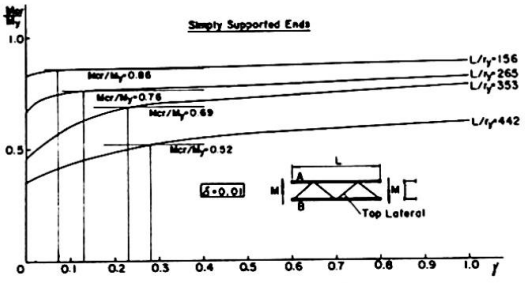

Fig. 6

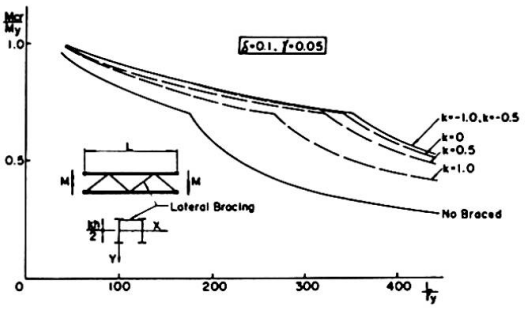

Fig. 7

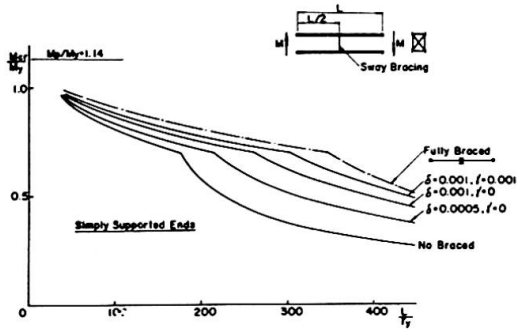

Fig. 8

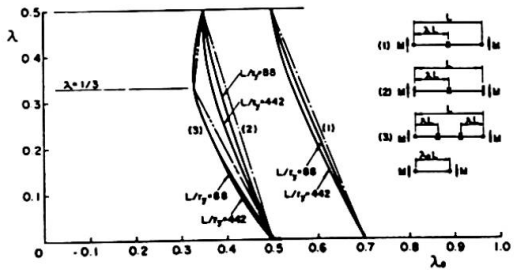

Fig. 9

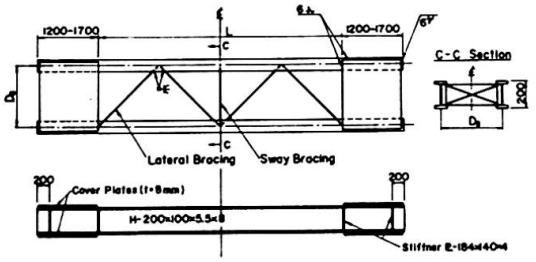

Fig. 10

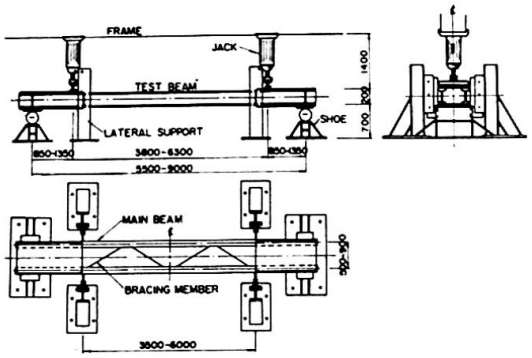

Fig. 11

cases. Theoretical solid lines for L/r_y=88 to 442 may be approximated with sufficient accuracy by chain lines in each case as,

(1) $\lambda_e = -0.4 + 0.7$ for $0 \leq \lambda \leq 0.5$
(2) $\lambda_e = -0.3 + 0.5$ for $0 \leq \lambda \leq 0.5$
(3) $\lambda_e = -0.5 + 0.5$ for $0 \leq \lambda \leq 1/3$
$\lambda_e = 0.1 + 0.3$ for $1/3 \leq \lambda \leq 0.5$

TEST PROGRAM

Test Specimens and Test Setup : Total of eleven specimens are tested in bending under clamped end conditions against lateral buckling. Rolled beams of H-200×100×5.5 ×8mm section are used as main girders throughout and steel round bars are as bracing members. The detailed dimensions of the test specimens are given in Fig. 10 and Table 1, and the test setup is shown in Fig. 11 and Photo 1.

Load-Deformation Curves : A typical example of load-deformation curves is shown in Fig. 12 where M versus u, v and β at span center are plotted for Type B11. From this figure it is observed that u_A and β_A remain unchanged during test and the full bracing condition is, thus, ensured at the bracing point.

Test Results : All of the test results are

Table 1

Specimens	Dimension of Test Beams	Bracing Systems
TYPE A1	H-200 × 100 × 5.5 × 8	Not Braced
TYPE B11		Lateral(D=19mm)
TYPE B12	D_s= 50cm	Lateral(D= 9mm)
TYPE C1	L= 350cm	Sway(D= 9mm)
TYPE D1	L/r_y=158	Lateral(D= 9mm) Sway(D= 9mm)
TYPE E1		Lateral(D=19mm) Sway(D= 9mm)
TYPE F1		Strut(D=19mm)
TYPE A2	H-200 × 100 × 5.5 × 8	Not Braced
TYPE B2		Lateral(D=19mm)
TYPE C2	D_s= 90cm	Sway(D= 9mm)
TYPE D2	L= 600cm	Lateral(D= 9mm) Sway(D= 9mm)
	L/r_y=270	

D : Diameter of Steel bars used for bracing members

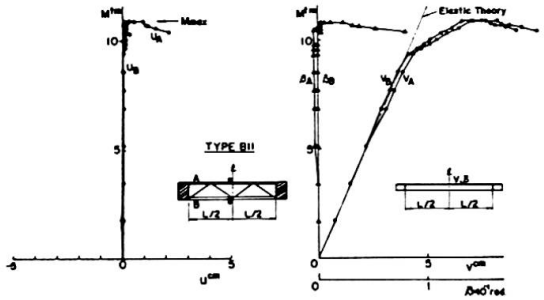

Fig. 12

Table 2

Specimens	L=350cm (L/ry=158), Ds=50cm					Specimens	L=600cm (L/ry=270), Ds=90cm				
	Test		Theory				Test		Theory		
	M_{test} (t-m)	Effect of Bracing	$M_{theo.}$ (t-m)	Effect of Bracing	$\frac{M_{test}}{M_{theo.}}$		M_{test} (t-m)	Effect of Bracing	$M_{theo.}$ (t-m)	Effect of Bracing	$\frac{M_{test}}{M_{theo.}}$
TYPE A1	4.95	1.00	4.83	1.00	1.02	TYPE A2	4.05	1.00	4.23	1.00	0.96
TYPE B11	5.40	1.09	5.27	1.09	1.02	TYPE B21	5.13	1.27	4.87	1.15	1.05
TYPE B12	5.35	1.08	5.26	1.09	1.02	TYPE B22	-	-	4.84	1.14	-
TYPE C1	5.25	1.06	5.06	1.05	1.04	TYPE C2	4.79	1.18	4.51	1.07	1.06
TYPE D1	5.55	1.12	5.27	1.09	1.05	TYPE D2	5.23	1.29	4.87	1.15	1.07
TYPE E1	5.50	1.11	5.27	1.09	1.05	TYPE E2	-	-	4.87	1.15	-
TYPE F1	5.23	1.06	5.06	1.05	1.03	TYPE F2	-	-	4.51	1.07	-

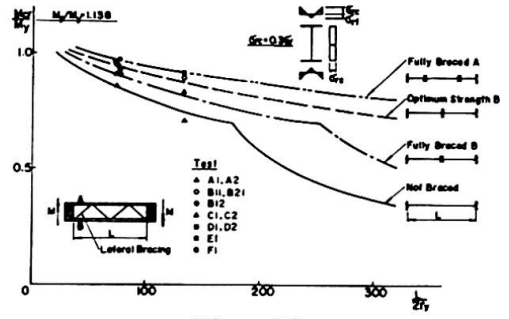

Fig. 13

Table 3

Specimens		F (kg)	F/F_{by}		P (kg)	P/P_f	Remarks
TYPE B11	1	-806	0.089	1	432	0.019	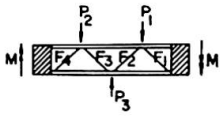
	4	-819	0.091	2	417	0.018	
	2	-80	0.009	3	113	0.005	
	3	-142	0.016				
TYPE B12	1	-565	0.278	1	470	0.021	
	4	-598	0.294	2	296	0.013	
	2	-178	0.088	3	138	0.006	
	3	-74	0.036				
TYPE B21	1	-604	0.067	1	445	0.020	
	4	-666	0.074	2	445	0.020	
	2	-62	0.007	3	50	0.002	
	3	-80	0.009				

plotted in Fig. 13 together with the theoretical buckling curves of unbraced and full bracing beams. Test points for the braced specimens B11-F1 are all above the fully braced B-curve.

A summary of test results is given in Table 2. The bracing effect which is defined by the strength ratio of each braced specimen to the unbraced beam is compared between theory and tests. Since all of the specimens are buckled in the inelastic range, the bracing effect may not be expected as it would be in the elastic range. Photo 2 illustrates several examples of specimens after test showing the buckled patterns of beams with full bracing.

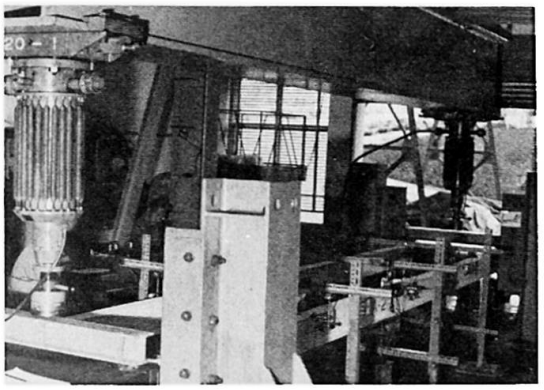

Photo 1

Bracing Forces : Bracing forces such as axial force F_α and bending moments M_ξ and M_η are measured during test. Table 3 summarizes the measured bracing forces F's and the resultant lateral forces P's which are composed of F's at the ultimate load. The maximum value of bracing force P is obtained as 2% of the compressive flange force P_f.

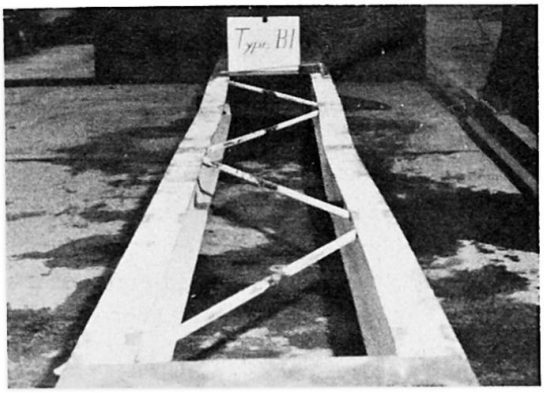

Photo 2(a)

CONCLUDING REMARKS

Followings are the main subjects which are discussed in this paper.
(1) Elastic and inelastic lateral buckling strength of beams with lateral and/or sway

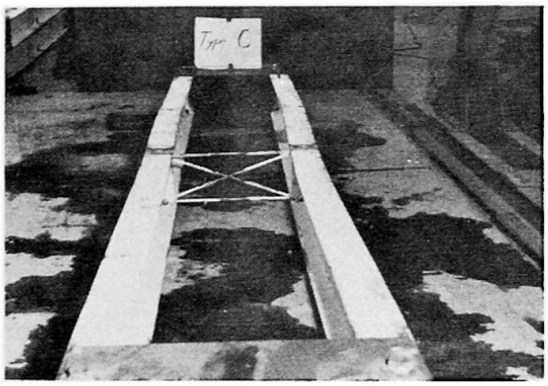

Photo 2(b)

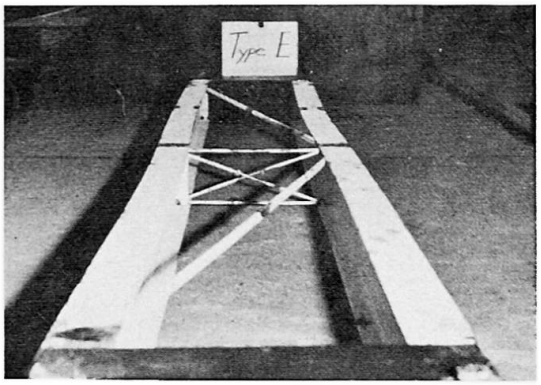

Photo 2(c)

bracings is determined theoretically including an arbitrary distributed residual stresses.
(2) Optimum relative stiffnesses δ and γ in bracing members are defined and the bracing effect of bracing systems are discussed.
(3) Tests are conducted for eleven specimens with different bracing systems and bracing effects are compared with the theoretical results.

REFERENCES

1) Lay, M.G. and Galambos, T.V., Proc. ASCE, Vol. 92, No.ST 2, April, 1966.
2) Lee, G.C. and Galambos, T.V., Proc. ASCE, Vol. 88, No.EM 1, February, 1962.
3) Lee, G.C., Ferrara, A.T. and Galambos, T.V., Bulletin No. 99, Welding Research Council, New York, N.Y., September, 1964.
4) Hartmann, A.J., Proc. ASCE, Vol.93, No.ST 4, August, 1967.
5) Hartmann, A.J., Proc. ASCE, Vol.96, No.ST 7, July, 1970.
6) Klöppel, K. und Unger, B., Der Stahlbau, Heft 7, 1969.
7) Schmidt, L.C., Proc. ASCE, Vol. 91, No.EM 6, December, 1965.
8) Taylor, A.C. and Ojalvo, M., Proc. ASCE, Vol.92, No.ST 2, April, 1966.
9) Massey, C., Proc. ASCE, Vol.88, No.EM 6, December, 1962.
10) Winter, G., Proc. ASCE, Vol.84, No.ST 2, March, 1958.
11) Zuk, W., Proc. ASCE, Vol.82, No.EM 3, July, 1956.
12) Apparao, Errera and Fisher, Proc. ASCE, Vol.95, No.ST 5, May, 1969.
13) Errera, S.J., Pincus, G. and Fisher, G.P., Proc. ASCE, Vol.93, No.ST 1, February, 1967.
14) Pincus, G. and Fisher, G.P., Proc. ASCE, Vol. 92, No.ST 2, April, 1966.
15) Finzi, L., 9th IABSE Congress Introductory Report, Amsterdam, 1972.
16) Fukumoto, Y., Kubo, M., Proc. JSCE, No. 196, December, 1971.
17) Galambos, T.V., "Structural Members and Frames," Prentice-Hall, Inc., Englewood Cliffs, N.J. 1968.
18) Fukumoto, Y., Fujiwara, M. and Watanabe, N., Proc. JSCE, No.189, May, 1971.

SUMMARY

Elastic and inelastic lateral buckling strength of two parallel girders with lateral and/or sway bracing systems between them is determined theoretically and the bracing effects on the buckling strength are discussed using stiffness parameters in the bracing. The optimum relative stiffnesses of the bracing which provide full bracing at the bracing points are obtained. Tests are also conducted in this study. Total of eleven specimens with different bracing systems are tested in bending, and the results of critical moments, buckled configurations and effective length are compared with the theoretical ones.

The Design and Testing of a Steel Building Taking Account of the Sheeting

Projet et essai d'une construction en acier, compte tenu du revêtement

Entwurf und Versuch an einer Stahlbaukonstruktion unter Berücksichtigung der Verkleidung

E.R. BRYAN
Professor of Structural Engineering
University of Salford, England

M.E. MOHSIN
Professor of Airframe Design
University of Cairo, Egypt

1. Introduction

The conventional method of designing steel framed buildings is to assume that all the load is carried on the bare frames acting individually. It neglects the integral action of the building as a whole. In fact, the ability of roof and floor panels to resist shear in their own planes provides a stressed skin construction which causes the sheeted frames to behave very differently from that assumed by conventional theory. Stressed skin principles have been used in the design of aircraft, ships and cars, but until recently they have not been used in buildings.

In order to establish a theory for the stressed skin design of buildings, it is necessary to first study the individual behaviour of the interacting components. The elastic and plastic behaviour of bare steel frames has been the subject of exhaustive research and is now well established. The other interacting component, the sheeted panel, has been the subject of theoretical and experimental investigation during recent years. In the United States, the work has resulted in a design method for specific types of construction (1), and in Britain a general theory has been developed (2) which gives very satisfactory results when applied to panels using different types of sheets and fasteners. This work is to be published shortly as a design manual (3).

2. General Principles of Design

Most buildings have two or more frames which are braced or sheeted in their own planes eg at the gable ends. In such buildings, the differential flexibility between the gable frames and intermediate frames will result in interaction between the frames and roof panels. The roof sheeting or decking will act like the web of a deep plate girder spanning from gable to gable and will transfer part of the spread or sway forces from the intermediate frames to the gable ends. Fig 1 illustrates the effect in a rectangular building under side load.

The extent of the interaction between the frames and panels depends on the ratio of panel shear flexibility to bare frame flexibility. For a rectangular portal frame, the bare frame flexibility is defined as the eaves displacement k per unit side load (Fig 2a)

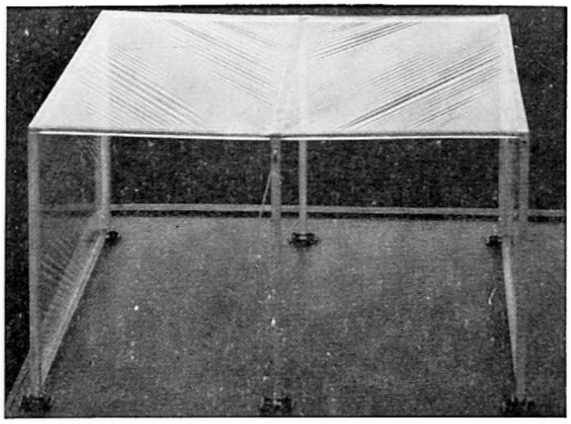

Fig 1. Membrane action in a rectangular building.

and for a pitched roof portal frame, the bare frame flexibility may be subdivided into that due to sway k_{sw} (Fig 2b) and that due to spread k_{sp} (Fig 2c). The panel shear flexibility is defined as the shear displacement c of a panel of sheeting or decking per unit shear load (Fig 3). The effect of the interaction is to reduce the moments and deflections in the frames.

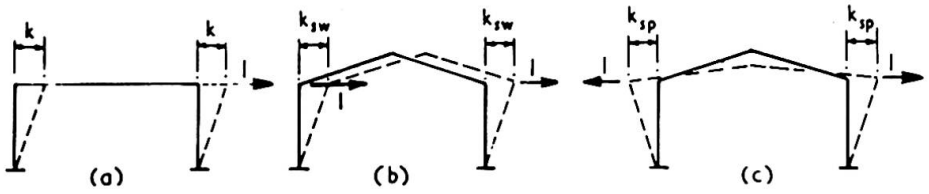

FIG.2. FRAME FLEXIBILITY

Previously tests have been carried out on full scale sheeted buildings to study the effect of sheeting on bare frames which have been designed in accordance with conventional methods (4). The purpose of the tests described in the present paper is different in that the sheeted building was designed in advance according to stressed skin theory. The philosophy on which the theory is based ensures the safety of the building at all stages of construction and use, and is given as follows:-

2.01 The steel framework must be strong enough by itself to withstand all the design loads. Under this condition, the maximum stress in the frames may be allowed to approach the guaranteed yield stress.

2.02 The effect of the sheeting will be to provide the factor of safety required by the various national standards.

This philosophy simplifies design and ensures the safety of the building at all times, even if sheeting is removed from the completed building.

3. Description of Test Building

The arrangement of the test building is shown in Fig 4. The six main frames were pinned base, pitched roof portals of 12m span and 6m spacing, so that the size of the building in plan was 12m x 30m. The columns were of 178mm x 102mm x 21.5kg/m

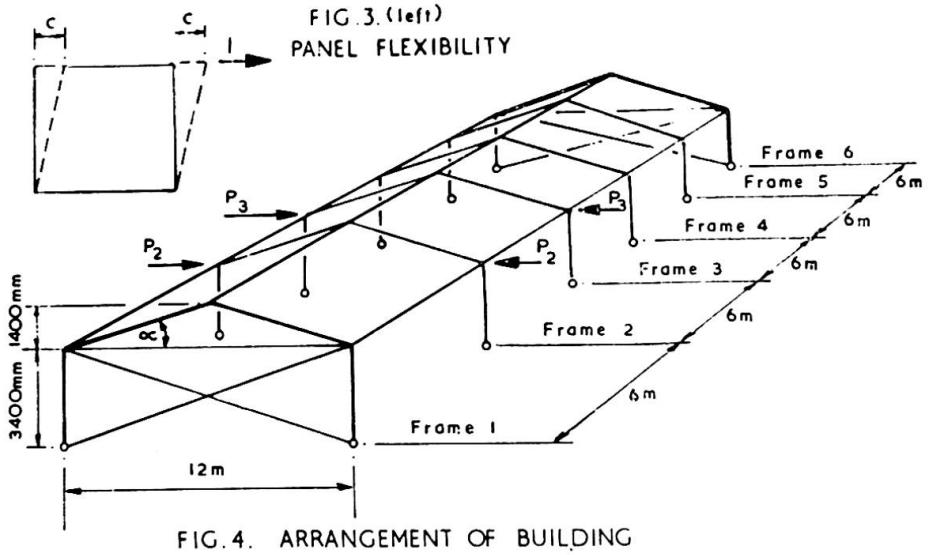

FIG.4. ARRANGEMENT OF BUILDING

joist section and the rafters were of 152mm x 89mm x 17.1kg/m joist. The purlins were spaced at about 1.5m centres and were of 140mm x 45mm x 2mm cold rolled Z section. The connections with the rafter were made through the flanges, without the use of angle cleats. Shear connectors made from short lengths of Z purlin (Fig 11) were used to transmit shear from the sheeting to the rafters and these also prevented twist in the purlin/rafter connection.

The roof was sheeted with 0.46mm thick plastic coated steel sheeting (Everclad L5 profile) interspersed with translucent sheeting of the same profile so that the area of the roof lights was 12.5 per cent of the roof area. The sheeting was fixed to the purlins with 6.1mm o.d. self tapping screws in every corrugation (15.2mm pitch) and the seams of adjacent sheets were fastened with 4.8mm aluminium pop rivets at 250mm centres. The sheeting was fastened to each shear connector with four 6.1mm o.d. self tapping screws.

The end gables of the building were braced, instead of sheeted, to allow access to the building during testing. In addition, the end bays of the building and the end roof panels were braced, in accordance with normal practice, to square up the building and provide stability during erection.

For comparison purposes, a separate steel frame, similar in all respects to an intermediate frame in the sheeted building, was erected and tested as a bare frame (Fig 7).

4. Design Criteria

The test building was designed for the superimposed loading specified for agricultural buildings, 480N/m^2, and the eaves deflection under a simulated wind load was checked. The design criteria, derived from the philosophy propounded in sections 2.01 and 2.02, were as follows:-

4.01 The stress in the bare frames was not to exceed the guaranteed yield stress of 247N/mm^2 assuming that all the design load was borne by the frames alone. The columns and rafters were also to satisfy the elastic stability criteria given in BCSA Publication No 23 using a load factor of unity.

4.02 In the sheeted building the stress in the frames was not to exceed the permissible working stress of 160N/mm^2 and the load factor for member stability was to be not less than 1.75. For the sheeting and fasteners, the load factor was to be not less than 2.25.

4.1 Design of Bare Frame (criterion 4.01)

The design loads and elastic bending moment diagram of a bare frame are shown in Fig 5. The maximum moments in the column and rafter occur at the ends of the haunch and give rise to bending stresses of 196N/mm^2 and 192N/mm^2 respectively. Although these stresses are well below the guaranteed yield stress of 247N/mm^2, and although the load factor against member instability is 1.54, the sections chosen are the smallest allowable to satisfy the criteria given in paragraph 4.01. This is because the choice of sections at the small end of the range is very limited.

4.2 Design of Sheeted Building (criterion 4.02)

In order to be able to check the design of the sheeted building it is first necessary to calculate the flexibilities of its components. The calculated sway flexibility of a bare frame is k_{sw} = 15.2mm/kN and the calculated spread flexibility of a bare frame is k_{sp} = 0.43mm/kN. The calculated eaves sway of the bare frame under horizontal wind loads at the eaves of 2.5kN is Δ = 37.8mm, and the calculated eaves spread of the bare frame under the design loads of Fig 5 is Δ = 17.8mm per eave.

Before the shear flexibility of a panel of sheeting can be determined, the parameters of the sheeting and fasteners have to be defined and their values listed. Using these values, the shear flexibility of a typical interior panel (eg panel 2-3) is calculated in accordance with the theory given in reference (3). From this, c_{2-3} = 0.30mm/kN. In the end panels (eg panel 1-2), the shear flexibility is modified by the erection bracing to c_{1-2} = 0.18mm/kN.

Let the design of the building under superimposed loads be considered first. From Fig 4 if P_2 and P_3 are the horizontal eaves forces exerted on frames 2 and 3 by the sheeting and if Δ_2 and Δ_3 are the eaves deflections of the sheeted frames 2 and 3,

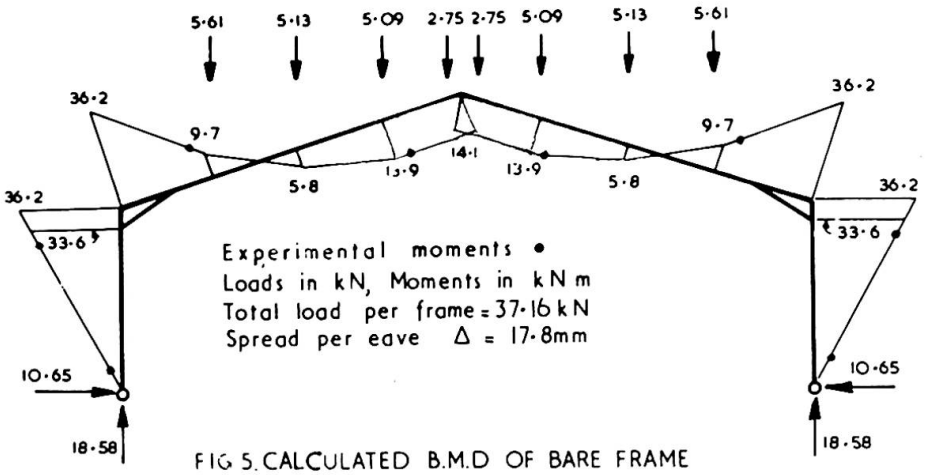

FIG 5. CALCULATED B.M.D OF BARE FRAME

then: -

For the frames, $\Delta_2 = \Delta - k_{sp} P_2$ ..... (1)

$\Delta_3 = \Delta - k_{sp} P_3$ ..... (2)

For the sheeting, $\Delta_2 \cos\alpha = c_{1-2}\left(\frac{P_2 + P_3}{\cos\alpha}\right)$ ..... (3)

$\Delta_3 \cos\alpha = c_{1-2}\left(\frac{P_2 + P_3}{\cos\alpha}\right) + c_{2-3}\left(\frac{P_3}{\cos\alpha}\right)$ ..... (4)

From equations (1) to (4), $P_2 = 24.3$kN, $P_3 = 14.0$kN, $\Delta_2 = 7.3$mm, $\Delta_3 = 11.8$mm

Under the action of these eaves forces, the bending moments in frames 2 and 3 of the sheeted building may be calculated to give the results shown in Fig 6. The maximum bending stress in frame 3 is 151N/mm^2 which is less than the design specification of 160N/mm^2 given in paragraph 4.02. In addition, the minimum load factor against member instability is 1.98 which is satisfactory.

Considering the sheeting and fasteners, it may be shown (3) that shear failure of an interior panel will occur at 44.1kN and will be due to tearing at the sheet/connector fasteners. This shear strength results in a load factor of 3.07 which is amply greater

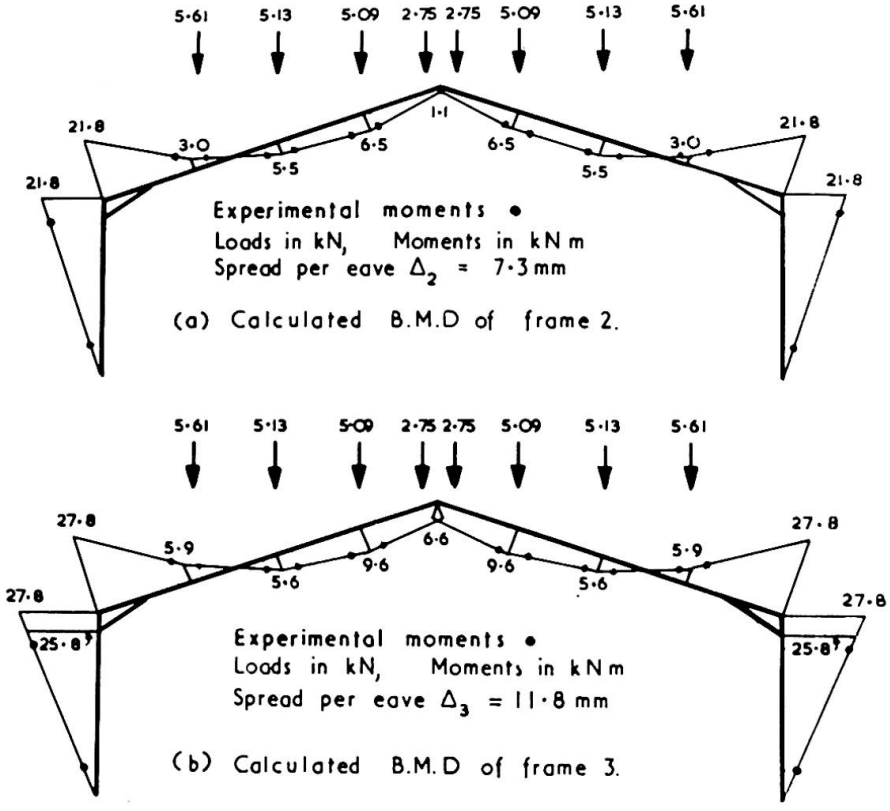

FIG. 6 CALCULATED B.M.D OF SHEETED BUILDING

than the value of 2.25 given in paragraph 4.02.

The behaviour of the sheeted building under wind load may be calculated using equations similar to (1) to (4) with k_{sp} replaced by k_{sw} and Δ replaced by the value for sway. These revised equations lead to a calculated eaves deflection at frame 3 of 1.7mm. If frame 3 were loaded by itself, the calculated eaves deflection would be 0.7mm.

5. Calculated Failure Loads of Frame

From control tests, the actual yield stress of the steel used in the frames was found to be 313N/mm^2. Using this value the failure loads of the bare frame and sheeted frame were calculated as given in Tables 1 and 2. In both the bare frame and sheeted frame failure should occur by collapse of the columns if the columns are laterally unsupported, or by simple plastic collapse of the frame if the columns are laterally supported.

6. Test Arrangements

6.1 Bare Frame

The superimposed load was applied at the purlin points of the bare frame through a steel linkage (Fig 7) using a 100kN jack. The side load was applied just below the eaves by means of a wire rope passing over a pulley and loaded with dead weights. Strains were measured by resistance strain gauges and deflections at the eaves and apex were measured with linear potentiometer transducers.

6.2 Sheeted Building

In the sheeted building, the superimposed load was applied through timber grillages (Fig 7) operated by 100kN hydraulic jacks fixed to the strong floor of the laboratory (Fig 8). The side load was applied as for the bare frame. The methods of measuring and recording strains were the same as for the bare frame.

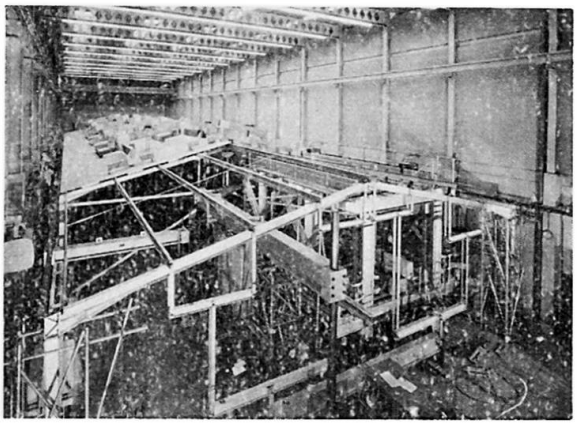

Fig 7. Loading arrangements for bare frame.

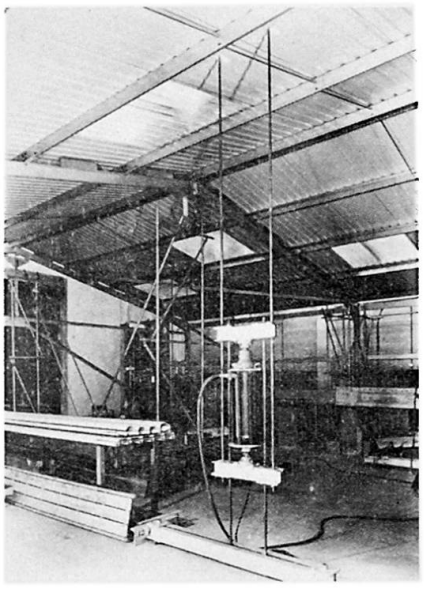

Fig 8. Jacking point.

7. Test Programme

Two series of tests (test series I and II) were carried out on the bare frame and sheeted building as follows: -

Test Series I - with the columns laterally unsupported

Test Series II - with the columns laterally supported at about two thirds of their height by rails.

In each series the following tests were carried out: -

7.01 Bare frame. Side loads at the eaves of 2.5kN.

7.02 Bare frame. Super loads at the purlin points increased to collapse.

7.03 Sheeted building. Side eaves loads of 2.5kN at each frame separately and then at all frames together.

7.04 Sheeted building. Super loads at each frame separately and then eventually increased to collapse at all frames together.

7.05 Sheeted building. Design super loads at all frames together. Loading and unloading for twenty cycles.

7.06 Sheeted building. Design super loads at all frames together. Sustained load for two days.

8. Test Results

8.1 Bare Frame

The results of the tests on the bare frame are summarized in Table 1. As expected there is close agreement between the calculated and observed deflections. There was also excellent agreement between the calculated bending moments and those derived from the strain gauge readings as shown in Fig 5.

	Calculated value	Observed value	Notes
1. Eaves deflection under side loads of 2.5kN	37.8mm	34.0mm	Test Series I
		31.7mm	Test Series II
2. Eaves deflection under design superimposed load	17.8mm	20.1mm	Test Series I
		18.2mm	Test Series II
3. Superimposed load to produce failure in columns	57kN	67kN	Test Series I
4. Simple plastic collapse load of frame under superimposed load	75kN	95kN	Test Series II

Table 1. Calculated and Observed Behaviour of Bare Frame

	Calculated value	Observed value	Notes
1. Maximum eaves deflection under side loads of 2.5kN (frame 3 only loaded)	0.7mm	0.9mm	Test Series I
		1.1mm	Test Series II
2. Maximum eaves deflection under side loads of 2.5kN (all frames loaded)	1.7mm	3.3mm	Test Series I
		3.1mm	Test Series II
3. Maximum eaves deflection under design superimposed load	11.8mm	16.3mm	Test Series I
		14.3mm	Test Series II
4. Superimposed load to produce failure in columns	73kN	82kN	Test Series I
5. Simple plastic collapse load of frame under superimposed load	110kN	122kN	Test Series II

Table 2. Calculated and Observed Behaviour of Sheeted Frame.

In Test Series I, with unsupported columns, failure occurred by column instability and in Test Series II, with supported columns, failure occurred by plastic collapse. In each case failure occurred in the predicted mode.

8.2 Sheeted Building

The results of the tests on the sheeted frames are summarized in Table 2. If allowance is made for the fact that the end gables were not completely rigid, as assumed in the calculations, then there is satisfactory agreement between the calculated and

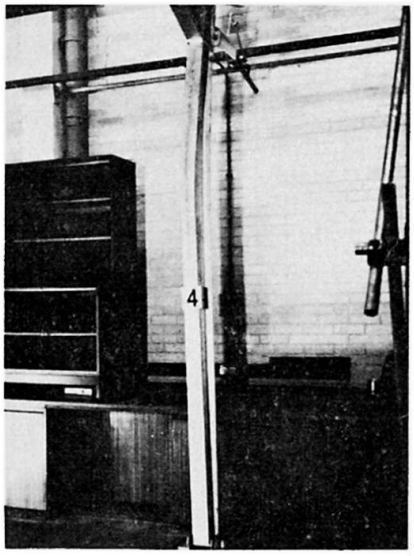

Fig 9. Instability in unsupported column in sheeted building

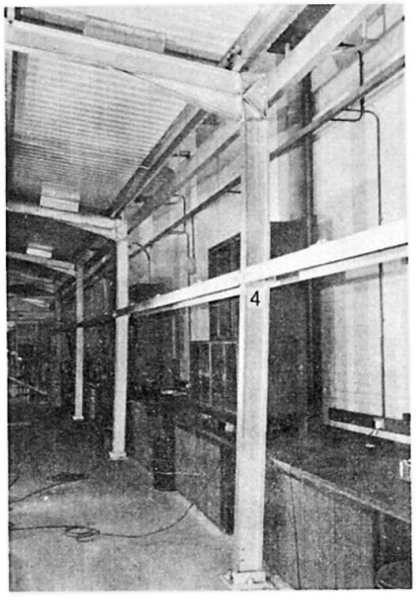

Fig 10. Plastic collapse in supported column in sheeted building

Fig 11. Plastic collapse of sheeted building.

observed deflections. There was also excellent agreement between the calculated bending moments and the measured moments as shown in Fig 6.

In Test Series I, with unsupported columns, collapse of the building started in frames 3 and 4 and extended to frames 2 and 5. The cause was column instability (Fig 9) which occurred immediately after the formation of a plastic hinge in the column below the haunch. After collapse, the sheeting and fasteners were inspected and found to be in perfect condition, but nevertheless the seam fasteners and shear/connector fasteners were replaced before Test Series II was carried out. In addition, all the buckled columns were replaced.

In Test Series II, with supported columns, simple plastic collapse of the frames commenced at the middle of the building (at frames 3 and 4, Fig 10) and extended towards the ends (to frames 2 and 5). The effect was therefore one of three dimensional collapse (Fig 11). After collapse, it was found that sheet failure had occurred by tearing at the sheet/connector fasteners at several frames. In both Test Series I and II, failure occurred in the mode predicted.

With regard to the tests listed in 7.05 and 7.06, ie loading and unloading cycles, and sustained load, the sheeted building behaved in an entirely satisfactory manner. At the design loads there was no evidence of shakedown in the building, nor of creep. It is therefore evident that these effects would not influence the design of the test building.

9. Conclusions

1. Compared with a conventional design, the stressed skin design of the building described saves 25 per cent of the weight of structural steel in the main frames. In view of the thinness of the sheeting, and low pitch of the roof, this is a considerable achievement.

2. From the tests under side load, it is apparent that the sheeting almost entirely eliminates sidesway in the frames. This fact could be a very important design consideration.

3. Although the sheeting was fastened to the purlins in every corrugation, the sheeting would have provided virtually as much restraint if it had been fastened to the edge purlins at every corrugation and to the intermediate purlins at alternate corrugations. This degree of fixity is quite common in roof sheeting as high suctions have to be withstood at the eaves

and ridge. Hence stressed skin design may involve little, if any, additional fasteners.

4. The test building illustrates one application of stressed skin design. Perhaps an even wider application is in roof and floor decks in flat roofed buildings. In these cases, the decking will be extremely effective in resisting horizontal forces.

5. One of the most important features of the work is that the design method reflects the actual behaviour of the complete building, not just the bare frame. Whether interaction effects are taken into account in design or not, they are bound to occur in practice; consequently it is only logical that they should be considered in the design method.

10. Acknowledgements

The work described was carried out at the University of Salford while Professor Mohsin was a British Steel Corporation Fellow. Without the support of the Corporation this project could not have been attempted, and the authors wish to record their deep appreciation.

11. References

1. AISI. "Design of light gage steel diaphragms". New York, 1967.

2. Bryan E R and El-Dakhakhni W M. "Shear flexibility and strength of corrugated decks". Jour.Struct.Div., ASCE, Vol 94, No ST 11, November, 1968.

3. Bryan E R. "The stressed skin design of steel buildings". To be published by Crosby Lockwood and Son Ltd, London.

4. Bryan E R. "Research into the structural behaviour of a sheeted building". Proc.Inst.Civ.Engrs., Vol 48, January 1971, pp 65-84.

SUMMARY

The interaction between the sheeting and frameworks of buildings may be taken into account in design to give a stressed skin design. The philosophy and principles of such design are discussed and applied to a 12m span by 30m long steel sheeted, steel framed pitched roof building. The building in question is tested under horizontal and superimposed loads and its performance is found to be closely in agreement with that predicted by stressed skin theory. The design saves 25 per cent of the weight of conventional frames and reflects the actual behaviour of the building which is very different from that of the bare frames.

Interaction Between Saw-Tooth Roof Truss and Latticed Girder for Minimum Weight Proportions

Interaction entre poutre maitresse de toiture de forme dentellée et porteurs en treillis, compte tenu d'un rapport de poids minimum

Wechselwirkung zwischen sägezahnförmigen Dachbindern und Gitterträgern bei minimalen Gewichtsverhältnissen

GUNVANTRAI N. DESAI MANHAR C. THAKKAR BAKUL S. BULSARI
Sardar Vallabhbhai Regional College of Engg. and Tech.
Surat, Gujarat State, India

1. Introduction

Structural steelwork for the roof system for any industrial shed or heavy work-shop, needs careful design consideration. Usually saw-tooth roof system is adopted to take the advantage of the natural north light available throughout the day. In structural design of this system, choice of basic configuration and proportions for structural elements like saw-tooth truss and latticed girder is, by and large made arbitrarily by structural engineers based on certain thumbrules and their intuition gained from experience. Such an arbitrary choice increases the weight of structural steelwork.

Structural steel is very costly material and in many developing countries it is in short supply. Economy in context of the basic structural units having large number of repetitions is therefore a governing selection criterion.

The authors here have considered several geometrical and topological configurations to arrive at minimum weight proportions by making systematic use of interacting behaviour of weight of saw-tooth truss and supporting latticed girder.

Design variables, constraints and assumptions have been listed for clarity. Influence on weight of structural steelwork per unit area; for both, saw-tooth truss and supporting latticed girder is studied. Combined effect determines the proportions for minimum weight per unit area. Influence on economy is illustrated by considering a typical example. This shows an overall saving to be 40 to 50 per cent over arbitrarily selected and conventionally designed saw-tooth roof system.

2. Design Variables

In Fig. 1 are listed various design variables considered in

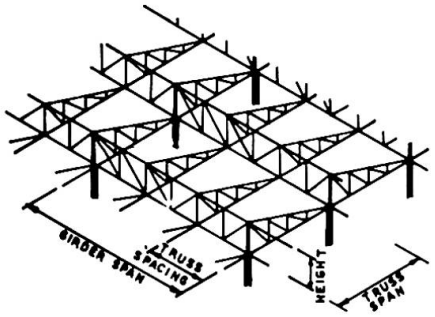

Fig. 1

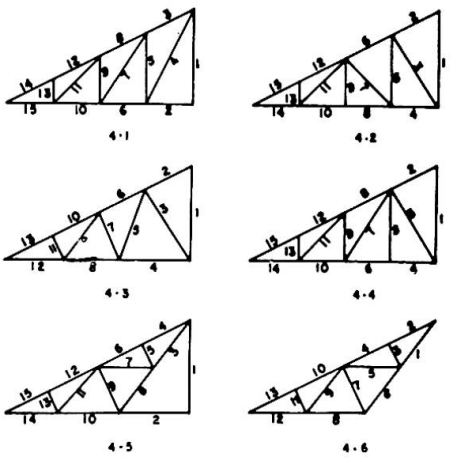

Fig. 2

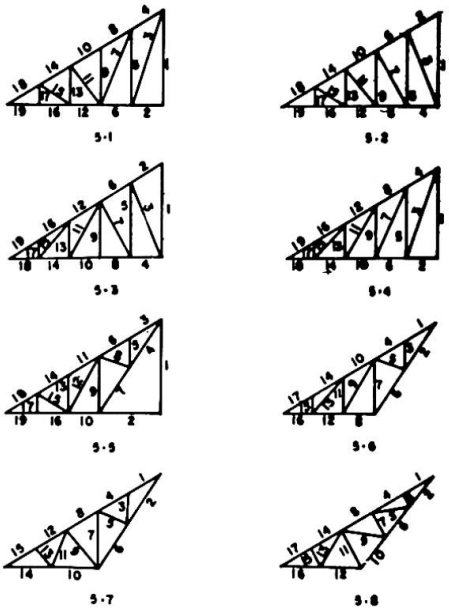

Fig. 3

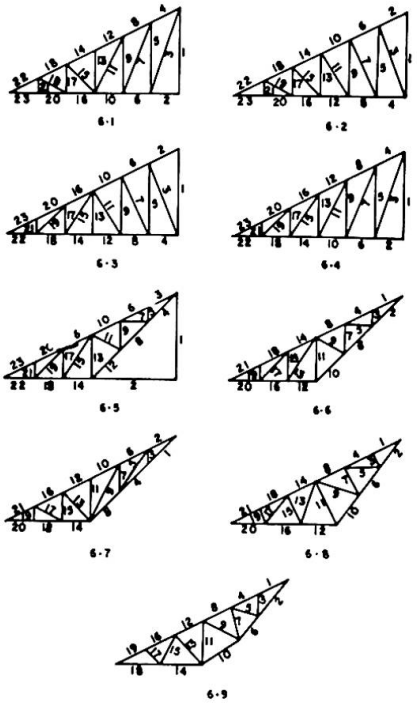

Fig. 4

the process to obtain minimum weight proportions. Number of panels in saw-tooth truss and in latticed girder are in addition to these. Only statically determinate configurations are considered.

3. Design Constraints

Minimum thickness of 6 mm for every section (1) is provided for weather resistance. Continuous members have the same cross-section, even though the forces in each of them differ.

Slenderness ratio is computed for least radius of gyration. The upper limits on slenderness ratio are 180 and 350 for compression and tension members, respectively (1). Effective lengths of continuous and individual compression members using welded connections, are taken as 0.70 and 0.85 times the member lengths, respectively (1). Permissible stresses in axial compression have been taken as specified in IS : 800-1962 (1). To account for reduced axial stress in outstanding leg of tension member, effective area is suitably derived (1).

Use of available single equal angle sections (2) is made for all members, except for the chords of latticed girders, which have two equal angle sections.

4. Design Assumptions

Following valid assumptions are made to simplify the design process, yet the structures designed are practicable and real ones.

1. Total uniformly distributed design load all inclusive of self-weight, sheeting weight and live load, on plan area is taken as 75 Kg/m^2 for all topological and geometrical configurations (3).

2. Only single loading condition with the design load mentioned above is considered. For the major portion of India stress reversals will not occur in general, with low degree of slope of saw-tooth truss (3). In particular cases, the effect of stress reversal will be very small and can be therefore neglected.

3. Bending of principal rafters of saw-tooth truss is neglected. Panel length is approximately fixed up considering maximum span which asbestos cement corrugated sheets, extensively used in India; can withstand without being overstressed or excessively deflected.

4. All joints are considered as hinged, though they are welded. Secondary stresses are neglected.

5. Influence on Weight of Saw-tooth Truss

Fig. 2 to 4 show various topological configurations considered for four, five and six panels, respectively.

From the direct search from various design solutions generated on CDC 3600-160A computer following inferences have been drawn by the authors.

With the increase in truss span, the weight increased. Larger truss spacings reduced the weight. These are quite obvious. Keeping even number of panels, increase in number of panels increased the weight. Odd number of panels appeared to increase the weight as compared to trusses with even number of panels. The optimum ratio of saw-tooth truss height to its span for minimum weight is observed to be 0.25.

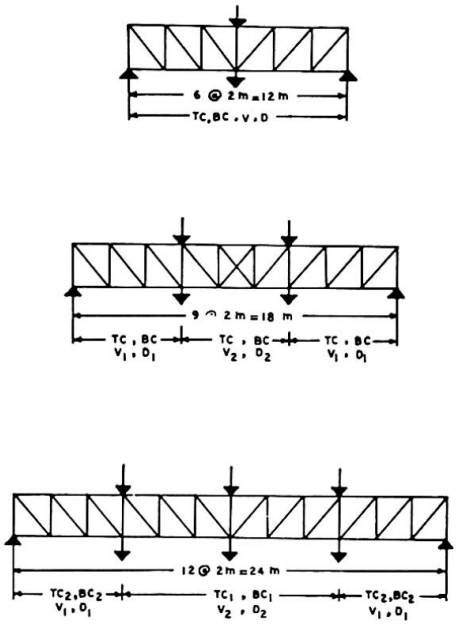

Fig. 5

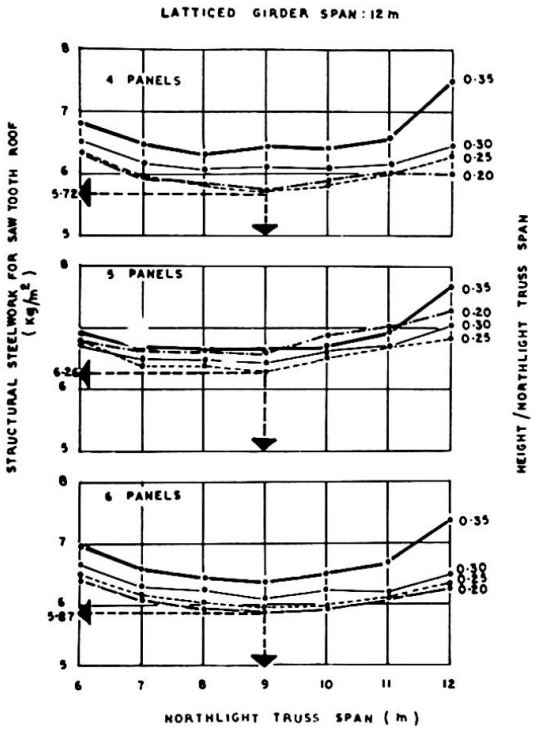

Fig. 6

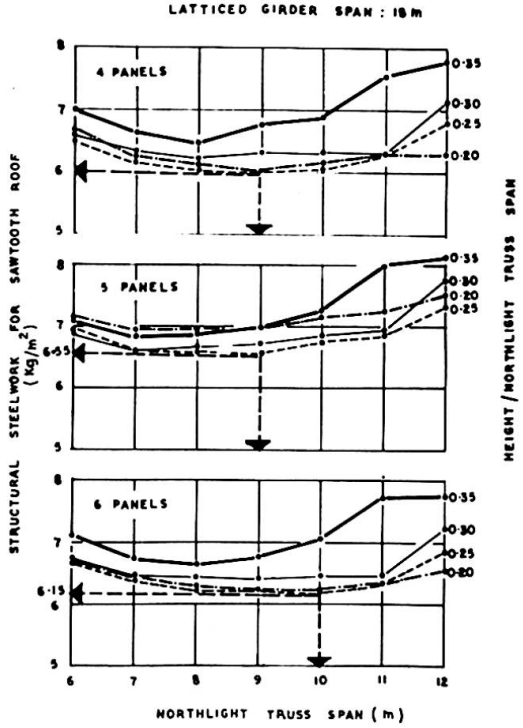

Fig. 7

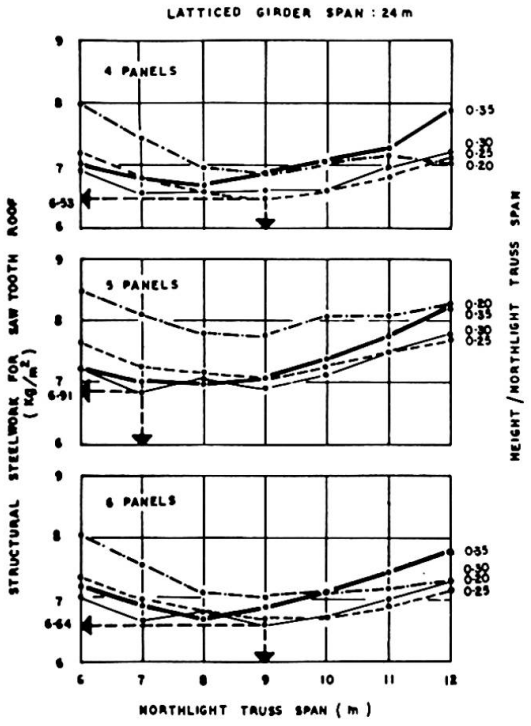

Fig. 8

Out of many topological configurations 4. 6, 5. 8 and 6.8 are found to give the minimum weight. Truss spacing should be large which can be easily accomplished using trussed purlin and a limit in this context has been drawn to 6 m. So, for further optimization, these variables are knocked out.

6. Influence on Weight of Latticed Girder

Three spans (in multiple of 6 m) (Fig. 5) are considered as 12 m, 18 m and 24 m. This covers fairly large range of spans which are normally constructed in saw-tooth roof system. The number of panels, correspondingly are 6, 9 and 12. This assumption made is in concurrence of actual practice and the chord length of 2 m has proved to be economical. Topology is assumed to be N type. It is advantageous with respect to the design of web members. Long diagonals are in tension and short verticals are in compression. This is in confirmation with the findings of Maxwell-Michells' theorems (4) which conclude that to obtain practical and yet relatively minimum weight truss, attempt should be made to minimize the weight of its compression members by proper selection of topology. Variations in the height are made but the uniformity to the height of saw-tooth truss is maintained. Keeping other parameters constant increase in girder span obviously increased its weight.

7. Weight Interaction of Saw-tooth Truss and Latticed Girder

Using topological configurations 4.6, 5.8 and 6.8 for saw-tooth truss with truss spacing as 6 m, interacting behaviour of saw-tooth truss weight and latticed girder weight is studied. Fig. 6 shows such a study for weight of structural steelwork for saw-tooth truss and latticed girder per unit area, for the latticed girder span as 12 m. Fig. 7 and 8 show similar studies for latticed girder spans of 18 m and 24 m, respectively.

It is quite clear from Fig. 6 to 8, that the minimum weight proportions are achieved if the saw-tooth truss span is 9 m, with a height/truss span ratio as 0.25 and the number of panels are only 4. Similar solutions for 6 panels are little higher and comparable, but solutions for 5 panels are quite higher in weight per unit area. This stresses that if proper choice on geometrical and topological configuration, plan dimensions and number of panels is not made, it will increase the total weight enormously.

8. Example

Using the approach presented above for a typical industrial shed of 18 m X 40 m in plan, in Western India total structural steel for saw-tooth roof system excluding purlins and wind bracings, worked out as 10,000 Kg. It will be interesting to know that a survey of similar structures in the same part of India revealed consumption of steel in the range of 17,000 Kg. to 21,000 Kg.

9. Conclusions

Systematic approach presented here can be easily used and can replace the intuitions or thumb rules, in determining proportions, geometry and topology.

Here only equal angle sections are considered, but where prefabrication is possible on huge scale other efficient sections such as tubes, can be easily dealt with.

Influence on economy will be worth noting in case of structures having large number of repetitions.

10. Acknowledgements

The authors are thankful to the authorities of University Grants Commission, New Delhi and S.V. Regional College of Engg. & Tech., Surat, India for the encouragement and financial support. The assistance of N.M. Dantwala for checking computer results and R.Z. Jani for preparation of the figures is acknowledged.

11. References

1. Indian Standard Code of Practice for Use of Structural Steel in General Building Construction, (Revised), IS : 800-1962 Indian Standards Institution, New Delhi, 1962.
2. Indian Standard Specifications for Rolled Steel Beam, Channel & Angle Sections, IS : 808- 1957, Indian Standards Institution, New Delhi, 1958.
3. Indian Standard Code of Practice for Structural Safety of Buildings : Loading Standard, (Revised), IS : 875 - 1964, Indian Standards Institution, New Delhi, 1965.
4. Khaachaturian, N., "Examples in Optimization of Trussed Structures", Lecture delivered at intensive course on Optimization in Structural Design, Preprint, Deptt. of Civil Engg. and Deptt. of Aero. Engg., Indian Institute of Tech., Kanpur, India, March 1969.

Summary

Various geometrical and topological configurations for saw-tooth truss and latticed girder are designed for practical design constraints such as availability of sections, limits on slenderness ratio and minimum thickness of section. Interaction between weights of saw-tooth truss and latticed girder is utilised in obtaining minimum weight proportions which are practicable. Influence on economy by a proper choice has been focussed.

Der Einfluss der Dachdeckung auf die Kippstabilität durchlaufender Pfetten aus Baustahl

The Influence of the Roof Decking on the Lateral Torsional Stability of Continuous Steel Purlins

L'influence de la couverture sur la stabilité de déversement des pannes en acier, calculées comme poutres continues

UDO VOGEL
o. Professor, Dr.-Ing.
Technische Universität Berlin, BRD

1. Einleitung

Im Einführungsbericht zum Thema II b "Wechselwirkungen zwischen verschiedenen Konstruktionsgliedern" weist L. F i n z i [1] im Abschnitt 4 auf den stabilisierenden Einfluß der Dachdeckung auf Pfetten hin und teilt diesbezügliche Forschungsergebnisse der Cornell University mit.

In Deutschland wurde dieses Problem in den vergangenen Jahren ebenfalls intensiv theoretisch und experimentell untersucht. Über einige der wichtigsten Ergebnisse dieser Forschungsarbeiten wird im Folgenden berichtet. Hierbei muß unterschieden werden zwischen Pfetten mit warmgewalztem doppeltsymmetrischen I-Querschnitt, die im allgemeinen "plastisch bemessen" werden, und solchen mit kaltverformtem dünnwandigen Profil, die wegen der Gefahr örtlichen Beulens im Bereich möglicher Fließgelenke i. a. "elastisch bemessen" werden.

2. Durchlaufende Stahlpfetten mit doppeltsymmetrischem Walzprofil

2.1. Allgemeines

Werden solche Pfetten nach dem Traglastverfahren bemessen, so muß sichergestellt sein, daß bis zur Ausbildung der für das Versagen maßgebenden Fließgelenkkette keine Instabilitäten, insbesondere kein Kippen, eintritt. Das Kippen ist stets zusammengesetzt aus einer seitlichen Verschiebung und einer Verdrehung des Querschnitts um die Balkenlängsachse ("lateral torsional buckling"). Um diese Verformungen ohne zusätzliche konstruktive Maßnahme (z. B. Verbände oder seitliche Abstützungen) auszuschließen, muß ent-

weder die Scheibenwirkung oder der quer zur Pfettenlängsrichtung vorhandene Biegewiderstand der Dachhaut oder beides aktiviert werden. Die Scheibenwirkung stellt eine seitliche elastische Bettung, der Biegewiderstand eine elastische Drehbettung dar. Welcher Anteil überwiegt, hängt von der Konstruktion und den Steifigkeitswerten der Dachhaut ab. Versuche von P e l i k a n [2] zeigten, daß z. B. für Wellasbestzementplatten, mit der üblichen Befestigung durch Hakenschrauben am 2. und 5. Wellenberg jeder Tafel, praktisch keine Scheibenwirkung vorhanden ist. Dagegen ergibt sich eine wirksame Kippbehinderung durch den Einfluß der elastischen Drehbettung infolge der Flächenlagerung der Dachhaut auf dem Obergurt der Pfette. Will sich nämlich die Pfette beim Kippvorgang verdrehen, so muß sich die durch die Auflast (Schnee) auf den Obergurt der Pfette aufgepreßte Dachhaut verbiegen und damit einen elastischen Verdrehwiderstand leisten.

2.2. Theoretische Untersuchungen

Die Überlegungen des Abschnittes 2.1 führen zu einer theoretischen Lösung des Kipp-Problems des durchlaufenden kontinuierlich drehelastisch gebetteten Trägers [3] . Dabei wird u. a. von folgenden Voraussetzungen ausgegangen:

a) Das Pfettenprofil bleibt beim Kippen - auch im plastischen Bereich formtreu.

b) Vor Erreichen der Traglast oder Kipplast tritt kein Beulen von Flansch oder Steg auf.

c) Ein Verdrehen des Querschnitts um die Pfettenlängsachse wird an den Auflagern (i. d. R. Binderobergurte) durch Auflagerwinkel oder andere konstruktive Maßnahmen verhindert.

d) Es gilt das bekannte idealelastisch-idealplastische Spannungs-Dehnungs-Gesetz.

e) Die Ausbreitung teilplastischer Zonen neben den Fließgelenken wird vernachlässigt.

f) An den Endauflagern und bei ausgebildeten Fließgelenken an den Zwischenstützen ist Gabellagerung vorhanden.

Die letzte Voraussetzung trifft näherungsweise zu, da bei Vollplastizierung eine Verdrehung der Endquerschnitte um die Querschnittshauptachsen möglich, in der Querschnittsebene wegen Voraussetzung c) jedoch unmöglich ist. Außerdem können sich die Endquerschnitte wegen der gegenläufigen Kippverformung zweier Nachbarfelder praktisch frei verwölben.

Die Näherungslösung wird mit Hilfe des energetischen Indifferenz-Kriteriums [4]

$$\delta\left\{\frac{1}{2}\int_{z=0}^{\ell}\left[EC_M(v'')^2+GI_D(v')^2-\frac{M_{x(z)}^2}{EI_y}v^2-(q\cdot v-\varepsilon)v^2\right]dz\right\}=\delta\{\mathcal{F}\}=0 \qquad (2.1)$$

und den Ritz-Ansätzen:

$$\vartheta_{(z)} = c_1 \cdot \sin \frac{\pi z}{l} + c_3 \cdot \sin \frac{3\pi z}{l} \qquad (2.2)$$

für ein Innenfeld, bzw.

$$\vartheta_{(z)} = c_1 \cdot \sin \frac{\pi z}{l} + c_2 \cdot \sin \frac{2\pi z}{l} \qquad (2.3)$$

für ein Endfeld und dem Übergang zum gewöhnlichen Minimalproblem

$$\frac{\partial f}{\partial c_i} = 0 \qquad \begin{matrix}(i = 1,3)\\ \text{bzw.}\,1,2)\end{matrix} \qquad (2.4)$$

gelöst. Man erhält durch Nullsetzen der Nennerdeterminanten des jeweiligen Gleichungssystems (2.4) die Kippbedingungen (2.5) für ein Innenfeld und (2.6) für ein Endfeld.

$$\begin{vmatrix} -(q_{Ki}\cdot v-\varepsilon) + 3.044\cdot\frac{32\,EC_M}{l^4} & +0.1520\cdot\frac{q_{Ki}\cdot l^2\cdot M_S}{4EI_\eta} \\ +1.2337\cdot\frac{8GI_d}{l^2}-\frac{M_S^2}{EI_\eta} & +0.1155\cdot\frac{q_{Ki}^2\,l^4}{32EI_\eta} \\ -0.8693\cdot\frac{q_{Ki}l^2\,M_S}{4EI_\eta}-0.3899\cdot\frac{q_{Ki}^2\cdot l^4}{32EI_\eta} & \\ \hline \text{SYMMETRISCH} & -(q_{Ki}\cdot v-\varepsilon)+246.57\cdot\frac{32\,EC_M}{l^4} \\ & +11.103\cdot\frac{8GI_d}{l^2}-\frac{M_S^2}{EI_\eta} \\ & -0.6892\cdot\frac{q_{Ki}\cdot l^2\cdot M_S}{4EI_\eta}-0.2682\cdot\frac{q_{Ki}^2\cdot l^4}{32EI_\eta} \end{vmatrix} = 0 \qquad (2.5)$$

$$
\begin{array}{|l|l|}
\hline
-(q_{Ki}\cdot v-\varepsilon)+\pi^4\cdot\frac{EC_M}{l^4}+\pi^2\frac{GI_d}{l^2} & \\
-0.2826\,\frac{\left(\frac{q_{Ki}\cdot l^2}{2}-M_s\right)^2}{EI_\eta} & +0.180\cdot\frac{\left(\frac{q_{Ki}\cdot l^2}{2}-M_s\right)^2}{EI_\eta} \\
+0.1740\cdot q_{Ki}\cdot l^2\cdot\frac{\left(\frac{q_{Ki}\cdot l^2}{2}-M_s\right)}{EI_\eta} & -0.1486\cdot q_{Ki}\cdot l^2\cdot\frac{\left(\frac{q_{Ki}\cdot l^2}{2}-M_s\right)}{EI_\eta} \\
-0.02852\cdot\frac{q_{Ki}^2\cdot l^4}{EI_\eta} & 0.02925\cdot\frac{q_{Ki}^2\cdot l^4}{EI_\eta} \\
\hline
\text{SYMMETRISCH} & -(q_{Ki}\cdot v-\varepsilon)+16\pi^4\cdot\frac{EC_M}{l^4}+4\pi^2\cdot\frac{GI_d}{l^2} \\
 & -0.3206\,\frac{\left(\frac{q_{Ki}\cdot l^2}{2}-M_s\right)^2}{EI_\eta} \\
 & +0.2310\cdot q_{Ki}\cdot l^2\cdot\frac{\left(\frac{q_{Ki}\cdot l^2}{2}-M_s\right)}{EI_\eta} \\
 & -0.04391\cdot\frac{q_{Ki}^2\cdot l^4}{EI_\eta} \\
\hline
\end{array}
= 0 \qquad (2.6)
$$

Diese Beziehungen könnten direkt zum Kippsicherheitsnachweis verwendet werden. Da man jedoch die Pfetten stets bis zur plastischen Grenzlast (Traglast) ausnutzen will, ist es für die Entwurfspraxis sinnvoller und einfacher, sich den erforderlichen Drehbettungskoeffizienten erf. ε zu errechnen, der notwendig ist, damit die Kipplast q_{Ki} gleich der Traglast q_T wird. Dieser Wert ist dem vorhandenen Drehbettungskoeffizienten vorh.ε gegenüberzustellen. Dazu nimmt man in den Kippbedingungen die folgenden Substitutionen vor:

$M_S = - M_{pl}$ für das Stützmoment,

$q_{Ki} = q_T = \frac{16\ M_{pl}}{l^2}$ für die Kipplast des Innenfeldes in (2.5),

$q_{Ki} = q_T = \frac{11\ M_{pl}}{l^2}$ für die Kipplast des Endfeldes in (2.6).

Die sich durch Auflösung der Determinanten ergebenden quadratischen Gleichungen für erf.ε besitzen immer noch relativ komplizierte Lösungen [3] , die jedoch mit dem auf der sicheren Seite liegenden Grenzübergang $l \longrightarrow \infty$ schließlich zu folgenden einfachen Werten führen:

$\text{erf. } \varepsilon = 0{,}855 \frac{M_{pl}^2}{EI_y}$	für ein Innenfeld	(2.7.a)
$\text{erf. } \varepsilon = 0{,}769 \frac{M_{pl}^2}{EI_y}$	für ein Endfeld	(2.7.b)

Weitere Lösungen für Pfetten, die seitlich durch Zugstangen gehalten sind, findet man in [5] und [6] .

Die numerische Auswertung von (2.7.b) für Pfetten mit I- und IPE-Profil zeigt das Bild 1:

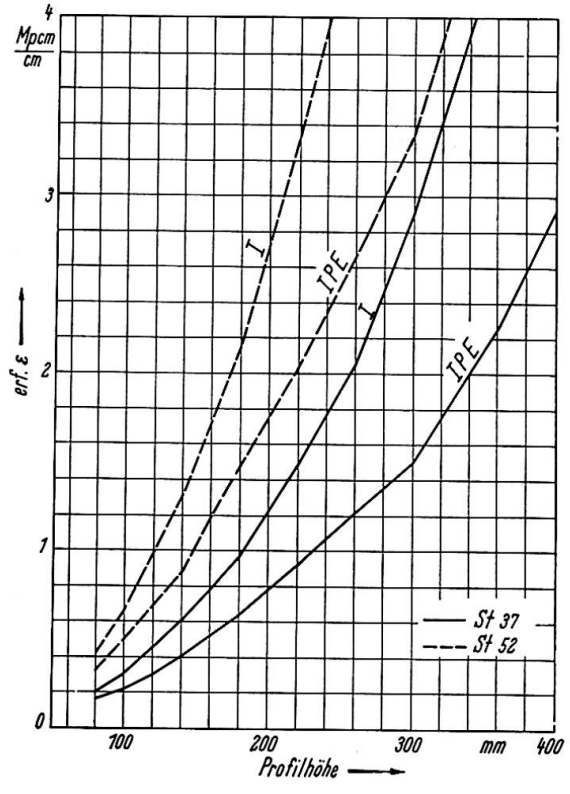

Bild 1:

erf. ε für das Endfeld einer durchlaufenden Stahlpfette

Der vorhandene Drehbettungskoeffizient ist aus der jeweiligen Biegesteifigkeit der Dachhaut zu ermitteln. Für den ungünstigsten Fall, daß nur zwei benachbarte Pfetten vorhanden sind, ergibt sich z. B. aus Bild 2:

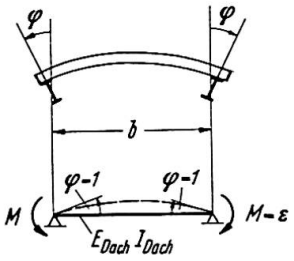

$$\varphi = \frac{1}{2} \frac{M b}{E_{\mathrm{Dach}} I_{\mathrm{Dach}}}$$

$$\text{vorh. } \varepsilon = M_{(\varphi = 1)} = \frac{2 E_{\mathrm{Dach}} I_{\mathrm{Dach}}}{b}$$

Bild 2: Ermittlung von vorh.ε

Der zu führende Kippsicherheitsnachweis lautet somit einfach:

$$\text{vorh. } \varepsilon \geqslant \text{ erf. } \varepsilon \qquad (2.8)$$

Für übliche Pfettenspannweiten und Dacheindeckungen ist er in der Regel erfüllt.

2.3 Einige experimentelle Ergebnisse

In den vergangenen 8 Jahren wurden in Deutschland eine Reihe von Traglastversuchen über die kippbehindernde Wirkung der Dacheindeckung durchgeführt. Dabei wurden Einfeldträger und Durchlaufende Träger in horizontalen und geneigten Dächern mit Eindeckungen aus Wellasbestzementplatten [2], [7], Trapezblechen aus Stahl [8] und Aluminium [9], Spanplatten [10] und Betonplatten [11] untersucht. In allen Fällen wurde die volle theoretische Traglast (plastische Grenzlast [12]), ohne vorzeitiges Kippen erreicht.

Die folgenden Bilder zeigen Fotos einige dieser Versuche:

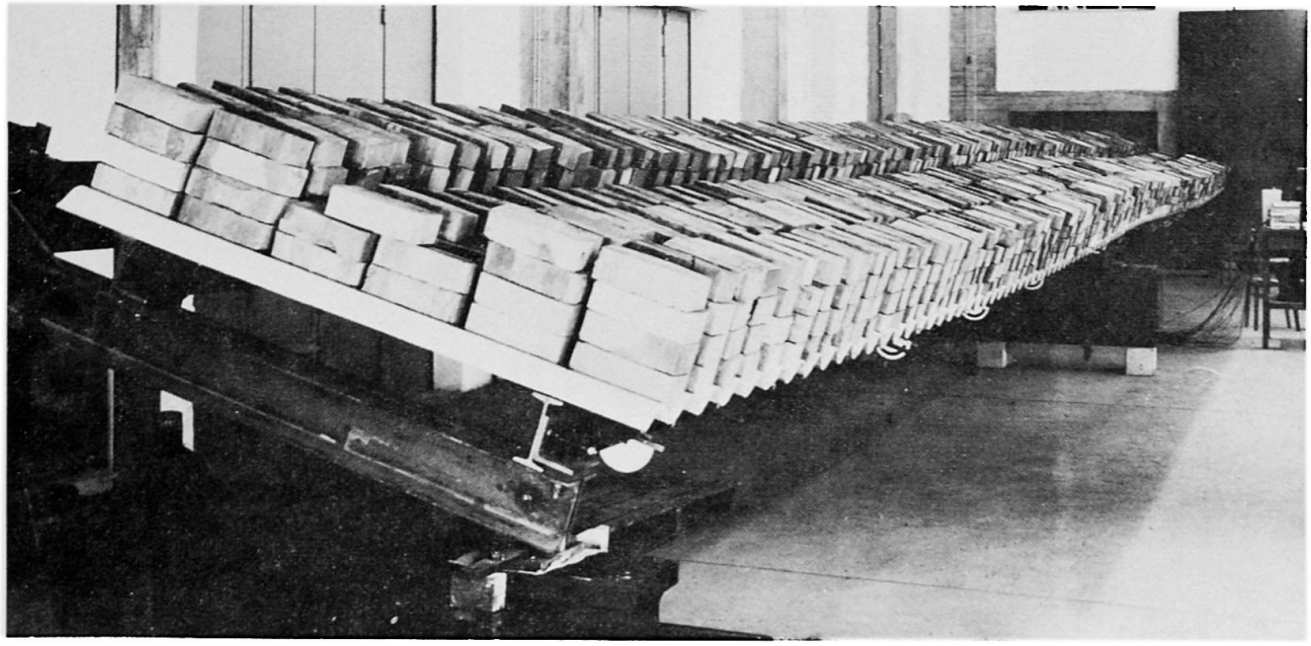

Bild 3: Versuch mit Wellasbestzementplatten; Pfetten I 160 über 2 x 10 m gestützt; Zugstangen in den Drittelspunkten; Dachneigung 30 % (16,7 °)

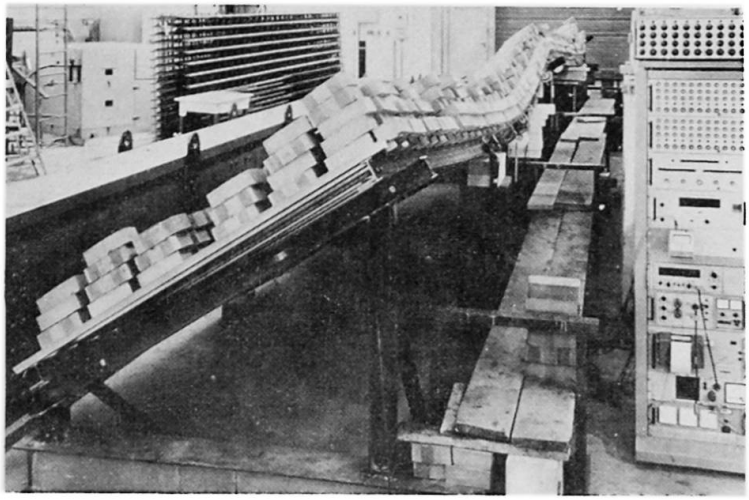

Bild 4: Versuch mit Trapezblechen aus Stahl; Pfetten IPE 100 über 2 x 8,25 m gestützt; Druckstreben in den Drittelspunkten; Dachneigung 62,5 % (32 °)

Bild 5: Versuch mit Flachsspanplatten; Pfetten IPE 100 über 2 x 5,50 m gestützt; horizontales Dach ohne Zugstangen

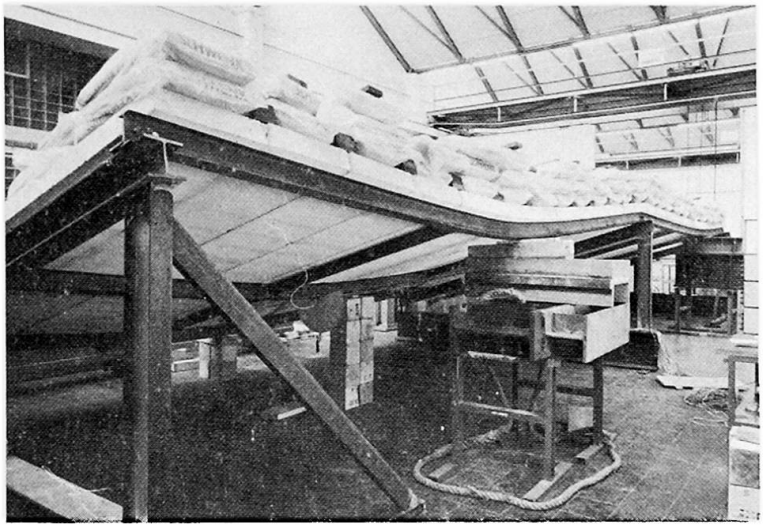

Bild 6: Versuch mit Gasbetonplatten; Pfette IPE 120 über 2 x 6,50 m gestützt; Druckstreben in den Drittelspunkten; Dachneigung 30 % (16,7 °)

3. Durchlaufende Stahlpfetten mit dünnwandigem Z-Profil

3.1. Allgemeines

Wegen der Dünnwandigkeit und der fehlenden Doppelsymmetrie des Querschnitts können i. a. für diese Pfetten das Traglastverfahren und damit die Ergebnisse des Abschnittes 2 nicht angewendet werden. Sehr häufig werden jedoch im Industriebau die Z-Profile so geformt, daß eine ihrer Querschnittshauptachsen bei geneigten Dächern vertikal verläuft (Bild 7).

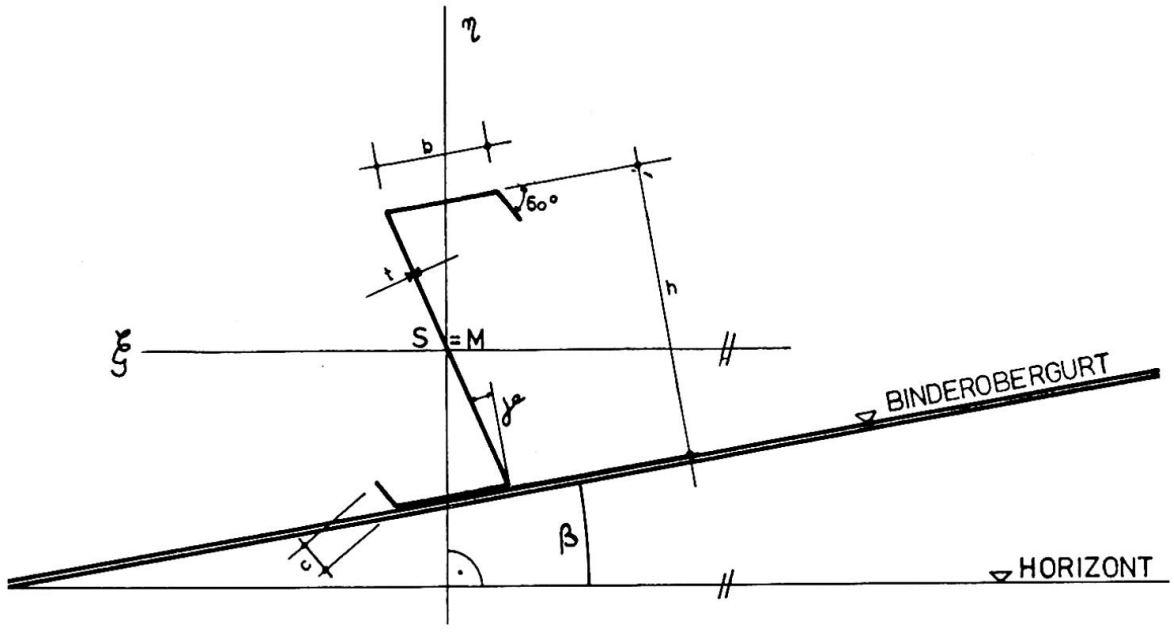

Bild 7: Z-Profil mit schrägem Steg und vertikaler Hauptachse

Dann sind bei vorhandener Punktsymmetrie und vertikalen Lasten (Eigengewicht + Schnee) die für den doppeltsymmetrischen Querschnitt aufgestellten Differentialgleichungen auch hier gültig [13] . Nach DIN 4114 [14] ist für solche Pfetten eine Kippsicherheit von $\gamma_K = 1{,}71$ unter Berücksichtigung der abgeminderten Kippspannungen im unelastischen Bereich nachzuweisen. Wie dieser Nachweis bei vorhandener elastischer Drehbettung infolge der Dachhaut geführt werden kann, wird im Folgenden gezeigt:

3.2. Theoretische Untersuchungen

Zunächst gelten auch hier die Kippbedingungen (2.5) und (2.6). An den Stützen kann jedoch kein Fließgelenk entstehen; es sind daher z. B. für ein Innenfeld die für den elastischen Träger gültigen Biegemomente

$$M_S = -M_{Ki} = -\frac{q_{Ki} \cdot \ell^2}{12} \quad ; \quad \text{bzw.} \quad q_{Ki} = \frac{12\, M_{Ki}}{\ell^2} \qquad (2.9)$$

$$\text{mit} \quad M_{Ki} = \sigma_{Ki} \cdot W_\xi \Longrightarrow \text{erf.}\,\sigma_{Ki} \cdot W_\xi \qquad (1.10)$$

einzusetzen. Dabei wird unter "erf. σ_{Ki}" diejenige ideale Kippspannung verstanden, die zu der abgeminderten Kippspannung $\sigma_K = 1{,}71 \cdot \max \sigma_{vorh.}$ führt.

Durch den Grenzübergang $l \longrightarrow \infty$ erhält man hier:

$$\text{erf.}\,\varepsilon = \sigma_{1,21} \frac{(\text{erf.}\,\sigma_{Ki} \cdot W_\xi)^2}{E\, I_\eta}$$

für ein Innenfeld (2.11 a)

$$\text{erf.}\,\varepsilon = \sigma_{,44} \frac{(\text{erf.}\,\sigma_{Ki} \cdot W_\xi)^2}{E I_\eta}$$

für das Endfeld (eines Dreifeldträgers [13]) (2.11 b)

Die numerische Auswertung der Gleichung (2.11 b) in Übereinstimmung mit DIN 4114, Bl. 1, Tafel 7, zeigt Bild 8.

An diesem Bild kann für bestimmte industriell hergestellte Z-Profile [13] der erforderliche Drehbettungskoeffizient direkt in Abhängigkeit von der unter Gebrauchslasten vorhandenen maximalen Spannung abgelesen werden. Ebenfalls sind vorhandene ε-Werte für verschiedene Dachdeckungen angegeben.

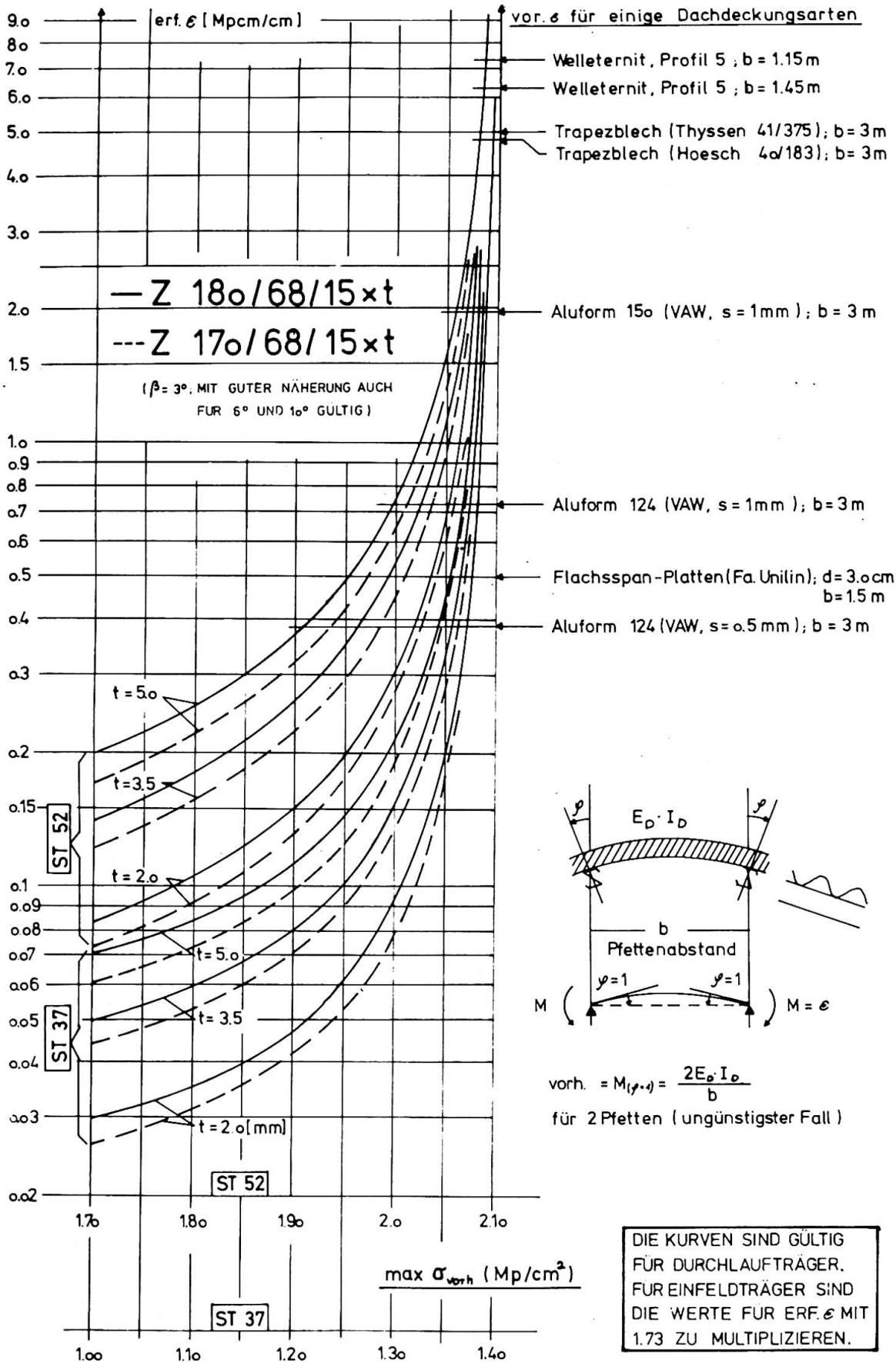

BILD 8: ERFORDERLICHER DREHBETTUNGSKOEFFIZIENT ALS FUNKTION DER SPANNUNG

3.3 Experimentelle Ergebnisse

Auch für Z-Profile sind in Deutschland Versuche durchgeführt worden [15] . Das folgende Bilde zeigt einen solchen Versuch, bei dem ebenfalls bis zu der für Biegung maßgebenden "elastischen Grenzlast" kein Kippen auftrat.

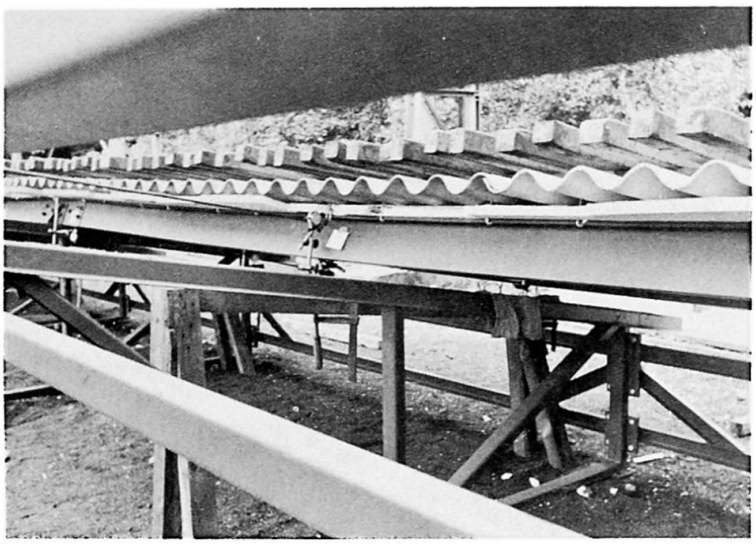

Bild 9: Ausschnitt aus Versuch mit Wellasbestzementplatten + 30 mm Isolierung; Pfetten Z 180/68/15 x 2,5 mit schrägem Steg über 6 x 6,00 m durchlaufend; Dachneigung ~18 % (10°); Belastung mit Stahlbarren.

4. Weitere Untersuchungen und noch ungelöste Probleme

Außer den hier behandelten theoretischen und experimentellen Ergebnissen wurden in Deutschland in den letzten Jahren weitere Fragen in diesem Zusammenhang behandelt, von denen einige hier kurz erwähnt werden:

a) Das Verhalten von Pfetten mit [-Profil [16].
b) Das Verhalten von Trägern, die mit über dem Obergurt gestoßenen Betonplatten belastet sind [17] .
c) Das Zusammenwirken von Pfetten und Dachhaut bei Unterwind-Belastung in offenen Hallen [18] .

Das zuletzt genannte Problem ist auch in Großbritannien experimentell behandelt worden [19] und wird z. Zt. an der Technischen Universität Berlin theoretisch untersucht.

5. Zusammenfassung

Es wurde ein kurzer Überblick über in Deutschland durchgeführte theoretische und experimentelle Untersuchungen zur Frage der stabilisierenden Wirkung der Dachdeckung auf Pfetten mit warmgewalztem oder kaltverformtem Profil gegeben. Die bisherigen Ergebnisse zeigen, daß bei den üblichen Abmessungen und Dachdeckungsarten eine volle Kippbehinderung durch die Dachhaut vorhanden ist, so daß zusätzliche konstruktive Maßnahmen entbehrlich sind. Das etwas schwierige noch ungelöste Problem der Windbelastung von unten, bzw. des Windsogs, wird zur Zeit genauer untersucht.

6. Literatur

[1] Finzi, L.: "Interaction of different Structural Elements", IVBH, Neunter Kongress in Amsterdam 1972, Einführungsbericht, Zürich 1971, S. 90/91.

[2] Pelikan, W.: "Traglastversuche mit kontinuierlichen Pfetten und Welleternit-Eindeckung", Der Bauingenieur 41(1966),S.440-44.

[3] Vogel, U.: "Zur Kippstabilität durchlaufender Stahlpfetten", Der Stahlbau 39 (1970), S. 76 - 82.

[4] Chwalla, E.: "Kippung von Trägern mit einfach-symmetrischen dünnwandigen und offenen Querschnitten", Sitzungsbericht der Akademie der Wissenschaften, Wien II a, Bd. 153 (1944), S. 47.

[5] Hildenbrand, P.: "Vergleich zweier Wege zur Ermittlung der Kippstabilität gerader gabelgelagerter Einfeldträger mit doppelt-symmetrischem I-Querschnitt nach der Energiemethode", Der Stahlbau 40 (1971), S. 18-23.

[6] Lindner, J.: "Mindeststeifigkeiten für den Kippsicherheitsnachweis beim Traglastverfahren", erscheint demnächst in der Zeitschrift "Der Bauingenieur".

[7] Pelikan, W.: "Ermittlung der Kippsicherheit von Stahlpfetten mit Welleternit-Eindeckung", Der Bauingenieur 40 (1965), S. 55-59.

[8] Prüfungsbericht Nr. S 11289 der Amtlichen Forschungs- und Materialprüfungsanstalt für das Bauwesen, Otto-Graf-Institut (Universität Stuttgart), vom 30. 4. 1969.

[9] Oxfort, J.: "Zur Kippsicherheit von I-Stahlpfetten mit ALUFORM-Profilblecheindeckung. Stellungnahme für Vereinigte Aluminium-Werke A.G., Bonn.

[10] Prüfungsbericht Nr. S 11638 der Amtlichen Forschungs- und Materialprüfungsanstalt für das Bauwesen, Otto-Graf-Institut (Universität Stuttgart), vom 25. 2. 1970.

[11] Oxfort, J. u. Hildenbrand, P.: "Traglastversuche an durchlaufenden Pfetten mit Leichtbetonplatten als Dacheindeckung", Der Bauingenieur 46 (1971), S. 131-135.

[12] Vogel, U.: "Zur Berechnung von durchlaufenden Stahlpfetten in geneigten Dächern nach dem Traglastverfahren", Der Stahlbau 33 (1966), S. 302-308.

[13] Vogel, U.: "Die Kippstabilität von Durchlaufträgern mit dünnwandigem Z-Querschnitt bei Belastung in Richtung einer Querschnittshauptachse", Der Bauingenieur 47 (1972).

[14] DIN 4114, Stabilitätsfälle (Knickung, Kippung, Beulung), Beuth-Vertrieb GmbH, Köln.

[15] Versuchsbericht Nr. 24/70 vom 22. 7. 70 der Firma Theodor Wuppermann GmbH, Leverkusen.

[16] Oxfort, J. u. Hildenbrand, P.: "Traglastversuch an durchlaufenden C -Pfetten mit Aluminium-Trapezblechen als Dacheindeckung", Der Bauingenieur 46 (1971), S. 338-342.

[17] Fischer, M.: "Das Stabilitätsproblem des in Höhe des oberen Flansches wirklichkeitsnah belasteten I-Trägers", Der Stahlbau 39 (1970), S. 267 - 275.

[18] Versuchsbericht Nr. 27/70 vom 10. 12. 70 der Firma Theodor Wuppermann GmbH, Leverkusen.

[19] Bryan, E.R.: "Asbestos cement sheeting and zed purlins under downward load and wind suction", Civil Engineering, Vol. 65, No. 765, p. 375-376, April 1970.

Die Wechselwirkung Boden—Bauwerk aus der Sicht des Konstrukteurs

Interaction between Soil and Structure from the Point of View of the Designer

L'interaction sol—structure du point de vue du constructeur

MICHAEL SORETZ
Dipl.-Ing.
Hannover, BRD

STEFAN SORETZ
Baurat h.c., Dr. techn.
Wien, Oesterreich

1. Einleitung

Die Lasten des Bauwerkes werden über die Gründung in den Boden geleitet. Im Boden werden dadurch Setzungen verursacht. Die absoluten und relativen Setzungen des Bodens müssen mit dem möglichen Verformungsverhalten der Gründung und des Bauwerkes verträglich sein. Zur Behandlung der Probleme ist zu unterscheiden zwischen der Wechselwirkung Boden - Bauwerk und der sekundären Wechselwirkung Boden - Gründung.

2. Wechselwirkung Boden - Bauwerk

Sind die Setzungen unter jedem Fundament gleich gross, oder ist das Bauwerk statisch bestimmt gelagert, dann entsteht aus den Setzungen keine Beanspruchung des Bauwerkes. Sind die Setzungen jedoch verschieden gross und das Bauwerk eine vielfach statisch unbestimmt gelagerte Konstruktion, wie es dem Regelfall entspricht, dann wird das Bauwerk durch die ungleiche Absenkung der Stützen und Wände beansprucht. Diesen unterschiedlichen Setzungen passt sich das schlaffe Bauwerk mit seiner Verformung an. Das starre Bauwerk widersetzt sich der Verformung,und durch Kräfteumlagerung wird die Setzungsmulde zu einer ebenen Fläche. Der Regelfall liegt irgendwo in der Mitte zwischen den beiden Extremfällen. Die Setzungen des Bodens haben also sowohl eine Deformation des Bauwerkes als auch eine Kräfteumlagerung durch die Biegesteifigkeit des Bauwerkes zur Folge.

Zur Beurteilung der möglichen Beanspruchung oder Deformation des Bauwerkes ist die Beurteilung der Steifigkeit der Konstruktion wesentlich. Dabei ist nicht die Konstruktion für sich allein zu betrachten, sondern in bezug auf die Grösse der Setzungen des Bodens. Es ist zwischen der Bauwerks-, der Boden- und der Systemsteifigkeit zu unterscheiden. Schultze

hat 1964 (1) die von verschiedenen Autoren gewählten Ansätze für die Systemsteifigkeit zusammengestellt. Die Ansätze gelten nur unter bestimmten Voraussetzungen, die jeweils zu prüfen sind. Für hochgradig statisch unbestimmte, räumliche Konstruktionssysteme sind die Ansätze nicht anwendbar. Es bleibt damit dem Konstrukteur überlassen, durch Näherungsrechnungen in jedem einzelnen Fall zu prüfen, welche Deformation das Bauwerk mitmacht und welche Kräfteumlagerungen infolge seiner Steifigkeit entstehen.

Häufig wird bei intuitiver Beurteilung die Steifigkeit der Bauwerke stark über- oder unterschätzt. Die Erfahrung aus Setzungsmessungen zeigt einerseits, dass mehrgeschossige Mauerwerksbauten mit geschlossenem Grundriss erstaunlich steif sind. Andererseits wird die Steifigkeit von Skelettkonstruktionen in aller Regel überschätzt. Nach der Erfahrung treten in solchen Konstruktionen bei Stützensenkungen, die rechnerisch zum Bruch führen, kaum die ersten Risse auf. Diese Tatsache erklärt sich einerseits daraus, dass der Werkstoff Stahlbeton, besonders im jungen Zustand, unter der Beanspruchung durch Zwangskräfte kriecht, andererseits daraus, dass sich die Systemsteifigkeit durch die Stützensenkung verändert (2). Weitgehend bekannt und unserer Erfahrung nach sehr praxisnahe sind die von Skempton (3) angegebenen Grenzwerte für die Verdrehung $\Delta s/l$ in üblichen Skelettbauten. Danach sind bei $\Delta s/l = 1/300$ die ersten "Architekturrisse" (Risse in Ausfachungsmauerwerk o.ä.) und bei $\Delta s/l = 1/150$ die ersten "Konstruktionsrisse" zu erwarten.

Wird nach Näherungsrechnung festgestellt, dass eine Konstruktion die Setzungen des Bodens nicht schadenfrei mitmachen kann, muss das Moment aus der erforderlichen Kräfteumlagerung ermittelt werden. Wenn dieses Moment vom Bauwerk nicht aufgenommen werden kann, dann muss entweder das Bauwerk zusätzlich ausgesteift werden, oder aber - konstruktiv richtiger und in der Regel billiger - es sind die Bauwerksabschnitte kleiner zu machen, und es ist durch die Steuerung des Bauablaufes die zeitliche Abfolge der Bauarbeiten so zu wählen, dass die Setzungsunterschiede geringer werden. Die Gründungskonstruktion ist in der Regel zu weich, um einen nennenswerten Einfluss zu haben. Bei den Betrachtungen ist zu berücksichtigen, dass das Bauwerk nicht im fertigen Zustand mit einem Kran in die Baugrube gehoben wird, sondern dass das Bauwerk Etage um Etage wächst und sich mit seiner Höhe auch seine Steifigkeit verändert. Es können also zum Teil unterschiedliche Setzungen von frischem oder jungem Beton des noch wenig steifen Bauwerkes ohne wesentliche Beanspruchung übernommen werden. Bei Bauwerken in tiefen Baugruben ist zusätzlich der Einfluss der Vorlast zu berücksichtigen. Es muss erst eine bestimmte Anzahl von Geschossen gebaut werden, ehe die Bauwerkslast die Vorlast übertrifft und damit setzungswirksam wird.

3. Wechselwirkung Boden - Gründung

Für einfache Gründungskonstruktionen, wie Streifen- und Einzelfundamente mit gedrungener Querschnittsform, hat sich der Ansatz gleichmässig verteilten Bodendrucks bewährt. Nach der Theorie ist in Abhängigkeit von vielen Parametern sowohl eine Konzentration von Bodendruck an den Rändern des Fundamentes als auch unter der Mitte desselben möglich. Nachdem sich mit der Annäherung der Last an die Bruchlast der Bodendruck zunehmend

unter der Fundamentmitte konzentriert, ist mit der gleichmässigen Bodendruckverteilung eine ausreichend sichere und trotzdem nicht unwirtschaftliche Bemessungsmethode gegeben.

Für biegeweiche Gründungskonstruktionen, wie Gründungsbalken und -platten konnte bisher noch kein allgemeingültiges und wirtschaftliches Bemessungsverfahren entwickelt werden. Wenn von der sicher unrichtigen und unwirtschaftlichen Annahme gleichmässig verteilten Bodendruckes unter einer biegeweichen Gründungskonstruktion abgesehen wird, sind das Bettungszahlverfahren und das Steifezahlverfahren als Bemessungsverfahren für biegeweiche Gründungskonstruktionen bekannt.

Die Anfänge des Bettungszahlverfahrens reichen in das 19. Jahrhundert. Das Verfahren setzt voraus, dass unter einer Last eine Setzung auftritt, die zu dieser Last proportional ist, $s = c \cdot p$. Neben der Last ist die Setzung definitionsgemäss $s = c \cdot o = o$. Der Proportionalitätsfaktor wird Bettungszahl genannt und bei diesem Verfahren als Bodenkonstante angesetzt. Nun ist einerseits bekannt, dass die Bettungszahl keine Bodenkonstante, sondern ausser vom Boden auch von der Grösse und Verteilung der Last abhängig ist. Andererseits ist bekannt, dass die Belastung eines Punktes der Bodenoberfläche auch eine Setzung benachbarter Punkte hervorruft. Damit ist also $s \neq o$ für $p = o$ und das Modell des Bettungszahlverfahrens $s = c \cdot p$ unzutreffend. In den letzten Jahren wurden Bemessungsverfahren mit variablen Bettungszahlen aufgestellt, die eine quantitative Verbesserung bringen, jedoch nicht den grundsätzlichen Widerspruch beseitigen.

Dem Steifezahlverfahren liegt die Form der Setzungsmulde der Oberfläche des elastisch isotropen Halbraumes für die Einheitsbelastung zugrunde. Hier wird die Steifezahl als Bodenkonstante eingeführt. Dieses Modell weist nicht mehr die offensichtlichen Widersprüche des Bettungszahlverfahrens auf. Die Annahme, dass der Boden elastisch und isotrop ist und die Steifezahl eine Bodenkonstante, ist jedoch zu vereinfachend. Die Setzungen des Bodens sind nicht den Bodenpressungen proportional. Der Boden ist nicht isotrop, sondern im Regelfall irgendwie geschichtet und häufig zerklüftet. Die Kompressibilität des Bodens nimmt oft mit der Tiefe ab.

Die erwähnten Verfahren haben die Bemessung der Gründungskonstruktion zum Ziel. Bisher können jedoch damit nur einfache Konstruktionselemente bemessen werden. Wird die Genauigkeit der Ausgangswerte für die Bemessung berücksichtigt, dann erscheint auch jeder grosse Rechenaufwand, wie er sich etwa bei vielfach statisch unbestimmten Systemen ergeben würde, nicht gerechtfertigt.

Das Problem liegt in der Verträglichkeit der Deformation des Bodens mit der Deformation der Gründung. Die Verteilung des von der Gründungskonstruktion aufzunehmenden Bodendruckes ist abhängig vom Verformungsverhalten des Bodens und der Gründung. Die Beanspruchung der Gründungskonstruktion wird also durch ihre Deformation gesteuert. Die Gründungkonstruktion kann daher auch nicht mit der tatsächlichen Bodendruckverteilung im üblichen Sinn bemessen werden. Wenn eine direkte Bemessung so schwierig bzw. unmöglich ist, sollte der auch sonst übliche Weg des Iterationsverfahrens gegangen werden. Im ersten Schritt wird die Gründung

mit einer ersten Annahme über die Bodendruckverteilung (z. B. linear, unstetig) entworfen. Mit diesen Annahmen sind die Setzungen und Durchbiegungen für kennzeichnende Punkte (z. B. Plattenmitte und Stützen) zu berechnen. Weichen diese Setzungen von den Durchbiegungen beträchtlich ab, sind die Annahmen in einem 2. Schritt entsprechend zu verbessern. In einem weiteren Arbeitsgang könnte für mehrere Punkte der Platte Übereinstimmung von Setzung und Durchbiegung und dadurch Annäherung an die tatsächliche Bodendruckverteilung erreicht werden. Bei der möglichen Genauigkeit der Randbedingungen ist dieser Aufwand jedoch nicht mehr sinnvoll. Häufig genügt es bereits, einfache Grenzfälle zu betrachten, und durch Vergleich der möglichen Deformationen der Gründungskonstruktion mit den Setzungen des Bodens eine Aussage über deren Verträglichkeit zu erhalten.

Bei den Betrachtungen ergibt sich, dass viele Kombinationen von Platten- oder Balkenabmessungen und Bodendruckverteilungen verträglich sind. Dies ist auf die hochgradige statische Unbestimmtheit der Wechselwirkung Boden - Gründung zurückzuführen. Daraus folgt auch, dass eine direkte analytische Bemessung nicht möglich ist.

Literaturverzeichnis:

(1) Schultze, E.: Zur Definition der Steifigkeit des Bauwerkes und des Baugrundes sowie der Systemsteifigkeit bei der Berechnung von Gründungsbalken und -platten. Mitt. Institut f. Verk. wasserbau, Grundbau und Bodenmechanik d. TH Aachen, Heft 32, 1964

(2) Rüsch, H.: Die wirklichkeitsnahe Bemessung für lastunabhängige Spannungen. Vortrag, gehalten auf dem deutschen Betontag 1965 in Berlin

(3) Skempton, A. W.: The Allowable Settlements of Buildings. J. Inst. Civ. Engrs. 5, London, 1956, Sept.

4. Zusammenfassung

Es wird ein allgemeiner Überblick über die anstehenden Probleme und ihre Lösung vom Standpunkt des Konstrukteurs gegeben. Die Betrachtungen beim Entwurf der Gründung von Bauwerken müssen in die Wechselwirkung Boden - Bauwerk und Boden - Gründung getrennt werden. Das Problem Wechselwirkung Boden - Bauwerk kann nach Ermitteln der Setzungen durch Abschätzen der Steifigkeit und der daraus folgenden Beanspruchung des Bauwerkes gelöst werden. Für das Problem Wechselwirkung Boden - Gründung erscheint zur Zeit eine direkte analytische Lösung nicht möglich. Bei der gegebenen Genauigkeit der Randbedingungen - Steifigkeit der Gründungskonstruktion und Bodenkennwerte - ist ein grosser Aufwand für hohe Genauigkeit der Berechnung nicht sinnvoll. Entscheidend ist die intuitive Erfassung der Wechselwirkung Boden - Gründung durch den entwerfenden Ingenieur, die durch Abschätzen der Verträglichkeit der Deformation des Baugrundes mit den Deformationen der Gründung überprüft werden kann.